Surgical Restoration of Maxillofacial Defects by Transport Disc Distraction Osteogenesis: Engineering Aspects

By James Angus Boonzaier

A thesis submitted in fulfilment of the requirements for the degree of Master of Science in the Department of Mechanical Engineering, University of Cape Town.

ABSTRACT

Transport disc distraction osteogenesis (TDDO) harnesses the natural healing mechanisms of bone to regenerate, and thus repairs, bone defects. Presently, no system is available for applying TDDO to the maxillary anatomy; specifically anterior-to-posterior distraction on a three-dimensional curvilinear vector. The objective of this study was to devise a system to enable repair of the defective maxilla.

The mechanical and ergonomic requirements of treatment by TDDO were investigated in the literature and through consultation with experts in the medical and bio-medical engineering fields. These requirements were distilled into a definitive Product Requirement Specification.

Three iterative versions of the device were manufactured and tested. After satisfying the functional requirements in bench-tests, each version of the device was evaluated clinically. The operational performance of each device directed refinement of subsequent versions, directing major improvements to ease-of-use and comfort.

The project culminated in a fully-functional maxillary TDDO device that addresses the requirements of both surgeon and patient. Proven in practice, the prototype can be easily and accurately customised by the surgeon to suit a wide range of defective maxillofacial geometries. The current version of the device performed successfully in bench-testing, confirming the strength of critical features and demonstrating the presence of adequate safety factors. The current version of the device has been implemented in two clinical cases where it successfully facilitated the repair of substantial defects of the maxillary alveolus and hard palate.

In total, four patients with large maxillary defects were treated with successful outcomes using devices developed in this project. One case has reached completion, with structural restoration of the maxillary alveolus and hard palate, and supporting permanent implanted dentition. Three ongoing cases are awaiting consolidation of the bone regenerate before final dental rehabilitation can commence.

Keywords: distraction; osteogenesis; bone; transport; maxilla; reconstruction; device; human; design; healthcare.

DECLARATION

I declare that the Master's submission titled *"**Surgical Restoration of Maxillofacial Defects by Transport Disc Distraction Osteogenesis: Engineering Aspects**"* is my own work, that it has not been submitted for any degree or examination at any other university, and that all sources of information have been acknowledged by complete referencing. I understand the meaning of plagiarism and declare that all the work elaborated in this document, save for that which has been properly acknowledged, is my own.

Signed.....

Full name.....

Date.....

Place.....

ACKNOWLEDGEMENTS

This engineering project would not have been possible without the innovative efforts of Dr Rushdi Hendricks, who conceived the underlying medical protocol. Over the course of this project Dr Hendricks' role developed from a professional collaborator to a valued mentor. His often challenging words kept me focused and directed.

My sincere gratitude is offered to my supervisor, Dr George Vicatos. He provided me with unwavering support and encouragement and gave me the space to work freely and independently; though always within the safety of his guidance.

Mr Kevin Katz and his team at Titamed deserve special mention for their assistance in manufacturing of the final prototype device. Their extensive experience in micro-machining proved invaluable in the final stages of development, and the quality of their workmanship was exceptional.

Mr Johann Muller of Wagner Systems provided valuable encouragement early in this project and always offered a sincere and experienced opinion. His insightful advice on design reporting proved its worth as I began putting pen to paper, and undoubtedly contributed to the level of detail in this document.

Four patients underwent treatment with devices developed over the course of this project. The patience and co-operation of these participants was crucial to the development process, providing essential operational experience and feedback. For this I am deeply grateful.

On a more personal note, I thank my mother, Jane Angus, my father, Dr David Boonzaier, and my partner, Catherine, without whose love and support I could not have managed.

I am grateful for the financial support of the South African Medical Research Council (MRC).

CONTENTS

LIST OF FIGURES

LIST OF TABLES

GLOSSARY OF TERMS

activation arm:	the interface between the distractor with the user, e.g. the head of the worm-screw.
activation mechanism (cf. traction mechanism):	the mechanism that translates the user's physical input into the distraction effect.
activation:	actuation of the distraction device to produce the distraction effect.
alveolar ridge, or alveolus:	the bony arch of the jaw into which the dental roots extend.
amelioblastoma:	invasive benign tumour, especially prevalent in the craniofacial complex.
autoclave:	sterilisation by high-temperature/pressure steam.
bifocal – cf. unifocal, multifocal:	in a two-dimensional curvilinear trajectory.
biocompatibility:	the extent to which a material causes no noxious effects to living tissue.
bone transport disc, or transport disc:	the distinct bone fragment that propagates the bone regenerate as it progresses along the distraction trajectory.
buttress plates:	metal mountings used to support the posterior end of the trajectory rail on the zygomatic arch and alveolar ridge.
callus:	the bone regenerate formed across the healing fracture.
Computed Tomography (CT):	non-invasive imaging technique for constructing a three-dimensional visualisation from a set of wo-dimensional images.
confluence:	the meeting point of the trajectory rail and posterior buttress plates at the rear of the oral cavity.
congenital:	present at birth.
cortex:	the dense outer layer of the bone.
cradle plate:	mesh extensions from the distraction locomotive that are formed such that they envelop the bone ransport disc.

craniofacial:	pertaining to the facial region of the skull.
detritus:	a general term for food remnants in the mouth.
distractor:	a device that facilitates the distraction osteogenesis procedure.
distraction:	refer to Transport Disk Distraction Osteogenesis.
ductile:	capable of being stretched and bent.
endochondral bone:	new bone forming within the cartilage of healing callus.
fibrous tissue:	tissue toughened by collagen fibres.
fixation screws:	specialised screws for anchoring or fixing implanted components to living bone.
gingiva:	the gum tissue of the mouth, covered with mucous membrane.
guide channel:	a slot in the locomotive component of the distractor, which stabilises and guides the locomotive along the trajectory rail.
intramembranous healing:	the formation of normal calcified bone within a healthy periosteum.
lingual:	pertaining to the tongue.
locomotive:	the mobile element of the distraction device, which supports and propels the bone transport disc along the distraction trajectory.
mandible:	the lower jaw.
mastication:	chewing.
maxilla:	the segments of bone comprising the upper jaw and nasal floor.
maxillofacial:	pertaining to the oro-nasal region of the face.
micromotion:	small relative movement between the two ends of the healing callus.
morbidity:	the extent to which the patient's normal functioning is compromised.
mucosa:	in this document 'mucosa' refers to all intervening soft tissues, including the periosteum surrounding the transport disc.

multifocal (cf. unifocal, bifocal):	in a three-dimensional curvilinear trajectory.
neurovascular:	pertaining to the blood supply and nerves.
nidus:	a high-risk area for infection.
obturator:	a custom-made prosthesis for physically isolating the oral and nasal cavities, often including dentition.
occlusal plane:	the plane defined by the points of contact between the teeth in the upper and lower jaw.
orthopaedic:	pertaining to the practice of treating bone disease.
osteotome:	a bone chisel.
patient compliance:	the degree to which a patient adheres to the agreed-upon treatment protocol.
prosthetic:	an artificial functional replacement for anatomical deficiencies
regenerate:	the healing callus generated by tddo, which matures into calcified bone.
resorbable:	capable of being eventually absorbed by the body.
stereo-lithographic:	
trabecular bone:	the less-dense matrix of bone contained by the cortical layer.
traction mechanism (cf. activation mechanism):	the propulsion mechanism consisting of the worm-screw operating on the rack of the trajectory rail.
trajectory rail:	a customisable guide that defines the path to be followed by the bone transport disc.
transcutaneous:	protruding through the skin.
transport disc carriage:	see locomotive.
Transport Disc Distraction Osteogenesis (TDDO), or transport distraction:	a surgical technique for producing new bone by gradual separation of a healing bone fracture.
trismus:	reduced ability to open the jaws due to muscle spasm.
unifocal (cf. bifocal, multifocal):	on a linear trajectory.

unilateral:	to either side of the midline (sagittal plane) of the body.
vascular:	pertaining to the blood supply.
viscoelastic:	bulk behaviour of a material in response to strain; immediately elastic, but becoming increasingly plastic over time.
worm-rack:	a mechanism involving a helical screw engaged with a linear toothed rack, which converts rotation into linear displacement.
worm-screw:	a helically threaded rotating component of the traction mechanism.
zygoma, or zygomatic arch:	the arched protrusion from below the eye to the temple.

In text *italicised* items designate technical terms specific to this document.

1. INTRODUCTION

1.1 SUBJECT AND MOTIVATION OF THE STUDY

This report details the design of a device for the repair of defects in the adult maxilla by Transport Disc Distraction Osteogenesis (TDDO). TDDO is a specialist method of facial reconstruction that stimulates (see sections 2.1 and 2.2) the growth of new bone in order to correct various abnormalities. It offers significant benefits over the conventional technique of bone-grafting. As such, various transport distractors have been developed by companies such as BioMet, KLS Martin, Lorenz and Synthes to carry out TDDO in the lower jaw (mandible), achieving excellent results. However, the TDDO procedure has not yet been applied to reconstruction of defects of the upper jaw (maxilla), owing largely to the lack of an effective surgical protocol and the absence of suitable devices.

Conventional grafting methods require high levels of technical skill and intra- and post-operative clinical care, with large associated costs. As a result, in the developing world many patients with maxillofacial bone defects are excluded from suitable treatment. In the majority of cases, the only treatment available to such patients is a removable denture-type prosthetic device, known as an obturator. This approach restores only partial oral function and patients continue with impaired speech and eating ability, as well as chronic oro-nasal hygiene and infection problems. In comparison with bone-grafting, TDDO is considerably less demanding of the clinical environment, and thus has the potential to extend effective reconstructive treatment to large numbers of patients inadequately treated with prostheses.

A new protocol, which applies TDDO to reconstruction of the maxilla, is being developed by Dr. Rushdi Hendricks and Dr George Vicatos. In collaboration therewith, this work presents the successful development of a versatile device for TDDO in the maxilla, with a focus on not only the functionality, but also the ergonomics and aesthetics of the device. The aim was for this collaboration to culminate in a fully-functional TDDO device; to be implemented in a multi-centre clinical study to evaluate the efficacy of the new treatment protocol for maxillary defect repair.

1.2 PROJECT BACKGROUND

Transport Disc Distraction Osteogenesis (TDDO) was pioneered by Alessandro Codivilla in 1905 and formalised by Gavriel Ilizarov in 1957 (Burstein & Williams, 2004), as a method of long-bone lengthening in orthopaedics. In 1992 TDDO was extended to maxillofacial reconstruction by Snyder et al. (Burstein & Williams, 2004). Since then it has rapidly gained favour amongst surgeons for the treatment of structural bone abnormalities in the craniofacial complex.

The benefits of TDDO over conventional bone-grafting techniques include reduced patient trauma and morbidity, higher success rates, shorter recovery time, and a superior anatomical, aesthetic and cosmetic result. The critical benefit, however, is that TDDO stimulates the repair of not only sound bone with the correct internal structure, but also the surrounding soft tissue and neurovascular networks.

Existing maxillofacial TDDO devices are not practically suited to distraction in the anterior curved segment of the maxilla. There is a gap in the market for a device capable of performing intra-oral, curvilinear TDDO to large segmental bone gaps in the maxilla.

1.3 PROJECT OBJECTIVES

The distinct objectives of this project were to:

- Define and formulate the design problem, and provide a comprehensive set of research-based design criteria in the form of a Product Requirement Specification (PRS).
- Investigate and evaluate potential solution concepts, analyse and discuss their relative merits and shortcomings, and ascertain an optimal solution concept or combination of solutions.
- Develop the solution concept into a complete design that caters for the basic requirements of TDDO in the maxilla and caters for the needs of the surgeon and the patient alike: a platform that is simple and versatile in implementation; and comfortable and convenient in its day-to-day function.
- Conduct physical laboratory testing of critical features and functionality to confirm the capabilities of the device and to ensure that the PRS requirements are satisfied.
- Culminate in a fully functional device that satisfies mechanical, ergonomic and aesthetic requirements and to demonstrate and evaluate the success of the design through bench-testing and clinical evaluation.

1.4 Summary of Project Activities

This section summarises the main activities involved in this project. They are presented in the order in which they were carried out.

1.4.1 Background Research & Literature Review

Information was obtained from academic journals covering the TDDO technique, its mechanical requirements and devices currently available for its execution; patents; engineering publications and consultations with expert collaborators in the medical and engineering fields. The compiled literature review is presented in section 2.

1.4.2 Development of a Product Requirement Specification

Based on the aforementioned research, the design problem was formulated into a coherent set of recommendations and requirements both qualitative and quantitative. This was distilled into the Product Requirement Specification (PRS) presented in section 3.3.

1.4.3 Design & Development Process

The design process involved three cycles of iteration, each of which included prototype manufacture, bench-testing and successive refinement of key features, guided by the input of surgeons. These refinements initially focused on basic functionality and later addressed issues of patient comfort and usability.

Two 'draft' devices were designed and manufactured in turn – the *V1* and *V2* prototypes. Both prototypes were bench-tested and subsequently applied clinically, with positive results. One clinical case has reached completion.

1.4.4 Culmination of Development

The development process culminated in the manufacture of a fully-functional *V3* device that is tailored to the needs of both the surgeon and the patient; adaptable and customisable to suit the specific needs of the individual case. Having refined the device according to its ergonomic requirements, strength and reliability limits were verified by calculation and confirmed by physical testing. Subsequently, the *V3* distractor was implemented in two clinical treatment cases, where it performed satisfactorily. The *V3* device is described in section 5 and a complete set of working drawings is provided in Appendix A.

1.5 Project Constraints and Limitations

Operational funding of this project was provided by the South African Medical Research Council (MRC), covering prototype manufacture, purchasing of equipment and clinical costs. In terms of manufacture, limits on this funding constrained the iterative design process by limiting the frequency with which prototypes could be manufactured and tested.

This project is open-ended, and it is expected that future ongoing experience will reveal opportunities for further refinements. Nonetheless, within the time limitations of the present study a device was developed which demonstrably addressed the requirements of the maxilla-adapted treatment protocol. Expert collaborators recommended only minor further improvements.

2. LITERATURE REVIEW

2.1 TRANSPORT DISC DISTRACTION OSTEOGENESIS (TDDO)

Distraction osteogenesis (DO) originated as a method of leg lengthening to correct leg length discrepancies. It was formalised in 1957 by Gavriel Ilizarov, a Russian orthopaedic surgeon, based on the principles of the Italian surgeon Allesandro Codivilla in 1905. Since its extension to craniofacial reconstruction by Snyder et al. in 1973, with the first clinical reports of human maxillofacial DO in 1992 (Burstein & Williams, 2004), the technique has rapidly gained favour as a treatment for various craniofacial bone abnormalities.

Transport Disc Distraction Osteogenesis (TDDO), or transport distraction, is a surgical technique used to repair bone defects by means of the gradual, controlled movement of a living bone segment, known as the ***bone transport disc***, across the defect (Saunders & Lee, 2008).

The technique involves four main stages (Zapata, Elsalanty, Dechow, & Opperman, 2010):

1. Surgical fracture of the native bone, generating the mobile bone transport disc (Figure 1).
2. A latent period to facilitate the formation of a healing callus in the fracture gap.
3. A period of controlled, gradual distraction (separation) of the fracture surfaces, thus stretching the callus.
4. A consolidation period once distraction has ceased, for embryonic bone to form mature.

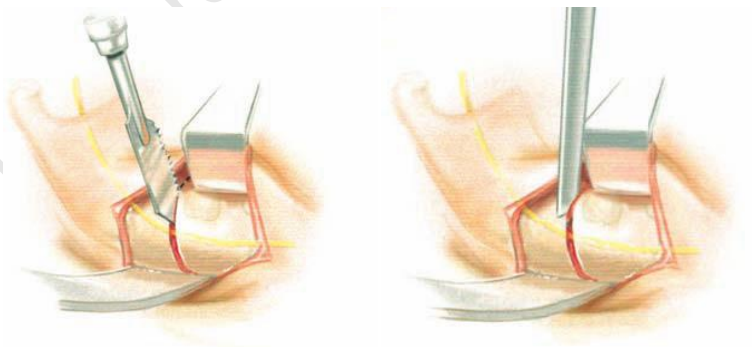

Figure 1: Producing the bone transport disc – the osteotomy process of sawing through the cortex and then fracturing the trabecular bone using an osteotome. (Burstein & Williams, 2004)

Distraction is generally carried out at a rate of approximately 1mm per day (in one or two increments per day), subsequent to a latent period of 5 to 7 days (Akay, 2011).

Distraction of the healing fracture accelerates the healing response of the body, and induces the regeneration of not only bone and cartilage, but also vital soft tissue components such as nerves, blood vessels and muscle (Akay, 2011). By directing this distraction along a defined trajectory, new bone can be produced by design, making the TDDO technique a flexible and effective tool in the treatment of various bone abnormalities (Saunders & Lee, 2008).

The benefits of transport distraction include (Burstein & Williams, 2004):

- Gradual stretching and generation of mucosa, muscle and nerves.
- Important neurovascular structures are slowly elongated, preserving continuity and function.
- Reducing or eliminating bone-grafting, saving time and decreasing patient morbidity.

In addition, TDDO is predictable and presents fewer complications than conventional bone-grafting techniques (Zapata, Elsalanty, Dechow, & Opperman, 2010).

In lieu of clinical studies of maxillary *transport distraction*, which is the area of focus in this project, the prolific application of the technique to the mandible has provided a useful proxy. Mandibular TDDO has produced excellent results, repairing defects as large as 50mm (Zapata, Elsalanty, Dechow, & Opperman, 2010) without any secondary grafting (Wang, Chen, Ping, & Yan, 2012). Yet, the literature presents few attempts to extend this technique to the maxilla, none of which involve human subjects, frequently citing the lack of appropriately designed hardware as a major reason.

2.2 TDDO: Physiology and Healing of Human Bones

The success of the distraction osteogenesis procedure is contingent on the mechanical environment of the healing fracture. Strain and stability of the fracture site have critical effects on the type of tissue that forms. While compelling theories exist, the effect of mechanical loading on TDDO in the craniofacial complex remains poorly understood. Nevertheless, this section documents current conceptions of distraction bone-healing.

The main mechanical factors in distraction bone healing are (i) the rate and rhythm of distraction and (ii) the stability of the healing fracture. The Interfragmentary Strain Theory developed by Stephen Perren in 1978, provides important physiological insight as to the effects of these factors on bone formation.

According to Saunders et al., Perren's theory 'predicts the type of tissue formed in fracture gaps as a function of the strain in the gap, with the strain being defined as the ratio of the gap end displacement to the width of the initial gap.' (Saunders & Lee, 2008) This is illustrated in Figure 2.

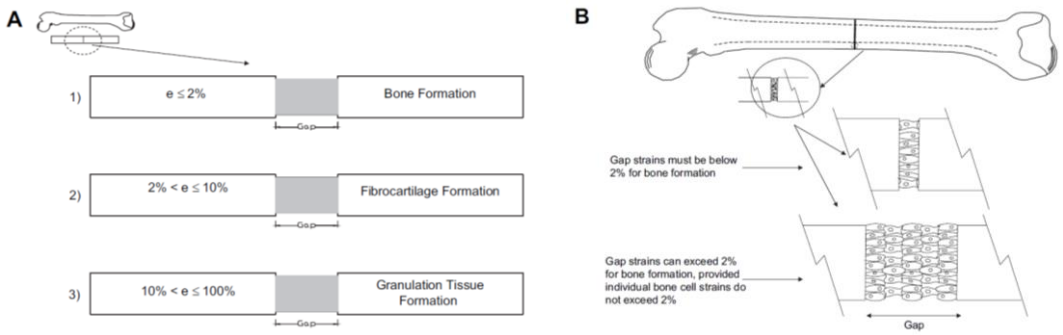

Figure 2: Illustration of the effects of strain due to callus stretching on bone formation. (Saunders & Lee, 2008)

In mathematical terms:

$$Strain = \frac{Change\ in\ gap\ length}{Original\ gap\ length}$$

According to Perren's Theory: (Saunders & Lee, 2008)

1. Primary, intramembranous healing occurs if strains in the gap region are below 2%;
2. Secondary, endochondral healing occurs if strains in the gap region are between 2-10%;
3. Fibrous tissue formation occurs if strains are between 10 and 100%; and a non-union occurs if strains are larger than 100%.
4. Intramembranous healing generates functional, calcified bone; endochondral healing generates cartilage and granulation healing forms fibrous scar tissue.

Perren's theory attributes the strain in the healing gap to two sources: Callus stretching due to controlled distraction, and 'micromotion' between the fracture surfaces – a measure of the stability of the fracture site.

In physiological terms, the strain theory relates the mode of healing to the types of cells that can survive the strain in the gap (see Figure 3):

1. If the micromotion is small (generating strain less than 2%), the fracture is relatively stable and osteoblasts can perform primary bone healing.
2. With increased micromotion (strain above 2%), the prevalence of osteoblasts in the healing callus is reduced and endochondral healing produces a cartilage matrix, known as secondary bone healing.
3. At strains between 10% and 100%, neither chondrocytes nor osteoblasts are able to survive and fibrosis healing occurs, forming a tough yet flexible union of scar tissue.

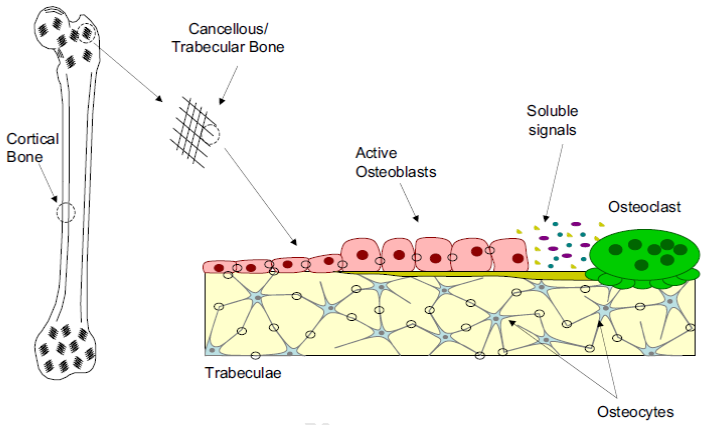

Figure 3: At the cellular level, bone consists of osteocytes, osteoblasts and osteoclasts. (Saunders & Lee, 2008)

Where large strains are present, the temporary, cartilaginous 'callus' serves two important mechanical functions:

- By uniting the bone ends, the fracture gap is stiffened.
- In the presence of the newly formed callus, the strain on the healing fracture is distributed over a greater length.

The predictions of Perren's theory provide a set of governing principles and are corroborated by clinical results by Bhatt (Bhatt, et al., 2007). A study by Sun (Sun, Rafferty, Egbert, & Herring, 2007) on swine presented several distraction cases where micromotion of 0.3mm was measured without adverse effects on bone formation. In certain cases it has been reported that even though primary bone can form under strains as high 20%, it is desirable that this be limited to a maximum of 10% to guarantee proper bone healing, thus confirming Perren's theory.

2.3 MAXILLOFACIAL ANATOMY AND GEOMETRY

The maxillofacial region is a complex arrangement of bone features and important musculature involved in eating[1], speech and facial expression. The design of an orally implanted device and its intrusiveness have profound implications for patient comfort and the ease of surgical installation. Device size, position, orientation and access must be compatible with the surrounding anatomical structures and functions.

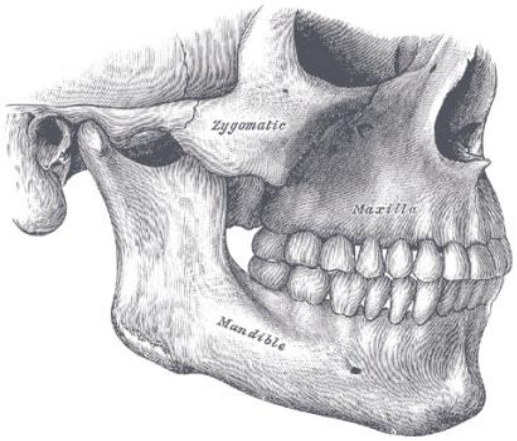

Figure 4: The craniofacial complex (Gray & Banniser, 1995)

Figure 4 illustrates the bony structures of interest in the maxillofacial complex: the maxilla, mandible and zygoma.

The **maxilla** (Figure 6 & Figure 5) consists of the alveolar ridge, the arch-shaped bone from which the upper teeth protrude; the hard palate; and the frontal process, which supports the nose. The alveolar ridge has a fairly constant triangular cross-section (Figure 5), with approximate height and width of 25mm and 10mm respectively, making it appropriate for reconstruction by TDDO. The radius of curvature of the maxillary arch ranges from 25mm to 55mm. The presence of a functional hard palate is important for eating and speech.

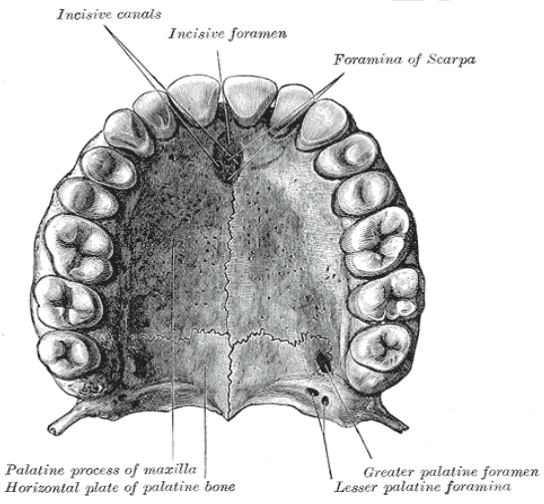

Figure 6: Inferior view of the maxillary arch (Gray & Banniser, 1995)

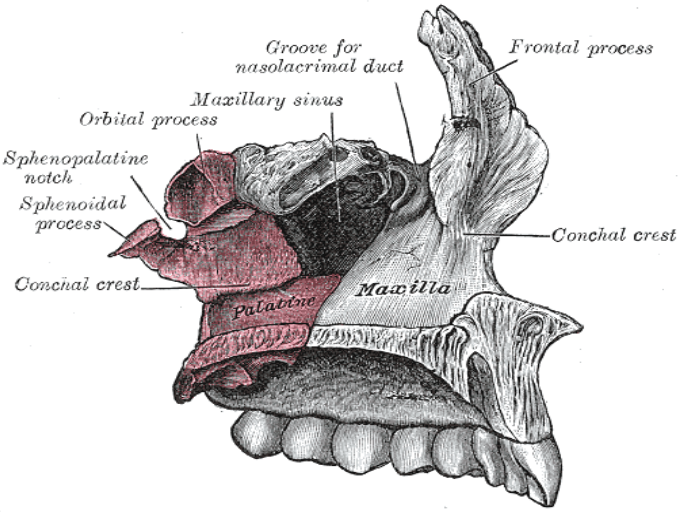

Figure 5: Coronal section of the maxilla (Gray & Banniser, 1995)

[1] In the current context eating includes mastication, swallowing and the requisite separation of the oral and nasal cavities.

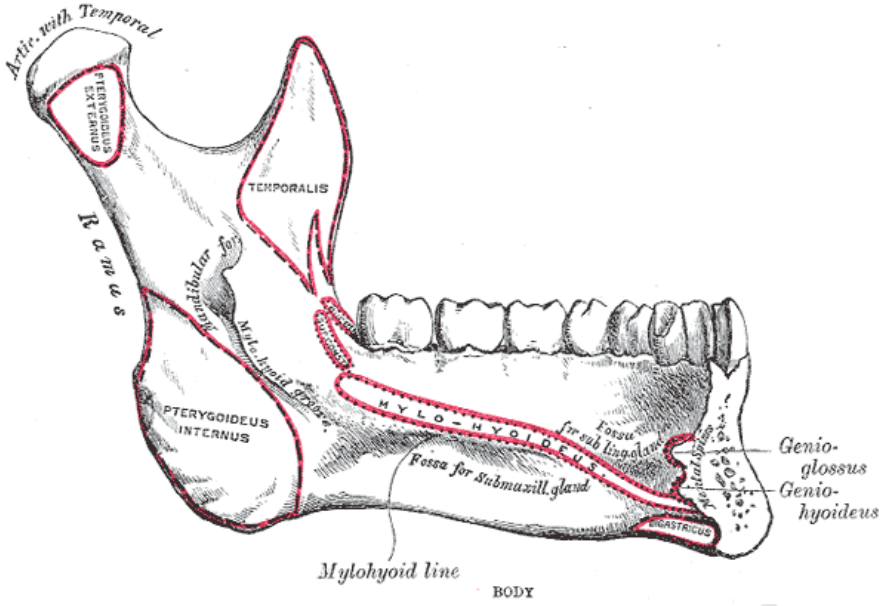

Figure 7: Coronal section of the mandible (Gray & Banniser, 1995)

The **mandible** (Figure 7) consists of the arched segment that supports the teeth, and the ramus and temporalis, which provide the hinge mechanics for control of the mandible. The geometry is less complex than that of the maxilla. It consists of straight sections linked by a curved central segment. The cross section is fairly constant and oval in shape, with approximate height and width of 30mm and 15mm respectively.

2.4 Applications & Indications – The Medical Problem

2.4.1 Maxillary Defects and their Implications

The maxillofacial complex is central to facial cosmetics and the essential human functions of eating[1], speech and facial expression (Wang, Chen, Ping, & Yan, 2012). Accordingly, any damage to the region compromises the patient's ability to function normally. Common causes of maxillofacial damage include surgically removed tumours (see Figure 8) such as amelioblastoma, congenital defects such as cleft lip and acute trauma such as gunshot wounds or vehicular accidents (Zapata, Elsalanty, Dechow, & Opperman, 2010). Surgical tumour removal is the most prevalent cause of maxillofacial defects, due its high incidence and severity. In the United States of America, 22 000 new cases of oral cancer are diagnosed annually and treatment thereof usually involves the removal of both hard and soft tissues from the face and mouth (Elsalanty, et al., 2009).

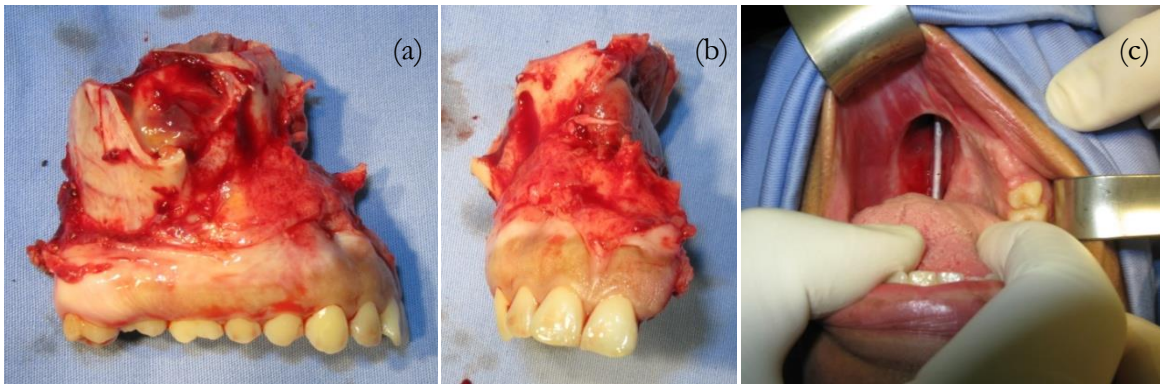

Figure 8: Typical tumour excision. (a, b) The excised bone segment and (c) the resulting defect. [2]

2.4.2 Existing Methods of Treatment

According to Elsalanty (Elsalanty, et al., 2009), the main aims of maxillofacial reconstruction are to restore normal physiology, function and appearance. In the maxilla, the ideal treatment should restore:

- Sensibility of the mucosa.
- Sufficient alveolar height and thickness to support dental implants.
- Lip competence.
- Normal function, e.g. chewing, swallowing and speech.
- Correct geometry and symmetry.
- Normal appearance of the reconstructed soft tissues.

The conventional treatment for large maxillary defects (see Figure 8) is vascularised bone-grafting (VBG). This involves the transplant of a living bone segment, including an intact vascular network, usually from the fibula, scapula or hip bone. While VBG is commonly used successfully to restore maxillofacial defects, it has four major shortcomings (Elsalanty, et al., 2009), (Wang, Chen, Ping, & Yan, 2012):

1. High rates of complication and 5% failure rate.
2. Highly demanding technique, requiring specialised personnel and clinical environment.
3. Bone graft donor site morbidity and complications.
4. Grafted bone does not match native bone in structure and physical dimensions, limiting prospects for dental prosthetic implantation.

[2] Consultation with Dr Rushdi Hendricks and Dr George Vicatos, the medical and engineering collaborators.

In comparison with non-vascularised bone-grafting, VBG patients spend, on average, 3 more hours in surgery, 12 more days in hospital, and lose 500cc more blood. According to Elsalanty et al., high rates of complication and the limited applications of grafting methods necessitate the development of new and effective alternatives (Elsalanty, et al., 2009).

In South Africa only 5 centres are capable of performing free fibula flap VBG. In contrast, there are more than 100 maxillofacial surgeons capable of executing the transport distraction technique [3]. According to the medical collaborator [4] there are hundreds of cases per year in South African for which maxillary TDDO is an appropriate treatment.

2.4.3 TDDO AS AN ALTERNATIVE

Bone generated by transport distraction mimics native bone in both physical dimensions and mechanical properties, and involves a less invasive surgical procedure than bone-grafting.

With a growing understanding of its capabilities, transport distraction is becoming an increasingly compelling alternative to conventional grafting techniques for the following reasons (Elsalanty, et al., 2009), (Wang, Chen, Ping, & Yan, 2012), (Akay, 2011):

- Surgical trauma is reduced: no donor site needed, reduced operating time.
- TDDO involves a comparatively simple surgical protocol.
- Regenerated bone quality and geometry is comparable to the native bone of the maxilla, making it ideal for restorative dental implantation.
- The surrounding mucosa, nerves and blood supply are regenerated in tandem, restoring broad oral functionality.

Dental rehabilitation is of utmost importance in maxillary reconstruction, which demands sufficient bone bulk for long-term prosthetic implants. A randomised controlled trial by Elsalanty (Elsalanty, et al., 2009) concluded that TDDO techniques produced far superior results to grafting. TDDO in the mandible produced an alveolar regenerate with an average height and width of 96% and 87.5% of the native bone respectively, compared to 26% height in the case of treatment by VBG.

[3] Consultation with Hendricks and Vicatos, 2011-2012.
[4] Dr Rushdi Hendricks, B.Ch.D, M.Ch.D

Nevertheless, TDDO has intrinsic shortcomings (Akay, 2011), (Zapata, Elsalanty, Dechow, & Opperman, 2010):

- Failure of devices during treatment.
- The need for two distinct surgeries for device installation and removal.
- Reliance of patient compliance, given that TDDO generally requires home activation of the device.
- Requires adequate healthy bone stock for harvesting the *bone transport disc* and anchoring the distraction device.

These shortcomings are, however, largely specific to the distraction device in question, and are fairly superficial in comparison to the overall physiological benefits of TDDO.

In short, the literature has demonstrated that TDDO may indeed offer a viable method of treating large maxillofacial bone defects, both in theory and in practice. It is implied in the literature that the extension of the TDDO technique to the repair of maxillary defects is restricted primarily by the lack of suitable devices (Zapata, Elsalanty, Dechow, & Opperman, 2010).

2.5 TDDO – Understanding the Physical Environment

2.5.1 The Distraction vector

The trajectory followed by the bone transport disc is known as the distraction vector. Zapata classifies this vector as follows (Zapata, Elsalanty, Dechow, & Opperman, 2010):

1. Unifocal, if the distraction vector follows a one-dimensional linear path.
2. Bifocal, if the distraction vector is curvilinear within a flat plane, i.e. two direction components.
3. Multifocal, if the distraction vector incorporates a third spatial dimension.

The activation mechanisms employed by most intra-oral devices limit their application to unifocal distraction. Such devices do not cater for craniofacial deformities that require a curvilinear distraction vector (Saunders & Lee, 2008), such as defects of the maxilla. In order to accommodate such cases, devices have been developed that make use of a ductile[5] rail, which can easily be customised by the surgeon to suit the geometry of a particular patient (Wang, Chen, Ping, & Yan, 2012) & (Zapata, Elsalanty, Dechow, & Opperman, 2010). These curvilinear devices cater for curvilinear TDDO in the

[5] Bendable and formable by applying mechanical force.

mandible (Zapata, Elsalanty, Dechow, & Opperman, 2010). However, as discussed in section 2.7.3, the peculiarities of these devices are not suited to TDDO applied to the maxilla.

2.5.2 Distraction Rate and Rhythm

Manually activated distraction, the current standard for craniofacial applications, involves two main components: (i) the rate of distraction, i.e. the total displacement of the bone transport disc per day and (ii) the rhythm, or frequency, of activations. According to Zapata (Zapata, Elsalanty, Dechow, & Opperman, 2010), rates vary from 1mm to 2mm per day at frequencies of up to 5 activations per day for craniofacial TDDO.

Maintaining the correct rate and rhythm is crucial. If the osteotomy is separated too rapidly (>2mm per day), the bone will not heal, and fibrous scar tissue will form in the gap, whereas if the gap is separated too slowly (>0.5mm per day), the regenerate will consolidate prematurely and impede further distraction (Akay, 2011), (Saunders & Lee, 2008). The same is true if the latent period is too long. There is consensus in the literature that 1mm per day, activated twice daily is satisfactory (Akay, 2011).

Continuous distraction is considered the ideal mode of distraction, as it minimises acute trauma in the healing gap by distributing the distraction over a greater period of time, while still achieving the required overall strain rate. However, attempts at continuous distraction involving actuation by small motors, hydraulics or stored spring energy have proved impractical for reasons of size, patient comfort and reliability (Zapata, Elsalanty, Dechow, & Opperman, 2010) & (Romanyk, Lagravere, Toogood, Major, & Carey, 2012)

2.5.3 The Callus Stretching Force

In TDDO, tensile forces in the healing callus and surrounding soft tissue provide the only resistance to distraction. In order to achieve the desired strain in the fracture gap, a distraction device must overcome this resistance.

Actual mandibular distraction forces reported in the literature generally ranged from 20 N to 60 N, with an average of approximately 35 N (Burstein, Lukas, & Forsthoffer, 2008), (Suzuki & Suzuki, 2011). In an entirely different application, a study by Burstein (Burstein & Williams, 2004) concludes that resorbable midface distraction devices provide a safety factor of 4.4 over the maximum expected distraction load of 60 N. However, this large safety factor is attributed to the relatively unpredictable

nature of the polymeric materials used. Furthermore, the fact that resorbable materials weaken over time must be compensated for by an initial overdesign.

According to Meyer et al., the distraction force is proportional to the cross-sectional area of the healing callus (Meyer, Kleinheinz, & Joos, 2004). Since the cross-sectional dimensions of the mandible are marginally higher than those of the mandible, the forces required by maxillary TDDO are likely to be proportionally less than those in the mandible. It is thus reasonably assumed that the maximum mandibular distraction force presented by the literature of 60 N provides a safe benchmark for the design of a maxillary TDDO device.

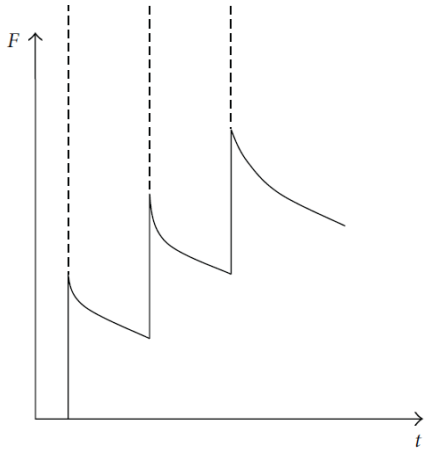

Figure 9: Stepwise relaxation of the distraction force during TDDO. (Romanyk, Lagravere, Toogood, Major, & Carey, 2012)

Romanyk (Romanyk, Lagravere, Toogood, Major, & Carey, 2012) models the distraction force as a stepwise relaxation function (see Figure 9). Daily activation of the distraction produces displacement of the bone transport disc that is effectively stepwise. The viscoelastic behaviour of the stretched tissues generates resistive forces in the callus that peaks at the instant of activation, and decays exponentially as the callus tissue relaxes.

A study by Suzuki et al. (Suzuki & Suzuki, 2011) supports this model, finding that distraction force increases over the course of the procedure, rising to a local peak at the moment of activation and then decreasing until the next activation due to increasing consolidation of the regenerate. Meyer (Meyer, Kleinheinz, & Joos, 2004) found that for a rate of 2mm per day, mandibular distraction force remains relatively constant throughout the distraction process, implying that distraction of up to 2mm per day remains within the elastic range of the distracted tissues.

Thus, devices for transport distraction must withstand cyclic force spikes of the order of 60 N, with intermediate residual loads.

2.5.4 Accidental Disturbance due to Lingual Forces

The stability of the bone transport disc is largely dependent on extraneous forces that might disturb the healing fracture, i.e. micromotion of the fracture site. Repetitive movement at the fracture site can lead to fibrous healing rather than proper bone formation. Forces due to the tongue have been investigated in various studies. For the force exerted by the tongue in the vertical direction, Trawitzki (Trawitzki, Borges, Giglio, & Silva, 2011) found a maximum force of approximately 1.3kgf for the anterior tip and 1.8kgf for the dorsum of the tongue. In both cases the maximum applied lingual force was measured in male test subjects.

Valentim et al. present a summary of various studies on tongue force in the anterior and lateral directions. The maximum lateral force of 16 N was found in a study by Dworkin. Other studies presented lateral lingual forces in the region of 12 N. The maximum tongue force in the anterior direction was approximately 26 N (Valentim, et al., 2012).

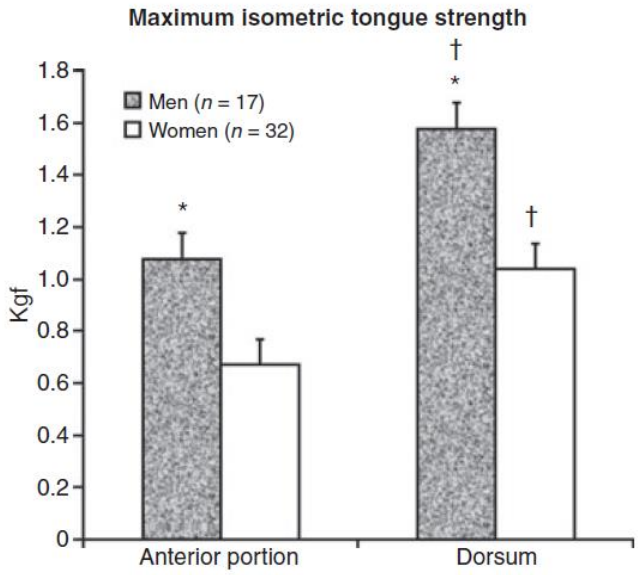

Figure 10: Mean maximum vertical tongue force exerted by the anterior portion and dorsum of the tongue. (Trawitzki, Borges, Giglio, & Silva, 2011)

2.5.5 The Bone Transport Disc: Size and Stability

The geometry of the regenerated bone is largely dependent on aspects of the initial bone transport disc, illustrated in Figure 11. The literature suggests that the bone transport disc should be approximately 20mm long (Wang, Chen, Ping, & Yan, 2012) and that more than 4 screws should be used in order to stabilize the bone transport disc (Elsalanty, et al., 2009).

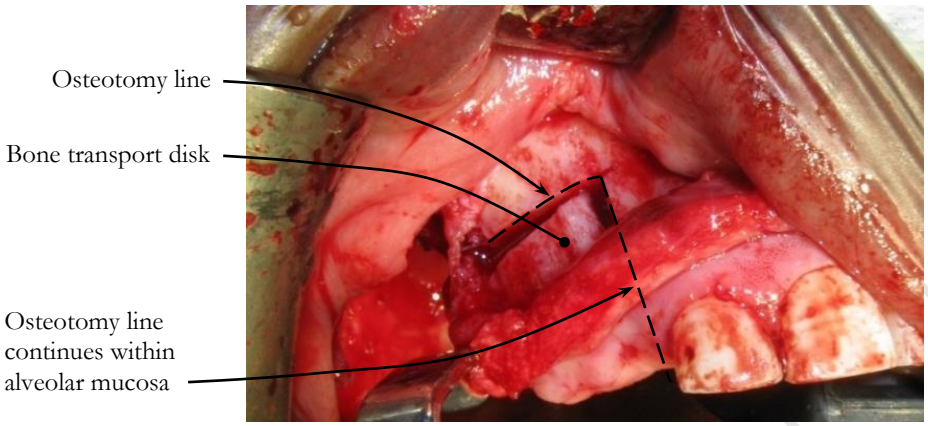

Figure 11: Intra-operative photograph of the surgically produced bone transport disc. [6]

[6] Consultation with Hendricks and Vicatos, 2011-2012.

2.6 ERGONOMICS: PATIENT COMPLIANCE AND COMFORT

For especially large defects, the active distraction period can last more than 2 months. Many maxillofacial TDDO protocols therefore allow patients to return home within two weeks of the initial surgery and enjoy a close-to-normal daily routine. In such cases, daily distractions are carried out by the patients themselves (see Figure 12) or by a trained nursing aid; the rate and rhythm of distraction prescribed by the surgeon.

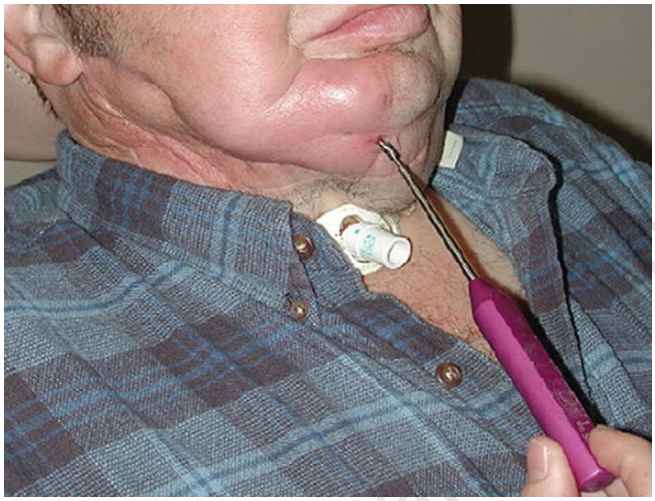

Figure 12: Patient activation of intra-oral mandibular distractor. (Zapata, Elsalanty, Dechow, & Opperman, 2010)

While in general patient compliance has been satisfactory (Zapata, Elsalanty, Dechow, & Opperman, 2010), Romanyk et al. suggest that patient involvement during treatment should be minimised to eliminate potential risks and to reduce inconvenience caused to the patient (Romanyk, Lagravere, Toogood, Major, & Carey, 2012). However, in the absence of automated distraction mechanisms (see section 2.5.2) patient-activated devices currently offer the only practical solution. As such, activation of distraction devices must be simple, intuitive and produce repeatable results, despite the lack of experience and training of users[7].

Intra-oral devices should minimise the presence of voids that might provide traps for food, detritus and infection, as it leads to unpleasant smells and taste and can provide a ***nidus*** for infection. To this end, ISO standard 7153-1 specifies that this category of device be produced with smooth contours and highly polished surfaces, which are easy to clean, resist corrosion and tend not to accumulate adherent debris. However, it should be noted that highly reflective surfaces can cause glare under operating lights. Where appropriate, non-glare finishes are preferable. Newson et al. recommend an anti-glare final finish using a Scotch-Brite™ polishing mop (Newson, 2002).

[7] Consultation with Hendricks and Vicatos, 2011-2012.

2.7 TDDO Device Design: Existing Concepts

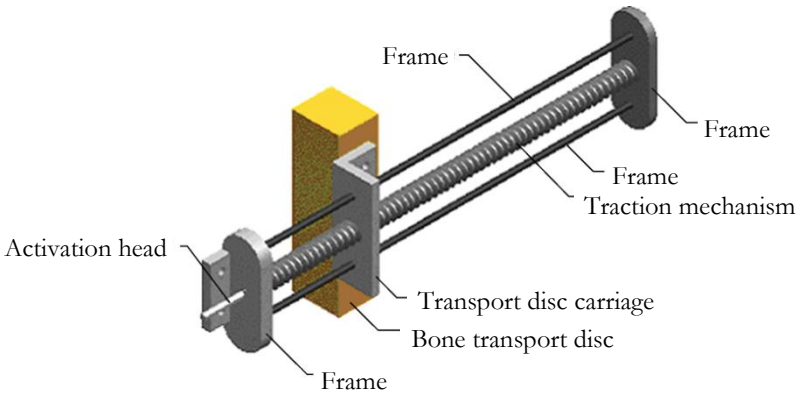

Figure 13: Typical format of existing TDDO devices. (Zapata, Elsalanty, Dechow, & Opperman, 2010)

Transport distraction devices generally consist of the following fundamental components (see Figure 13):

1. The ***frame*** supports the components of the device and designates the trajectory to be followed by the bone transport disc.
2. The ***transport disc carriage*** supports the bone disc, while navigating the trajectory/path.
3. The ***traction mechanism*** translates the operator's activation energy into displacement along the trajectory.

Zapata makes several pertinent suggestions for maxillofacial distraction devices (Zapata, Elsalanty, Dechow, & Opperman, 2010):

1. TDDO devices should be intra-oral, to lessen scar formation and small, to improve patient comfort and reduce stress on the soft tissues.
2. Devices should be stable, with the use of a strong frame, attached directly to the bone to diminish shear stresses within the newly formed callus.
3. The devices should follow the desired vector plan.
4. Device customisation and installation should be as simple as possible in order to minimise operating time.
5. Devices should be capable of *bifocal* or *multifocal* distraction (defined in section 2.4.3) to mimic the natural curvilinear continuity in the newly formed bone when reconstructing the facial contours.

The following sections analyse aspects of existing maxillofacial TDDO devices in terms of these suggestions.

2.7.1 INTRA-ORAL VS. EXTRA-ORAL DISTRACTION

Depending on the clinical application, intra-oral and extra-oral distraction methods possess individual benefits and shortcomings. In short, intra-oral distraction is superior in the context of the maxilla. Extra-oral distraction methods are preferred when complicated three-dimensional bone reconstruction is required. Table 1 summarises the superiority of intra-oral methods in the maxillofacial context.

Table 1: Comparison of extra-oral vs. intra-oral distraction devices (Zapata, Elsalanty, Dechow, & Opperman, 2010), (Burstein & Williams, 2004). Table by author.

INTRA-ORAL	**EXTRA-ORAL**
✗ Generally only capable of bifocal distraction	✓ Capable of multifocal distraction
✓ Excellent stability of anchorage pins	✗ More susceptible to loosening of anchorage pins
✓ Relatively small: Good patient comfort	✗ Relatively large: Poor patient comfort
✓ Intra-oral: no scarring	✗ Transcutaneous protrusions: scarring
✓ Low infection rates	✗ Pin-tract infection common
✓ No activation arm extension: Less error	✗ Long activation arm extension: Greater error

Figure 14 illustrates the size of extra-oral devices. Such devices compromise the patient's quality of life and the prominent transcutaneous protrusions can lead to noticeable scarring. Intra-oral devices must be small enough to be situated entirely within the oral cavity, without significantly compromising normal oral function and hygiene. The methods of fixation must consider the surrounding anatomy in terms of installation, *distraction activation* and the ultimate removal of the device. Access at all stages of treatment is a critical consideration. [8]

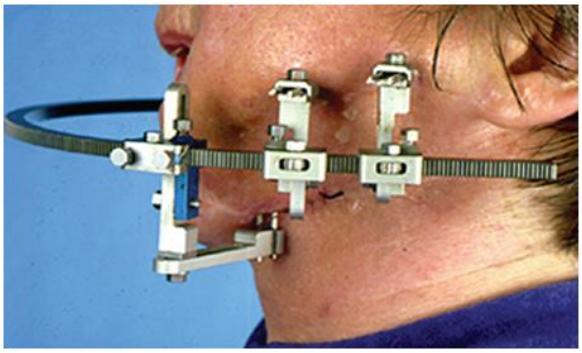

Figure 14: Example of an extra-oral mandibular TDDO device (Zapata, Elsalanty, Dechow, & Opperman, 2010)

[8] Consultation with Hendricks and Vicatos, 2011-2012.

2.7.2 ANCHORAGE OF THE DEVICE & STABILITY

The major factors affecting the mechanical integrity and stability of the distractor are the:

1. Manner in which the device frame is **anchored** to the surrounding bone.
2. Number, length and diameter of **anchorage screws**.
3. **Orientation** of the various components of the device and the effect thereof on the distraction vector.
4. **Material** properties of the device.

Anchorage of maxillofacial TDDO devices is commonly achieved in one of three ways: Bone borne, tooth-borne or a hybrid of the two. Tooth-borne and hybrid fixation are less secure and can damage the teeth and gums. Bone-borne anchorage, which uses fixation screws placed directly into native bone, provides the most stable anchorage condition. (Zapata, Elsalanty, Dechow, & Opperman, 2010)

Fixation screws are of two types: Anchoring screws (2.0mm to 2.5mm) that secure the distractor to the surrounding native bone; and the ***bone transport disc*** fixation screws (1.5mm) used to secure the distracted bone segment to the mobile part of the device. Depending on the application and the integrity of the surrounding bone, Elsalanty recommends using more than 4 screws in the bone transport disc to mitigate tipping of the disc during distraction (Elsalanty, et al., 2009).

The **orientation** of the device during installation dictates the distraction vector to be followed by the ***bone transport disc***. Thus, the ideal device should provide the surgeon with maximum versatility in device placement, and adjustment of the vector after device installation (Meyer, Kleinheinz, & Joos, 2004).

A review of **materials** is presented in section 2.8.

2.7.3 ACTIVATION MECHANISMS: CASE STUDIES

The literature presents four types of activation mechanism used historically in TDDO:

- Screw-type with or without a traction wire (Figure 15)
- Rack-and-pinion, or worm-rack
- Spring-type
- Hydraulically driven

For intra-oral TDDO in the maxilla, the literature suggests screw-type and traction wire devices as the most appropriate solutions. Spring and hydraulic appliances are impractical for reasons of size, reliability and limitations on the extent of distraction. (Zapata, Elsalanty, Dechow, & Opperman, 2010), (Wang, Chen, Ping, & Yan, 2012)

Romanyk (Romanyk, Lagravere, Toogood, Major, & Carey, 2012) cites the main benefit of screw-type devices as the simple and well-understood mechanics. The pitch of the screw defines the relationship between rotation and axial displacement, and thus the strain induced. Since distraction-induced healing is strain- rather than stress-related, it is preferable that the operator has control over the distance by which the callus is stretched (strain), rather than the force applied (stress). On the contrary, spring devices provide control of the force applied (Meyer, Kleinheinz, & Joos, 2004). An important benefit of screw-type devices is that they can be easily scaled to suit the size and loading requirements of a range of applications, whereas the scalability of spring-type devices is limited.

Hydraulically powered devices were generally found to be impractically large and required an auxiliary device to pressurise and meter the working fluid.

In the past, screw-type devices have been supplemented with a traction wire. A power-screw mechanism, equal in length to the distraction trajectory, is situated at least partially outside of the mouth. This mechanism is known as the ***activation arm***. It generates a displacement which is transmitted to the ***transport disc carriage*** by the traction wire. Such devices require protrusion through the skin and are thus prone to infection and scarring. In the case of mandibular devices, where the bulk of the device is submerged in the tissues, where it cannot be accessed directly, it is desirable that the activation arm be available extra-orally (see Figure 12).

Figure 15: Traction-wire device (Elsalanty, et al., 2009)

For power-screw type devices, the literature reports distraction lengths of up to 50mm with or without the traction wire adaptation, and by incorporating a customisable guide-rail both formats have facilitated ***bifocal*** distraction in the mandible.

In the case of certain screw-type devices, the actuation screw mechanism and the guide rail can be incorporated into a single unit, substantially reducing the size of the device. Elsalanty (Elsalanty, et al., 2009) proposes one such device for mandibular distraction (Figure 16 & Figure 17). The device consists of a guide rail, formable to the desired trajectory, and a transport disc carriage. The guide rail features a toothed rack on the outer surface (Figure 16A). A worm-screw housed within the transport disc carriage engages with the toothed rack, providing the traction mechanism.

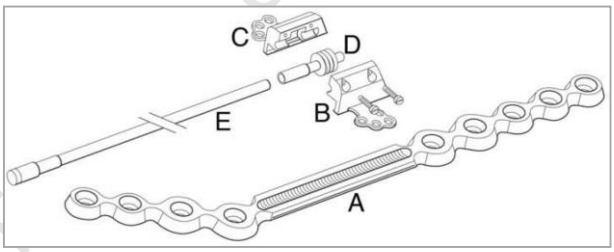

Figure 16: Exploded view of device proposed by Elsalanty. (Elsalanty, et al., 2009)

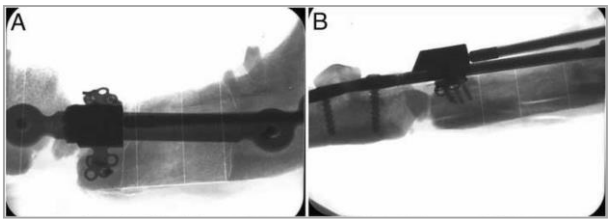

Figure 17: X-ray images of implanted device: straight vector and high profile. (Elsalanty, et al., 2009)

In a study of thirteen beagle dogs, Elsalanty's report concluded that the toothed guide-rail mechanism provided adequate stability of the ***bone transport disc*** and accurate control of distraction.

2.8 IMPLANTABLE MATERIALS: A REVIEW

The choice of suitable materials is a critical consideration in the design of implanted medical devices. Materials must be suitable for close and prolonged contact with human tissue in warm, saline conditions (Newson, 2002).

According to Elias (Elias, Lima, Valiev, & Meyers, 2008), the most important criteria for medical implant materials are biocompatibility and corrosion resistance. The popular biomaterials are titanium alloys, stainless steel alloys and resorbable polylactide polymers.

2.8.1 TITANIUM ALLOYS

Titanium offers the highest level of biocompatibility and corrosion resistance, causes minimal image scatter in CT scanning and is compatible with ultra-sound and magnetic resonance imaging (Cheung, Chow, & Chiu, 2004). Five grades of titanium have been developed specifically for dental implant applications, specified according to ASTM as grades 1 to 5 (Elias, Lima, Valiev, & Meyers, 2008). More recently Grade 23 has been introduced, as a higher purity version of grade 5, and is considered the ultimate material for dental implantation due to its high bio-compatibility, and good fatigue strength.

2.8.2 STAINLESS STEEL

Stainless steels for medical applications are specified in ISO standards 7153-1 for non-implant devices and 5832-1 & 5832-9 for implants. Stainless steels are desirable for their good corrosion resistance, but with the development of highly biocompatible titanium alloys, stainless steel is seldom used for long-term implants.

2.8.3 RESORBABLE MATERIALS: POLYLACTIDE

Use of resorbable materials is growing in maxillofacial reconstruction, as this often removes the need for secondary surgery to remove plates and screws. The literature reports cases of distraction systems that can be removed non-invasively after treatment, by making use of resorbable materials.

Polylactide is the most widely-used of these materials in maxillofacial applications. It begins to dissolve within 6 weeks and is fully resorbed within 12 months; with chemical modification the material can be engineered to last multiple years. It has been used in maxillofacial transport distraction procedures where forces present are similar to those in the mandible and maxilla (Cheung, Chow, & Chiu, 2004). However, polylactide loses strength long before it loses volume (Burstein &

Williams, 2004), leading to ongoing concerns about the reliability of resorbable materials for distraction applications. Also, it is reported that during resorption these materials can fragment into large particles, which are often extruded through the skin, causing severe irritation and discomfort (Burstein & Williams, 2004).

A controlled trial of resorbable vs. titanium alloy distraction devices by Cheung (Cheung, Chow, & Chiu, 2004) found:

1. A high incidence of broken screws and fixation plates in the resorbable group only.
2. Customisation of devices in the resorbable group was more time-consuming than that of the titanium-alloy group.
3. Placement of resorbable screws took twice as long as in the titanium-alloy group.
4. Resorbable screws required pre-tapping of the drilled hole, whereas the titanium-alloy screws were self-tapping.

3. DEFINING AND FORMULATING THE DESIGN PROBLEM

3.1 PROBLEM DEFINITION

According to the medical collaborator[9] no device currently exists for Transport Disc Distraction Osteogenesis (TDDO) in the maxilla that is capable of anterior-to-posterior distraction along a three-dimensional curvilinear vector, for repair of segmental defects of the maxilla.

Maxillary TDDO is a pioneering method of treatment never before applied in humans. While new theories constantly add insight into the basic mechanisms of TDDO, the exact mechanical requirements are not fully understood. Furthermore, the literature generally only discusses cases in the mandible, with no reference to TDDO in the maxilla. While the biomechanics of mandibular and maxillary TDDO are similar, there are distinct practical differences between the two procedures, particularly in the ergonomic requirements of the devices that facilitate each procedure.

Given the lack of definite information pertaining to maxillary TDDO, this project involved the parallel evolution of both the physical design of the new device and its functional requirements; both clinical- and patient-related. Clinical observations, patient feedback and recommendations from expert collaborators provided valuable insight into the diverse needs of both the surgeon and patient.

Over the course of this project, the multifarious design considerations were distilled and formulated into a coherent set of requirements – both quantitative and qualitative. This is presented in the form of a Product Requirement Specification in section 3.3.

[9] Dr Rushdi Hendricks, B.Ch.D, M.Ch.D

3.2 The Medical Environment

It was a priority of this project to develop a solution that can be easily adopted by surgeons and is compatible with the medical environment. It was thus necessary to consider the practicalities of surgery, existing technology and tooling and how the device affects the experience of the patient.

What follows is a discussion of the problem as it was understood at the outset of the design process. These concepts were based on the literature and consultation with the medical collaborator[10].

3.2.1 Surgical Installation of the Device

While the application of TDDO to the maxilla is unprecedented, it has been used successfully in the mandible. The basic surgical protocol for installation of mandibular TDDO devices generally involves the following procedure:

Pre-operatively:

1. Using life-sized models of the patient's skull, the key aspects of the surgery are planned, including customisation of the device. (see section 3.2.2)

Intra-operatively:

2. The accuracy of any pre-operative planning is checked and adjusted if necessary.
3. The locations of bone anchorage screws are demarcated as well as the osteotomy line for the transport disc.
4. The transport disc osteotomy is performed, creating a distinct vital bone segment.
5. The device is installed; anchored to the native bone place using bone screws.
6. The transport disc segment is affixed to the bone transport unit using bone screws.
7. Once installed, the distraction device is activated to ensure that there is visible separation at the transport disc osteotomy.
8. The distraction device is reversed to bring the osteotomy surfaces back into forced contact so that healing can begin.
9. The osteotomy is allowed to heal at the discretion of the surgeon (usually 1 week) to allow formation of healthy callus.

[10] Dr Rushdi Hendricks, B.Ch.D, M.Ch.D

3.2.2 PRE-OPERATIVE PLANNING AND PREPARATION

Maxillofacial reconstruction demands accurate reconstruction of both facial functionality and geometry, where even the slightest disparities can compromise the aesthetics of the result (Saunders & Lee, 2008). In TDDO, this relies upon the anatomical accuracy of the distraction trajectory prepared by the surgeon. In addition, the points of anchorage to the native bone must be stable and structurally sound to prevent excessive ***micromotion*** at the fracture site (See section 2.2).

Modern computed tomography (CT) and rapid-prototyping technology provide surgeons with accurate full-scale cranial models, facilitating detailed pre-operative surgical planning and device customisation, thereby enhancing the predictability of surgery.

This facility separates the planning aspect from the surgical installation procedure, reducing operating time, patient trauma and cost, while affording the surgeon additional time for hardware customisation. (Wang, Chen, Ping, & Yan, 2012), (Burstein & Williams, 2004), (Meyer, Kleinheinz, & Joos, 2004)

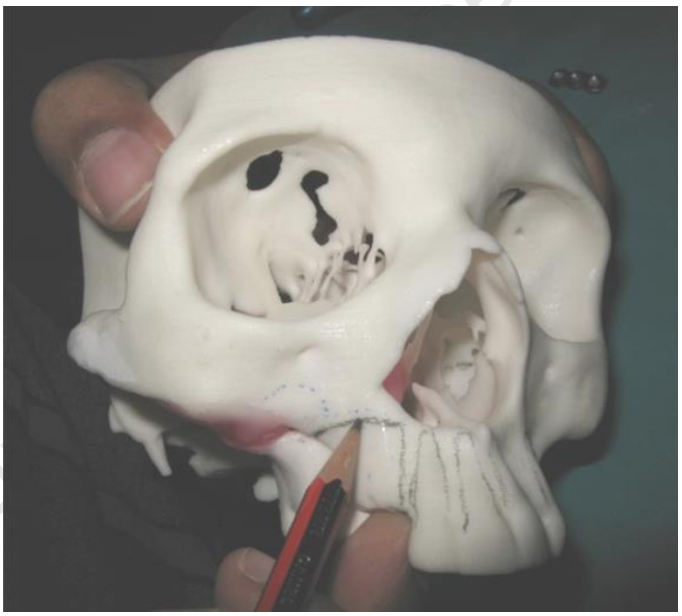

Figure 18: Pre-operative planning of surgery facilitated by CT imaging and rapid-prototyped cranial models.

3.2.3 DESIGN FACTORS

The surgical protocol in section 3.2.1 hints at the diversity of factors to be considered:

1. Case-specific customisability – adapting the device to the individual case.
2. Intra-oral access – the device must be installed and activated within the oral confines.
3. Stability – the influence of the intra-oral environment.
4. Patient experience – Comfort, compliance and postoperative oral hygiene.

3.2.3.1 CASE-SPECIFIC CUSTOMISABILITY

Maxillofacial geometry can vary considerably between patients depending on gender, age and ethnicity. Furthermore, the invasive and unpredictable nature of facial bone cancer produces defects that differ widely in severity and location. Thus, the ideal TDDO device should cater for a variety of facial geometries and defects, provided that adequate bone stock is available adjacent to the defect, from which to harvest a substantial and viable bone transport disc.

In order to accommodate the range of users, the device should be customisable by the surgeon according to the needs of the individual. This can be achieved by employing modular and/or customisable components; however, such customisation poses a risk of damage. To mitigate such risks, the customisation should be isolated to the relevant component, thereby ensuring that other critical components are not inadvertently affected. Knowing that the dexterity of individual surgeons varies, customisation should not demand highly trained personnel. [11]

This project focuses on segmental defects in the maxillary alveolar ridge. These defects can be 20mm or more, measured circumferentially along the outer surface of the alveolar ridge, and can extend to the nasal floor (see Figure 8c). Discussion with the medical collaborator revealed that a two-dimensional curvilinear trajectory was sufficient to reproduce the normal functional geometry of the maxilla; i.e. an arch within a flat plane. The minimum curvature of the maxillary alveolar ridge varies from 25mm to 30mm[12]. The device should cater for a 25mm minimum radius of curvature.

3.2.3.2 INTRA-ORAL ACCESS

The installation, activation and ultimate removal of intra-oral devices requires manipulation of various components and tools within the oral cavity. The design of the device, its position and orientation

[11] Consultation with Hendricks and Vicatos, 2011-2012.
[12] 25-30mm curvature is based on measurements from CT images in various publications and stereo-lithographic models sourced from the medical collaborator.

must consider the tight constraints of the surrounding facial anatomy. Poor intra-oral access is exacerbated by the effect of ***trismus*** (reduced ability to separate the jaws). In maxillofacial surgery the main causes of ***trismus*** are prolonged contact with foreign bodies and infection. ***Trismus*** can be reduced by administering muscle relaxant and is thus not a prohibitive problem.

During its working life, the device should be accessed through the mouth without any protrusion through the skin. According to the literature, extra-oral activation may provide easier access, but this benefit is far outweighed by the reduced scarring and superior patient comfort offered by intra-orally activated devices.

3.2.3.3 STABILITY

In order for the device to function satisfactorily, it must provide a stable mechanical environment that promotes proper bone formation. The device must therefore be capable of withstanding certain loads within the mouth, which arise largely from the actions of the patient. Given the large magnitude of bite forces, a level of patient co-operation must be expected, trusting that the patient will take due care not to behave in any way that could compromise treatment or cause damage to the device. Such assumptions are common in any long-term medical treatment. Nonetheless, the device should withstand disturbance from the tongue, as this is very often unconscious and therefore inevitable.

3.2.3.4 PATIENT EXPERIENCE

Patients are required to live with the device installed for up to 6 months, making comfort a primary concern. For hygiene reasons, the prevalence of food-trapping voids in or around the device should be minimised, as they provide sources of infection and foul odours. In general, the treatment protocol includes a thorough hygiene regimen, involving oral brushing, rinsing and the use of water-jet oral cleaning systems such as the Waterpik™, if necessary.

Considering the long duration of treatment, the presence of the device within the mouth should not compromise normal functions, including eating, drinking, breathing, speaking and sleeping. Furthermore, any potentially abrasive or intrusive surfaces should be eliminated. In the interests of social interaction, it is highly desirable that the device is not visible externally.

3.3 PRODUCT REQUIREMENT SPECIFICATION

This section presents a summary of the design requirements of the maxillary Transport Disc Distraction Osteogenesis (TDDO) device. These requirements were based on a review of the literature, a survey of existing devices and consultation with the medical collaborator[13]. While initially qualitative – pertaining to ergonomics and basic functionality – these requirements evolved to define quantifiable force and strength requirements as the project progressed.

Quantitative criteria were included for the purpose of verifying the strength and reliability of the device. In general, these were not considered to be formal design criteria from the outset, as the early design was based on qualitative ergonomic requirements, i.e. dimensions were originally based on user convenience, rather than optimised for strength. It will be shown in section 5.2 that the dimensions of the device, as determined by ergonomics, are also sufficiently large in terms of its strength and reliability criteria.

3.3.1 SCOPE STATEMENT

This project involves the development of a device that achieves stable and controlled intra-oral transport distraction of a bone fragment along a planar curvilinear trajectory for reconstruction of unilateral defects of the maxilla in adults.

Treatment of unilateral maxillary tumours usually requires the removal of the entire posterior segment of the maxilla, resulting in a void at the rear of the affected side of the maxilla. This void implies a lack of bone on which to anchor the posterior end of the device, which must be accounted for by the method of anchorage of an effective distraction system.

The TDDO system should address the requirements of each stage of treatment, from pre-operative planning, through installation and daily operation, to removal of the device. The availability of auxiliary tooling has to be considered.

The responsibility of device installation and removal rests with a qualified surgeon.

[13] Dr Rushdi Hendricks, B.Ch.D, M.Ch.D

3.3.2 FUNCTIONAL CAPABILITIES

1. The device should accommodate patient-specific two-dimensional curvilinear[14] geometry, such that:
    a. A distraction path of up to 100mm length can be achieved, and
    b. A minimum radius of curvature of 25mm can be followed.
2. The device must secure the bone transport disc with at least 4 bone anchorage screws.
3. Installation and removal is to be as simple as possible.
4. The device must make use of existing installation/activation tooling, wherever possible.
5. The device should permit adjustment of the distraction vector at any stage during the surgical installation procedure.
6. The device should be capable of being driven along the trajectory in both the forward and reverse directions. [15]
7. Actuation of the device should require torque of no more than 20 Ncm. [16]
8. The device should produce an axial distraction force of at least 60 N. (See section 2.5.3)
9. The device must endure a cyclic distraction force for at least 500 cycles.
10. The device must withstand erratic tongue forces of up to 12 N vertically and 16 N laterally (See section 2.5.4).

3.3.3 SAFETY, USER-INTERFACE AND PATIENT EXPERIENCE

A review of existing devices and recommendations in the literature suggest the following:

11. The device should attach directly to native facial bone, with minimal intrusion on the local anatomy, such as disturbance of dental roots or irritation of soft tissue.
12. The device should be manually activated intra-orally, requiring no penetration of the skin.
13. Activation should be simple enough to be carried out by the patient or the patient's minder, in a non-clinical environment such as in their own home.

[14] Two-dimensional curvilinear refers to a curved line on a flat plane.
[15] It is assumed that 10mm of retraction is sufficient to position the bone transport disc during the initial latency period. According to Hendricks, in practice, retraction of no more than 5mm has been observed.
[16] 20 Ncm value is based on the activation torque of existing devices and provides a bench-mark.

14. Basic oral function must not be hindered, i.e. the device must not interfere with:
    a. the passage of air and food.
    b. movement of the tongue.
    c. movement of the mandible.
15. The device should not be visible externally.
16. The device should not protrude more than 10mm from the outer maxillary contour [17]
17. Suitable implantable materials should be used for all tissue-submerged components.
18. The device must withstand normal sterilisation procedures.

3.3.4 MAINTENANCE

19. The implanted device must endure a working life of at least 6 months.
20. The device should require no maintenance during its working life.

[17] 10mm dimension is based on qualitative comfort testing by author on consenting subjects.

4. DESIGN AND DEVELOPMENT

The design and development process aimed to produce a fully functional device, encompassing the various mechanical and ergonomic requirements as defined in the PRS in section 3.3. This was achieved through an iterative process of design, manufacture, testing and refinement.

The development and refinement process saw the design and manufacture of three successive prototypes:

1. *Version 1 (V1)*: Self-cutting traction mechanism (see section 4.3)
2. *Version 2 (V2)*: Metallic worm-rack traction mechanism (see section 4.4)
3. *Version 3 (V3)*: Metallic worm-rack traction mechanism with base plate (see section **5**)

Each of these devices was implemented clinically to treat large defects of the maxilla. During each case, observation of the surgical procedures and the device in practice provided crucial insight into the needs of the patient and surgeon; directing iterative refinement of the device in both form and function. Coupled with an ongoing research into the details of maxillofacial TDDO, these clinical observations provided a robust understanding of the mechanical and ergonomic requirements of the TDDO procedure.

The following section presents the development of the distraction device from a basic concept into the fully-functional *V3* device, via the intermediate *V1* and *V2* prototypes. The key design decisions, successes and failures are documented, as well as the observations and outcomes of clinical treatment.

4.1 BASIC FORMAT OF THE DEVICE

Based on various recommendations in the literature (see section 2), a survey of existing maxillofacial TDDO devices, and consultation with the medical and engineering specialists, it was established that the device should include the following basic elements:

1. A *transport disc carriage (*or *locomotive)* that supports and guides the transport disc.
2. A *traction mechanism* that actuates distraction of the transport disc carriage.
3. A *trajectory rail* that defines the path of the transport disc carriage.

4.2 TRACTION MECHANISM: SOLUTION CONCEPTS

Guided by the principles described in section 3, various solution concepts were generated for the basic actuation (or traction) mechanism. This section presents a brief summary of the three most promising solution concepts considered.

4.2.1 SIMPLE WORM-RACK MECHANISM

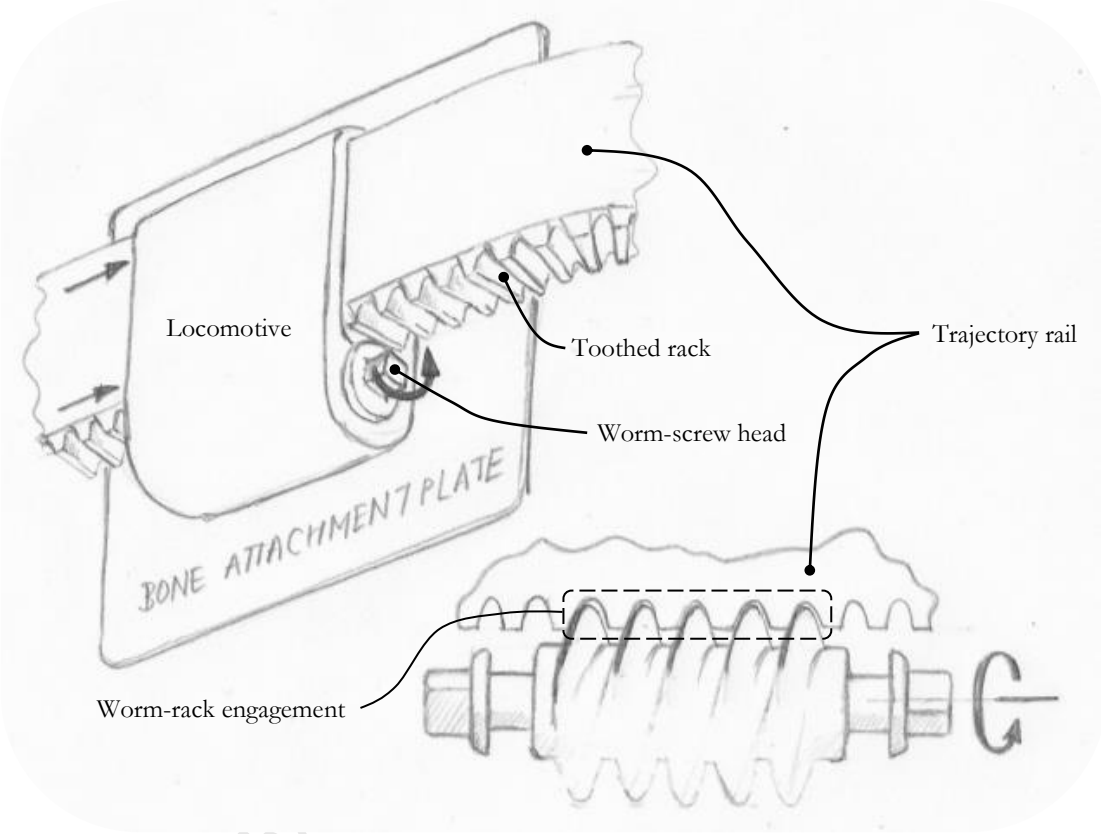

Figure 19: Sketch of worm-rack solution concept, with detail of the worm-rack engagement (hand-drawing by author).

The worm-rack concept, illustrated in Figure 19, involves a worm-screw that engages with a toothed rack on the narrow edge of the trajectory rail. The worm-screw is housed within the locomotive. By rotating the worm-screw the locomotive is propelled linearly along the trajectory rail. The trajectory rail can be bent and trimmed to form the desired distraction vector according to the geometry of the individual case. Aside from the rack teeth, the trajectory rail has a continuous rectangular cross-section along its length.

It is foreseen that ending of the trajectory rail would distort the rack teeth, causing the tooth spacing to widen on the outside of bends and narrow on the inside. In order to tolerate this distortion, the profiles of the engaged worm and rack would require a suitable amount of intentional play to be incorporated.

4.2.2 SELF-CUTTING WORM AND PLASTIC TRACK

This mechanism utilises a sharp-toothed worm-screw that cuts notches into a closely-coupled plastic track, thereby progressively forming a corresponding 'rack' in the previously virgin plastic (see Figure 20). When rotated, the worm 'crawls' along its track in the manner of a hose-clamp. The plastic track is bonded to a metallic trajectory rail, which provides the necessary rigidity to support the locomotive. The trajectory rail and plastic track can be bent and trimmed to form the desired distraction vector, according to the requirements of the individual case.

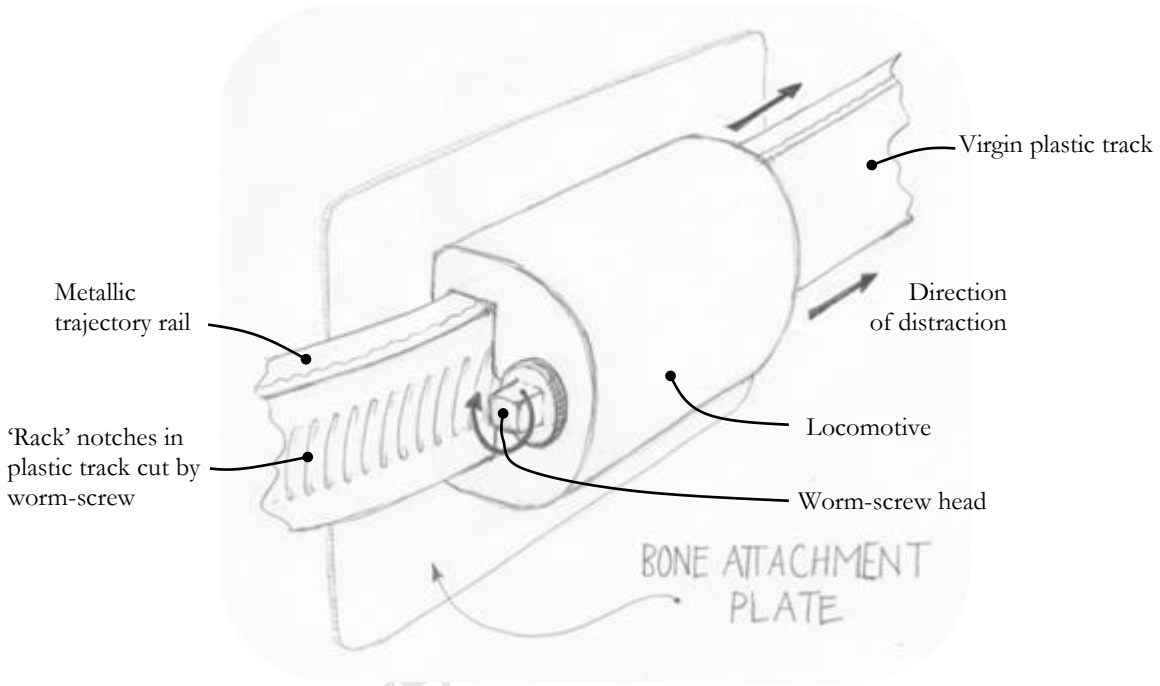

Figure 20: Sketch of self-cutting worm solution concept (hand-drawing by author).

In principle, the capability of the self-cutting concept to progressively form a unique corresponding rack in the plastic track accommodates potential irregularities in the trajectory rail and elegantly overcomes the trajectory rail distortion issue described in section 4.2.1.

4.2.3 DUAL-RAIL AND STRADDLED WORM

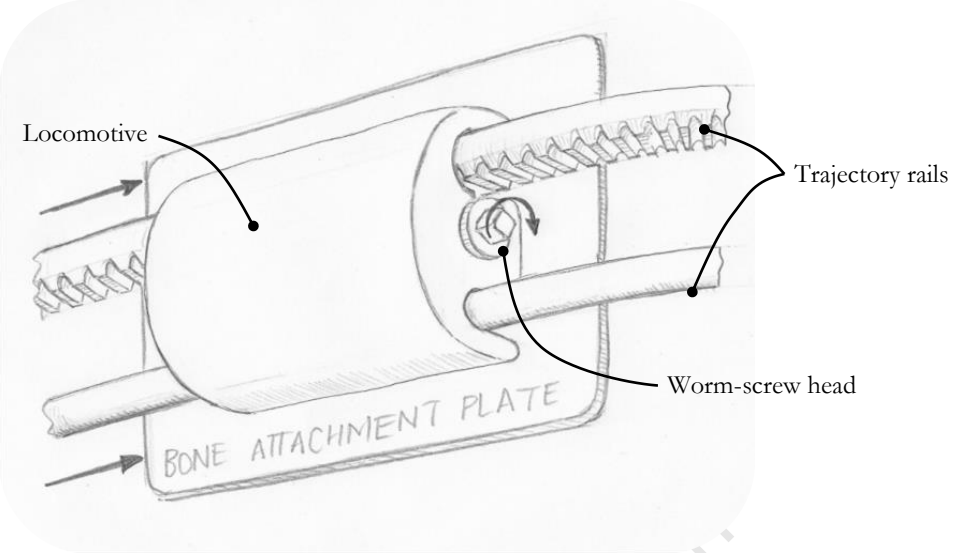

Figure 21: Sketch of dual-rail solution concept (hand-drawing by author).

This concept involves a pair of parallel metallic trajectory rails with a worm-screw housed between the two, as illustrated in Figure 21. One of the trajectory rails incorporates a toothed rack for engagement with the worm-screw, and the second rail provides additional stability and guidance. A variation of this concept utilises the plastic self-cutting mechanism described in section 4.2.1.

The benefit of this arrangement over the single trajectory rail is that the spaced trajectory rails provide a wider footprint for more stable constraint of the locomotive. On the other hand, this mechanism poses several significant problems: It requires accurate matching of the two trajectory rails, incurs the additional cost of more components and a more complex design, and the second rail implies a bulkier device than the two alternative concepts.

4.2.4 CHOSEN CONCEPT: SELF-CUTTING WORM AND PLASTIC TRACK

The 'self-cutting' concept originated in an undergraduate proof-of-concept study[18], wherein a basic prototype was manufactured and elementary strength tests yielded positive results. Having thus established its feasibility, it was decided that the versatility of the self-cutting concept demanded further investigation. The following sections demonstrate the evolution of the first prototype device, which employed the self-cutting concept.

[18] Available from author on request: "Device for Maxillary Transport Distraction Osteogenesis" by James Boonzaier.

4.3 VERSION 1 PROTOTYPE: SELF-CUTTING CONCEPT

The *V1* prototype focused on developing the self-cutting traction mechanism (see section 4.2.2) into a prototype device that would provide the required distraction force, adequate control and navigate the tight curvature of the maxillary anatomy. At this stage, ergonomic issues were not explicitly addressed as it was felt that these might detract from the primary focus on the traction mechanism.

4.3.1 V1: PROTOTYPE DESIGN AND DEVELOPMENT

During the first phase of development the design of the *V1* distractor evolved considerably, as illustrated by the initial and final designs in Figure 22 & Figure 23, respectively. In all its forms, the *V1* prototype consisted of the following core elements.

1. A metallic ***trajectory rail*** – section 4.3.2.1
2. A plastic track that attaches to the ***trajectory rail*** – section 4.3.1.1
3. A ***locomotive***, which secures and directs the bone transport disc along the trajectory rail and houses the worm-screw traction/cutting mechanism – section 4.3.1.2
4. Two ***buttress plates***, which support the posterior end of the trajectory rail – section 4.3.2.2

The following sections present the refinement of these elements during the first phase of the development.

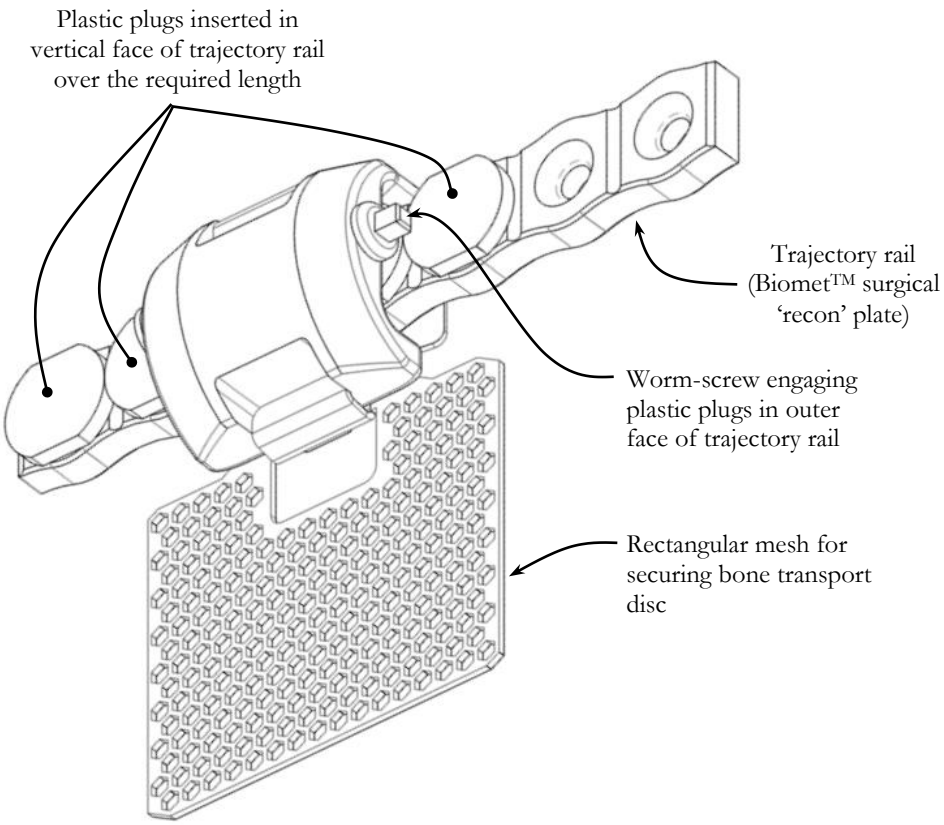

Figure 22: First conceptual version of the *V1* distractor as developed in the author's B.Sc. proof-of-concept project.

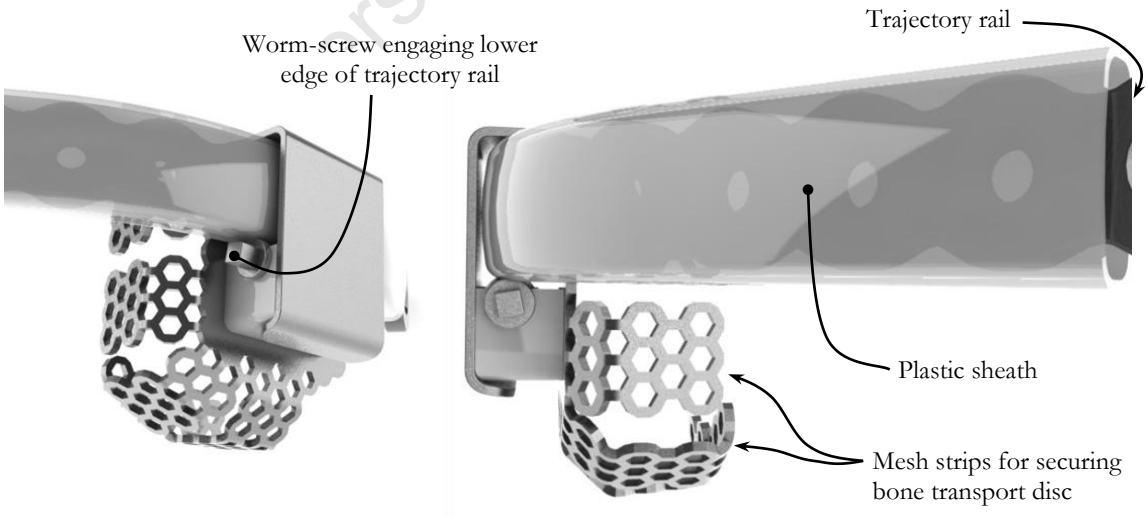

Figure 23: Final version of the *V1* distractor

4.3.1.1 PLASTIC TRACK: LOW DENSITY POLYETHYLENE

The plastic self-cutting concept employed a plastic track, in the form of a low-density polyethylene (LDPE) sheath, which was reinforced with a titanium trajectory rail. The LDPE track was problematic, as the material is susceptible to mechanical and thermal effects. The TDDO treatment protocol exposes the device to both of these in the form of:

- High-temperature sterilisation by ***autoclave***, and
- Forceful customisation of the device by bending and cutting.

It was therefore made a requirement that any plastic components should be separate, but attachable after customisation and sterilisation of the device. To this end, two distinct formats of plastic track were considered, both of which can be attached to the trajectory rail intra-operatively:

1. Multiple plastic plugs embedded in a metal rail (see Figure 22).
2. A single, continuous plastic tube on a metal rail (see Figure 23).

Figure 24 shows a photograph of a test model that was used to prove the viability of the self-cutting concept. This test model was used to establish the required depth of cut to produce the required traction force. The trajectory rail was provided by an existing mandibular reconstruction plate supplied by Biomet™.

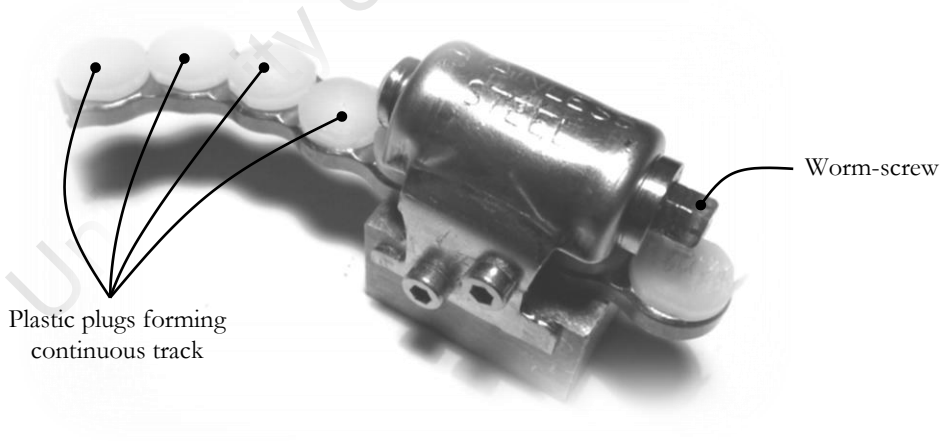

Figure 24: Apparatus for quantifying traction force of plastic self-cutting mechanism.

High- and low-density polyethylene specimens (HDPE & LDPE, respectively) were tested to establish whether the mechanism could produce the required distraction force. At this stage, the only known study of maxillofacial distraction force specified that a traction force of 35 N was adequate in mandibular TDDO (Robinson, O'Neal, & Robinson, 2001). Using this figure as a benchmark, it was

found that both high- and low-density polyethylene were suitable: HDPE provided a traction force of 100 N, and LDPE provided a traction force of 65 N before failure.

Although HDPE provided a significantly higher traction force than the LDPE, it had two shortcomings that made it impractical for the desired application.

- HDPE was found to be too rigid to accommodate the required curvilinear trajectories.
- HDPE offered particularly high resistance to rotation of the worm-screw, which raised concerns about the forces on the device and the bone transport disc during activation.

LDPE was therefore specified.

The initial design of the *V1* distractor engaged the worm-screw on the vertical face of the trajectory rail (see Figure 22). In this orientation, the worm-screw was located outboard of the trajectory rail, causing the device to intrude significantly on the adjacent cheek. In the interests of patient comfort, the design was revised such that the worm-screw engaged the trajectory rail on the inferior edge of the rail (see Figure 23) rather than its outer vertical face. This modification places the bulk of the device below the trajectory rail, in a less intrusive area.

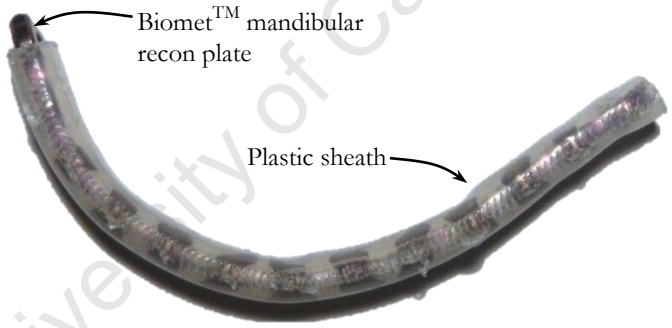

Figure 25: Biomet™ mandibular recon plate with LDPE 'sheath'.

To accommodate this modification the format of the plastic track was revised, abandoning the multiple plugs in favour of a single sheath (see Figure 25). The sheath, provided by LDPE tubing, can be slipped over the trajectory rail after it has been finally customised. Experimentation showed that in this format both the LDPE tube and trajectory rail could accommodate the necessary bend radius of 25mm.

The use of a single tubular track rather than multiple plastic plugs eliminated from the design the need for these small components and reduced the intricacy of the surgical installation procedure.

4.3.1.2 LOCOMOTIVE – HOUSING

The locomotive is the mobile element of the device that supports and guides the bone transport disc along the trajectory rail. The locomotive houses and constrains the worm-screw against the trajectory rail, ensuring that the thread of the worm-screw traction/cutting mechanism is reliably engaged with the plastic track.

The bone transport disc is secured to the locomotive by forming the integrated mesh strips (see Figure 26) into a cradle, as shown in Figure 23. This mesh cradle thus envelopes the bone fragment so that it can be firmly secured by screws from various angles.

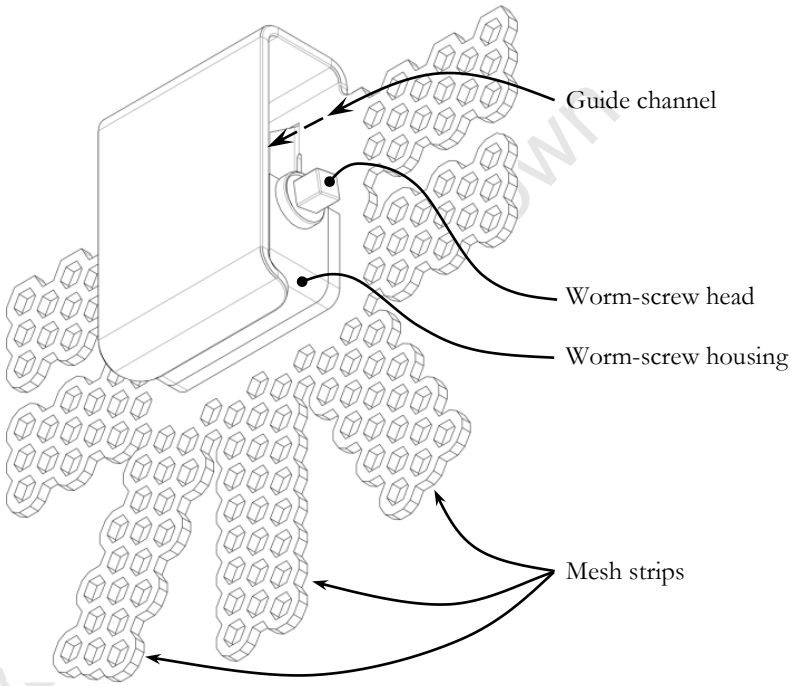

Figure 26: Labelled components of *V1* locomotive assembly.

The locomotive is stabilised by close contact with the trajectory rail that feeds through the ***guide channel*** (see Figure 26). According to the design specifications, the device must accommodate a radius of curvature of 25mm. In order for the locomotive to navigate along a trajectory rail with such tight curvature, the constraints between the locomotive ***guide channel*** and trajectory rail were relaxed. The sketches in Figure 27 illustrate an early study of locomotive stability using a protrusion on the inner surface (labelled A) which accommodates tight curvature, while maintaining at least two points of contact between the locomotive and trajectory rail.

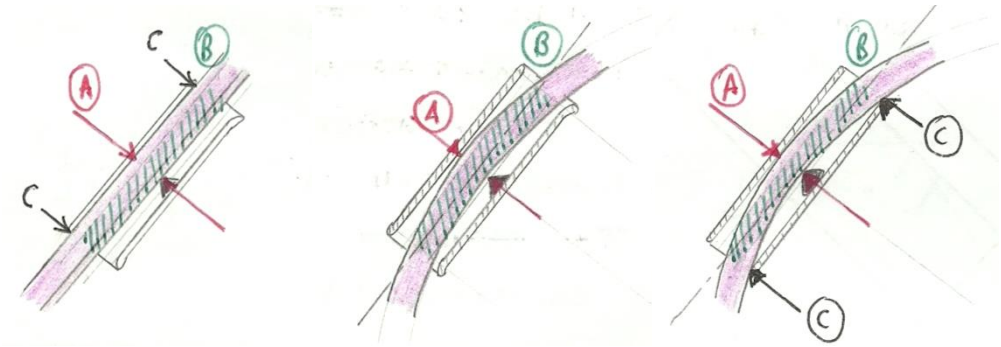

Figure 27: Early investigation of locomotive constraint and stability.

4.3.1.3 WORM ACTIVATION HEAD: COMPATIBILITY WITH EXISTING TOOLS

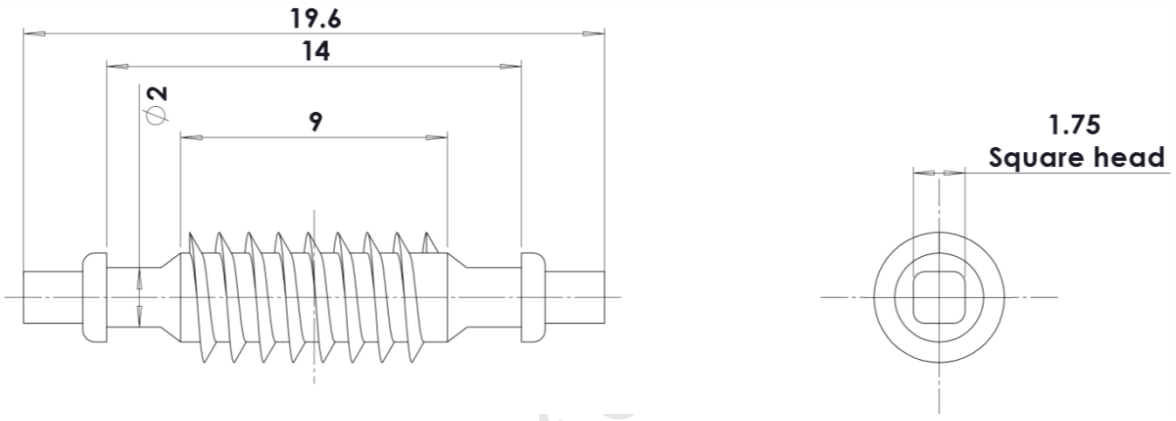

Figure 28: *V1* worm activation head design and overall dimensions (mm).

In an effort to utilise existing tools and to minimise cost, the worm activation head was designed to be compatible with an existing Biomet™ distraction driver, which prescribed a 1.75mm square head (see Figure 28). These distraction drivers were developed specially for activation of existing non-maxillary distraction devices, e.g. mandibular or midface distractors and are commonplace in surgery. The screwdriver in Figure 29 below provides a 'click' every 180° to promote accurate control.

Figure 29: Biomet™ 'click' distraction screwdriver

4.3.2 V1: Device Anchorage and Stabilisation

The device was supported and anchored using a scaffold of metallic plates and bone screws (see Figure 30), all of which were commercially available. These components had three distinct functions:

1. The ***trajectory rail*** supports and guides the locomotive along the desired path.
2. ***Buttress plates*** support and stabilise the trajectory rail.
3. Various sizes of **bone anchorage screws** anchor the device to the native bone.

Figure 30: Various Biomet™ plates and anchorage screws used in *V1* distractor.

4.3.2.1 Trajectory Rail – Biomet™ Mandibular Plate

At this early stage not enough was known about the rigidity, anchorage and patient comfort requirements of the trajectory rail to underpin the development of a unique proprietary rail. Thus, the *V1* device utilised the existing Biomet™ titanium mandibular reconstruction plate.

A compelling benefit of Biomet™ reconstruction plates is their 'locking head' feature, which binds the head of the bone anchorage screw to the plate, thereby locking its orientation. Locking head screws incorporate a tapered multi-start thread at the neck below the head of the screw. This threaded head engages with a corresponding internal thread at the entrance to the holes in the plate. By locking the screw to the plate, the screw is prohibited from shifting its orientation or position, improving the overall integrity of the bone-screw anchorage.

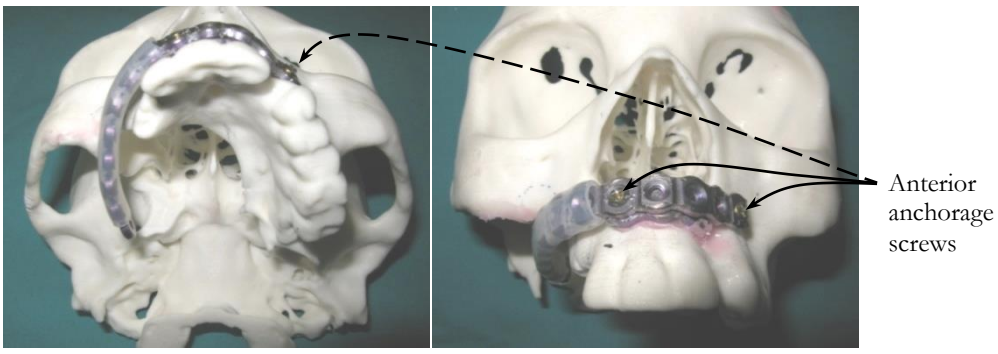

Figure 31: Inferior and frontal view of customised Biomet™ recon plate installed on a cranial model.

4.3.2.2 Stability of the Trajectory Rail – Zygomatic and Alveolar Buttress Plates

Figure 31 shows the trajectory rail anchored to the maxilla on a cranial model of a maxillectomy patient. This anchors the device at its anterior end. However, as mentioned in section 3.3.1, treatment of unilateral maxillary tumours usually involves total removal of the posterior segment of the maxilla, leaving a void in the bony anatomy to the rear of the mouth. In such cases there is no intact bone on which to anchor the posterior free end of the rail.

To address this, two 1.5mm Biomet™ plates were introduced to buttress the posterior end the rail against the adjacent zygoma and the opposite alveolar ridge (see Figure 32).

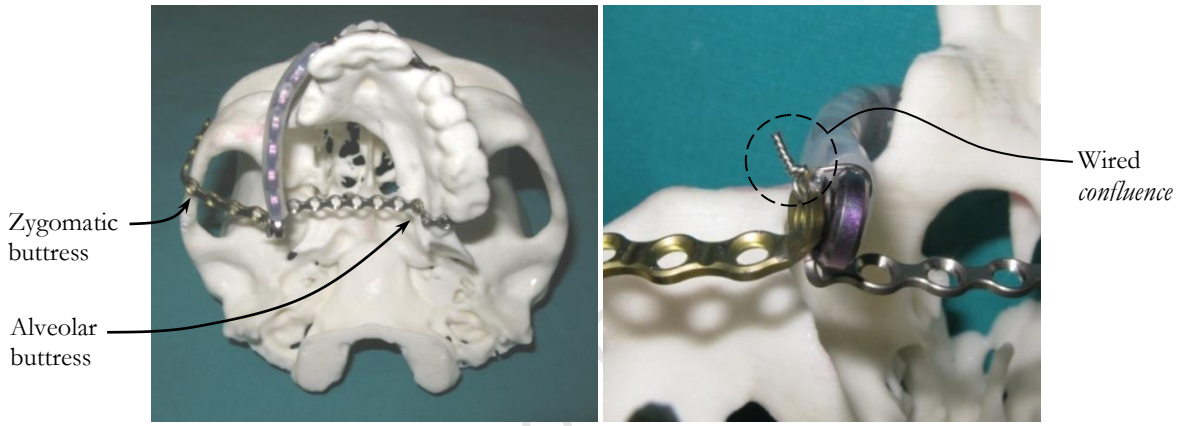

Figure 32: Trajectory rail and buttress plates installed on a stereo-lithographic patient model with a detailed view of the wired *confluence*.

These plates are referred to as the ***buttress plates***. The zygomatic buttress resists vertical- and the alveolar buttress resists horizontal deflection of the trajectory rail at its posterior end, providing three-dimensional stability.

For the *V1* prototype, the trajectory rail and buttress plates were linked by a simple wired joint using 0.6 mm titanium wire (see Figure 32, wired confluence), fed through the holes in the buttress plates and rail, and tightened by twisting. Titanium wire is commonly used in maxillofacial surgery and the wired ***confluence*** technique was endorsed by the surgeon for its simplicity and the relative ease-of-use within the confines of the posterior oral cavity.

According to the surgeon, this layout of the buttress plates is compatible with the maxillofacial musculature, although there were initial concerns raised about patient comfort.

4.3.3 V1: Laboratory Testing

Despite the encouraging results of preliminary testing (see section 4.2.4), there were concerns about the strength of the LDPE track. Laboratory testing of the manufactured *V1* prototype attempted to evaluate the effects of loading on the plastic track by simulating the basic aspects of the clinical distraction environment, namely:

1. Distraction along the worst-case curvilinear trajectory with the minimum expected bend radius of 25mm.
2. Distraction against a load of 60 N, representing the maximum callus stretching force.

4.3.3.1 Test distraction on worst-case trajectory

The *V1* device performed satisfactorily on the worst-case trajectory, encountering no significant mechanical interference. The distracted length was 40mm with a radius of curvature of 25mm. As expected, the sharp-threaded worm produced distinct ridges in the edge of the plastic track as it progressed. In general, these ridges were left intact, though some debris was observed – 0.2mm to 0.5mm thick and up to 3mm long. At some points, the worm cut through the LDPE track material completely.

The stability of the locomotive on the trajectory rail was unsatisfactory. 'Play' between the two components permitted the locomotive to rotate around the axis of the rail by ±10°. To address this stability concern, the constraint of the locomotive on the rail was tightened by removing the spacer shown in Figure 33. Thus, the rotational play was thereby reduced to less than ±5°.

Patient comfort was improved by countersinking assembly screws and removing any protrusions or sharp edges. Figure 33 presents the prototype before and after refinement.

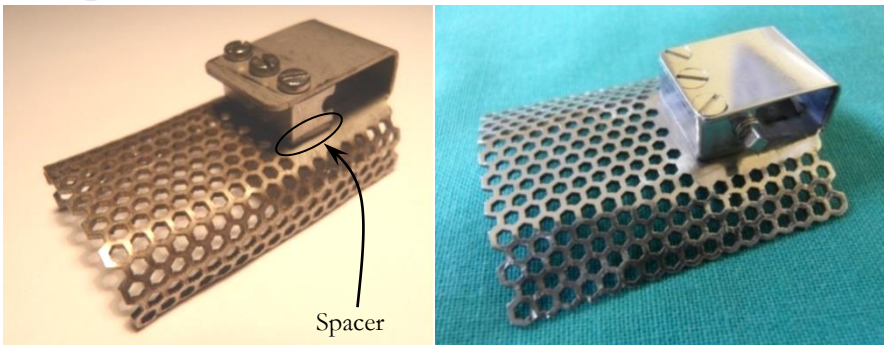

Figure 33: *V1* locomotive before and after refinement.

4.3.3.2 TRACTION FORCE TESTS ON A LINEAR TRAJECTORY

A linear distraction of 10mm was carried out under a load of 60 N, activated in increments of 2mm (=2 turns), allowing an hour between each activation. To achieve the desired 10mm distraction the device was thus activated 5 times. The 60 N load represented a safety factor of 1.7 over what was then considered to be the maximum expected distraction load of 36 N.

For the sake of brevity and compactness, full details of these tests are not presented here, but similar tests are described in detail in section 6.1.1, which describes testing of the most recent device version.

It was expected that 5 activations of 2mm each would displace the locomotive by a total of 10mm. However the actual displacement of the locomotive proved to be 9.1mm, i.e. 9% less than the intended distraction extent. This suggested that the LDPE track deformed under the load or that there was a degree of slippage of the traction mechanism. The clinical implications of this discrepancy is that in the worst case the daily distraction rate would be 9% less than intended, e.g. an intended distraction rate of 1.5mm, would actually generate 1.37mm per day. This was deemed acceptable by the medical specialist. Nevertheless, concerns were noted about the accuracy of control offered by the self-cutting concept.

Having satisfied the engineering aspects of laboratory testing, the *V1* device proceeded to clinical implementation.

4.3.4 V1: CLINICAL EVALUATION

The first clinical case involved the repair of a 45mm defect on the right side of the maxilla (see Figure 35), which was the result of surgical excision of an invasive tumour. This surgery led to a defect that included the majority of the hard palate, but left the nasal floor, the anterior segment of the maxilla and the zygoma intact.

A stereo-lithographic cranial model was produced which facilitated pre-operative customisation of the device and planning of the surgical installation procedure (see Figure 31 to Figure 34). This model was produced by the University of Cape Town based on CT images from the medical collaborator.

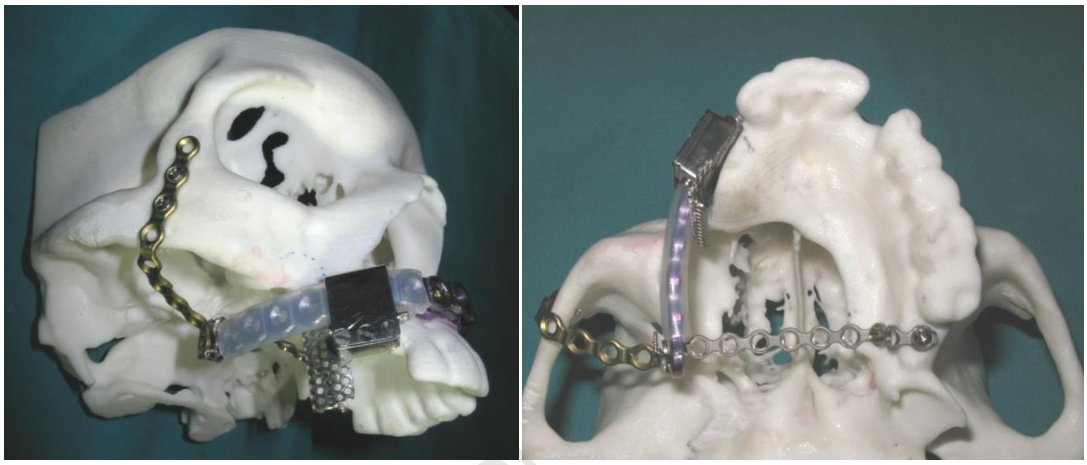

Figure 34: Oblique and inferior view of *V1* distractor installed on a cranial model

The timeline of treatment was as follows:

- 7 Sep 2011 Surgical installation of the device (see Figure 35 to Figure 37)
- 8-14 Sep 2011 Latent period to allow formation of the healing callus
- 14 Sep 2011 Distraction began
- 14 Sep – 3 Oct 2011 Daily distractions at a rate of 1.5mm per day
- 3 Oct 2011 Plastic track failure after 26mm of distraction (see Figure 38)
- 5 Oct 2011 Distractor repaired and distraction resumed (see Figure 39)
- 12 Oct End of active distraction
- 12 Oct – 1 Feb 2011 First period of regenerate consolidation
- 1 Feb 2012 Device removal
- 1 Feb – 5 Sep 2012 Second period of regenerate consolidation
- 5 Sep 2012 Placement of permanent dental implants in new maxillary arch.

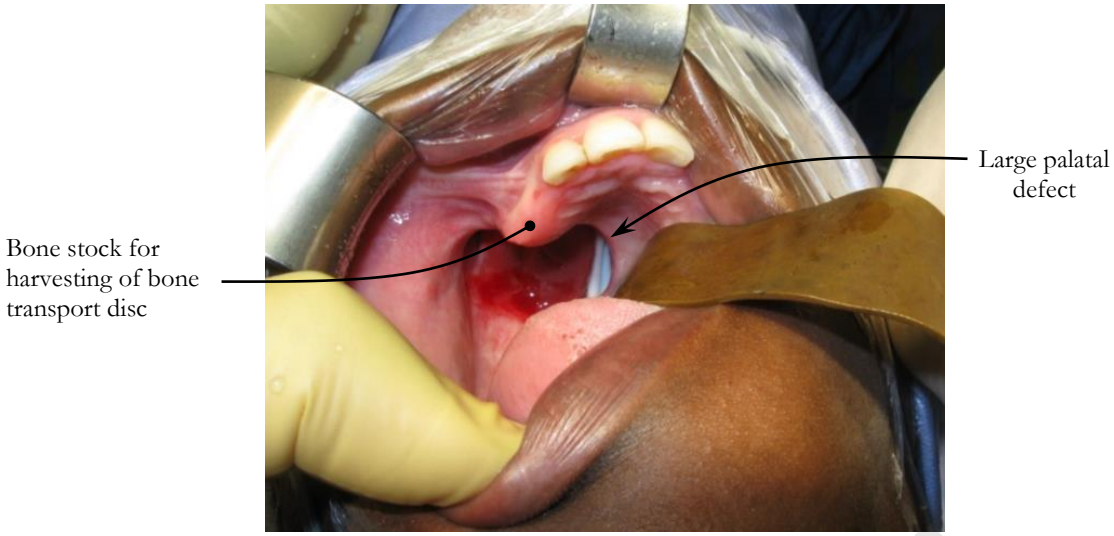

Figure 35: The defect before treatment.

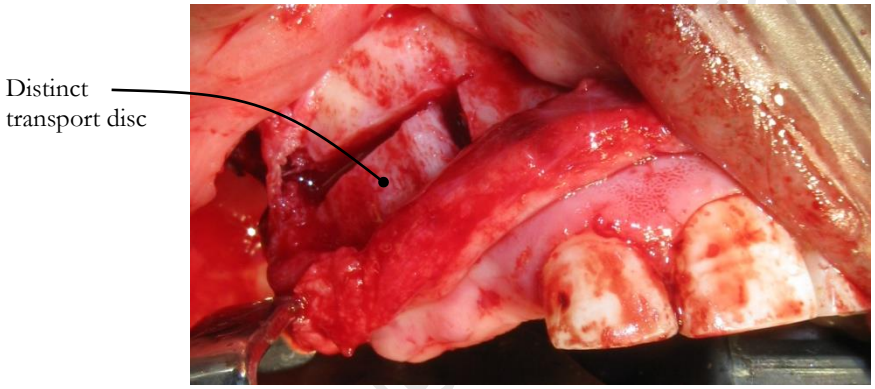

Figure 36: Surgical fracture to create transport disc.

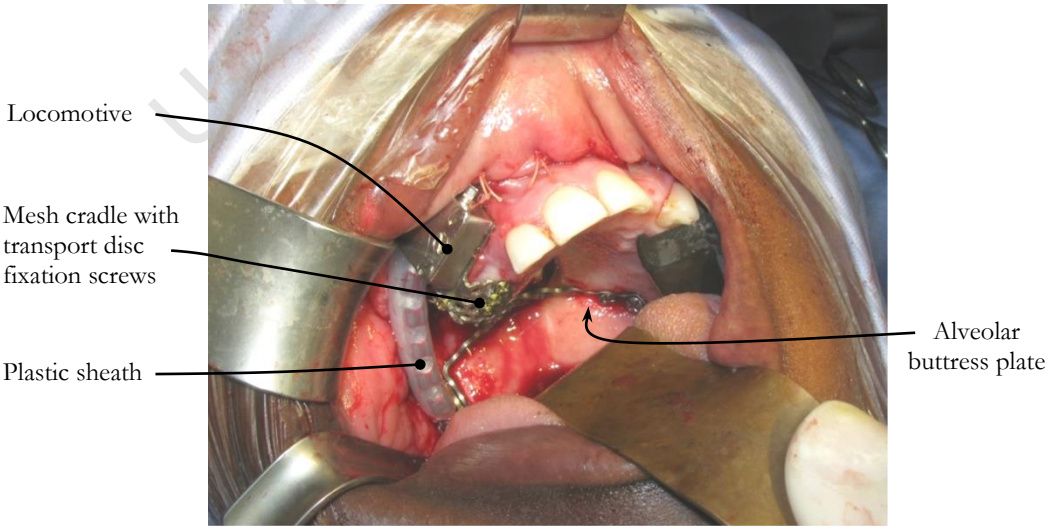

Figure 37: Installed *V1* distractor.

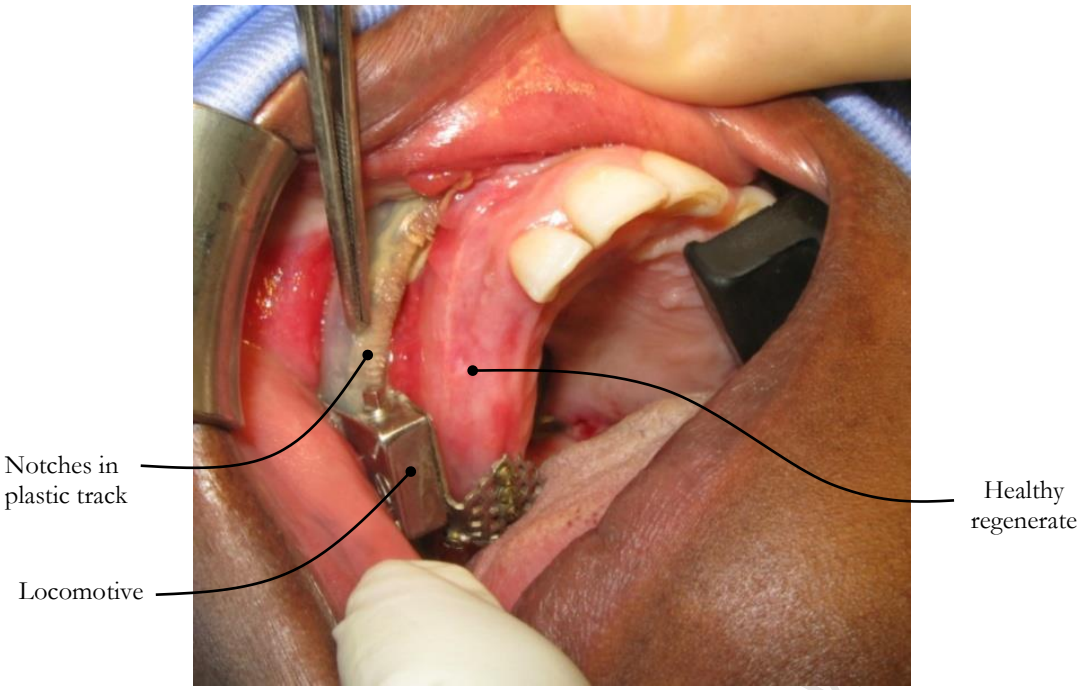

Figure 38: 3 Oct. 2011: Failure of device due to stripping of the plastic track; 26mm of healthy regenerate.

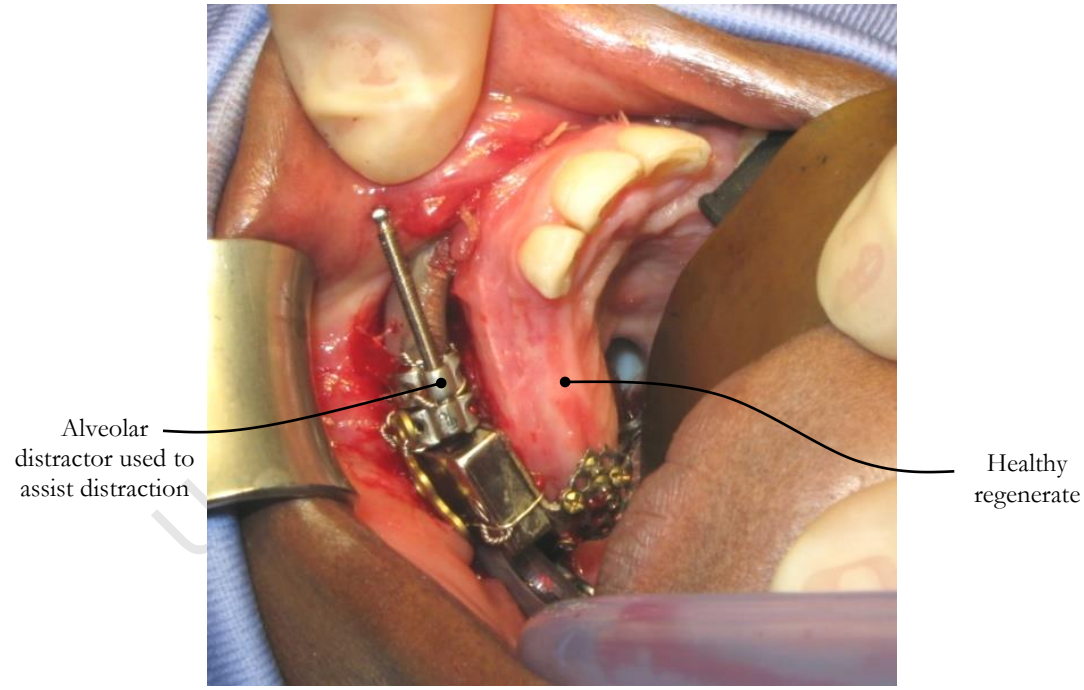

Figure 39: Repair using alveolar distractor; 26mm of healthy regenerate.

Installation of the first prototype on 7 September 2011 took 4½ hours. The following important observations were made during the installation procedure:

1. During surgical installation, the device underwent many adjustments in order to perfect the geometry of the rail and cradle and to designate secure fixation screw locations. These adjustments disturbed and sometimes damaged the plastic track. This was worsened by the protocol's demand for forward and reverse movement of the locomotive during installation and raised further concerns about the reliability of the track in delivering the necessary distraction force.
2. There were minor geometric discrepancies between the pre-operative cranial models and the real situation, particularly the surface contours of the frontal maxilla. This was attributed to the poor resolution of the original CT scan, which caused certain small details of the maxilla contours to be absent. In addition, the cranial models reproduce only the bone anatomy and give no indication of the surviving surrounding soft tissue. As a result, the device required more extensive intra-operative customisation than had been expected. The first draft design did not cater for repetitive attachment and removal of the trajectory rail for fine-tuning, having expected only minor adjustments to be made intra-operatively. Repetitive adjustment of the rail curvature disturbed the bone anchorage screws and compromised the rigidity of the installation.
3. During the installation procedure it was necessary to place metallic spacers between the trajectory rail and the anterior part of the maxilla (see Figure 40). These spacers accommodated the thickness of the soft tissues of the *gingiva*, and provided space for the locomotive to move freely without injuring the soft tissues.

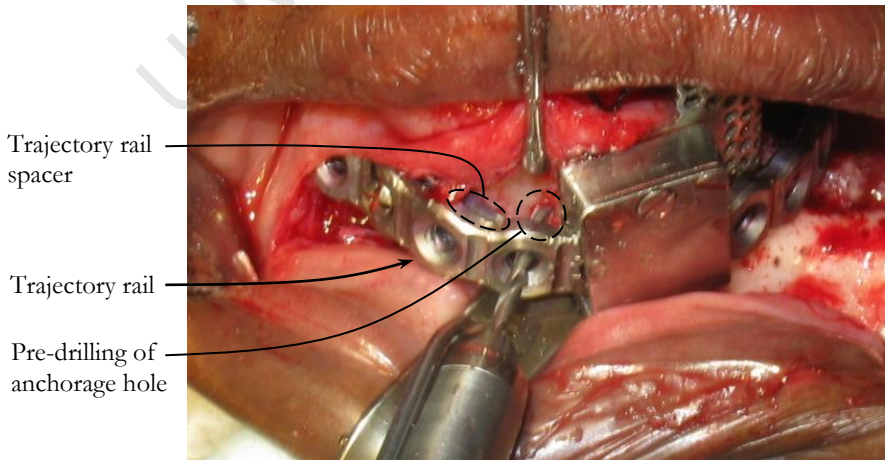

Figure 40: Photograph showing placement of trajectory rail spacers, and drilling holes for bone anchorage.

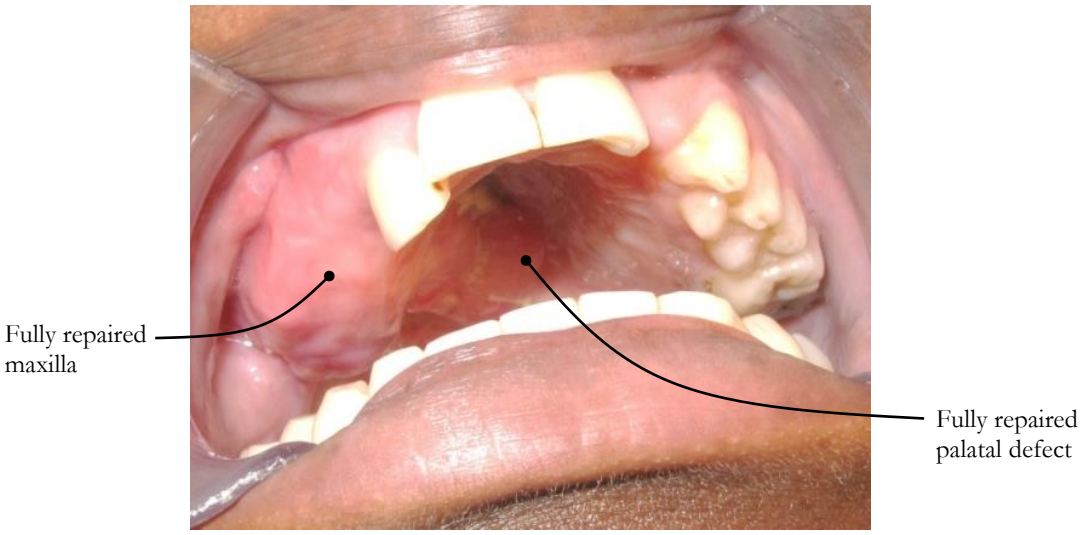

Figure 41: The fully repaired defect, 3 months after initial surgery

4.3.5 Discussion of V1 Clinical Performance

The *V1* prototype facilitated the repair of the clinical defect (see Figure 41), and experience during treatment provided valuable feedback on the design and insight into how it might be improved. Specifically, it provided a more refined understanding of the surgical protocol and the distraction force; it highlighted the need for improved ease-of-installation and removal and improved reliability of the traction mechanism.

Reviewing the performance of the *V1* prototype, the following shortcomings of the first clinical case were highlighted:

- The surgeon found that the transport disc mesh cradle was too rigid for easy shaping.
- The locomotive was not sufficiently stable on the rail after customisation. In particular, the locomotive was able to rotate excessively about the axis of the rail. This was due to the oval, rather than rectangular, cross-section of the LDPE tube.
- The wired *confluence* joint was easily customisable, and it was evident that there would be sufficient access for removal post-treatment. However, the surgeon felt that it was a crude solution which requires further development. The surgeon requested that a bolted or screwed fixation arrangement be developed.
- The void formed between the plastic tube and trajectory rail was a hygiene and infection concern.
- The self-cutting traction mechanism presented several intrinsic shortcomings. Fundamentally, the deformation and flow characteristics of the low-density polyethylene track material are inappropriate, given the magnitude of the expected loads. The strength provided by the plastic

track was found to be inconsistent; affected by irregularities in the trajectory and the inherent play between the locomotive and rail. It was observed that the depths of the grooves cut by the worm-screw varied unpredictably, whilst some segments of the worm-screw perforated the plastic tube entirely.

- An aspect of device functionality that was not properly considered when designing the *V1* distractor was the need to move the locomotive repeatedly over the same section of rail both forwards and backwards. As this was not foreseen in the design phase, it was not investigated during bench-testing, where it might have been discovered earlier. This deficiency alone rendered the plastic cutting concept inappropriate.

Therefore, future versions of the device should utilise of a rigid mechanism, rather than the plastic track used in the *V1* device, to generate the distraction force. This would ensure accuracy of distraction, predictable behaviour of the device and reliable force delivery.

- During the installation surgery, anchorage screws used to secure the anterior end of the rail to the maxilla were repeatedly inserted and removed in order to adjust the trajectory rail and transport disc attachment cradle. This compromised the integrity of the bone-screw anchorage and it was suggested that future versions should allow repeated attachment and removal of the trajectory rail without disturbing anchorage screws. This would ensure that the anchorage screws would be inserted only once during installation and removed only after treatment has been completed.
- The use of spacers, as described in the clinical observations, was cumbersome and it introduced small, loose components, adding significantly installation time.
- More information was required on the magnitude of the distraction force. The forces found in the clinical environment appeared to be greater than expected, leading to failure of the traction mechanism. While, at this stage these forces could not be quantified, *in vivo* there was noticeably more resistance to distraction than had been encountered in pre-clinical laboratory testing (see section 4.3.3), which evaluated the device based on data from the literature. It was assumed that mandibular distraction force data found in the literature was a suitable bench-mark.
- The *confluence* of the rail and support plates at the rear of the mouth was secured using titanium surgical wire. This solution accommodated substantial freedom of alignment of the buttress plates and was sufficiently strong. However, the surgeon requested that in the next iteration of the device the *confluence* connection should make use of a bolt- nut arrangement instead.

4.4 VERSION 2 PROTOTYPE: WORM-RACK MECHANISM

Based on the valuable experience of the *V1* distractor, the second phase of development began with a critique of how the problem had been defined and a revision of the design requirements. In response to the in vivo failure of the *V1* prototype, the priority of the *V2* design phase was to develop a more robust traction mechanism that would provide a greater distraction force and improved stability.

4.4.1 V2: MAJOR DESIGN REFINEMENTS

The *V2* distractor retained the basic format of the *V1* version, comprising distinct rail and locomotive components. The zygomatic and palatal support plates were also retained, having performed suitably in the first case – supporting the posterior end of an otherwise cantilevered trajectory rail.

The major design modifications were as follows:

- A metallic worm-rack traction mechanism replaced the plastic self-cutting mechanism. This necessitated a purpose-built metallic trajectory rail with a preformed toothed rack for engagement of the worm-screw (see Figure 42 & Figure 43).
- The locomotive profile and mesh cradle were refined to improve patient comfort and customisability.
- The wired *confluence* used in the *V1* device to link the posterior buttress plates was replaced with a bolted connection.

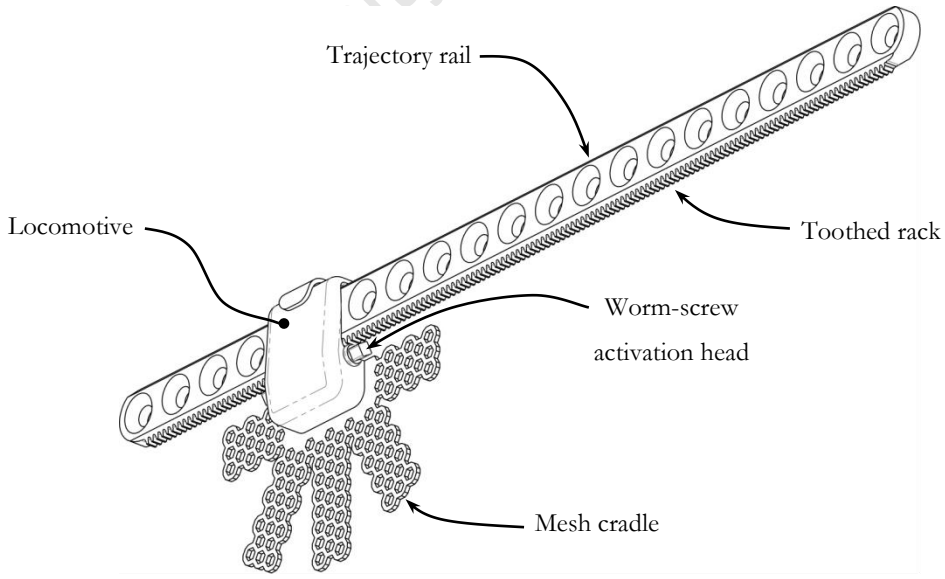

Figure 42: Labelled *V2* distractor with toothed rail.

4.4.1.1 WORM-RACK TRACTION MECHANISM

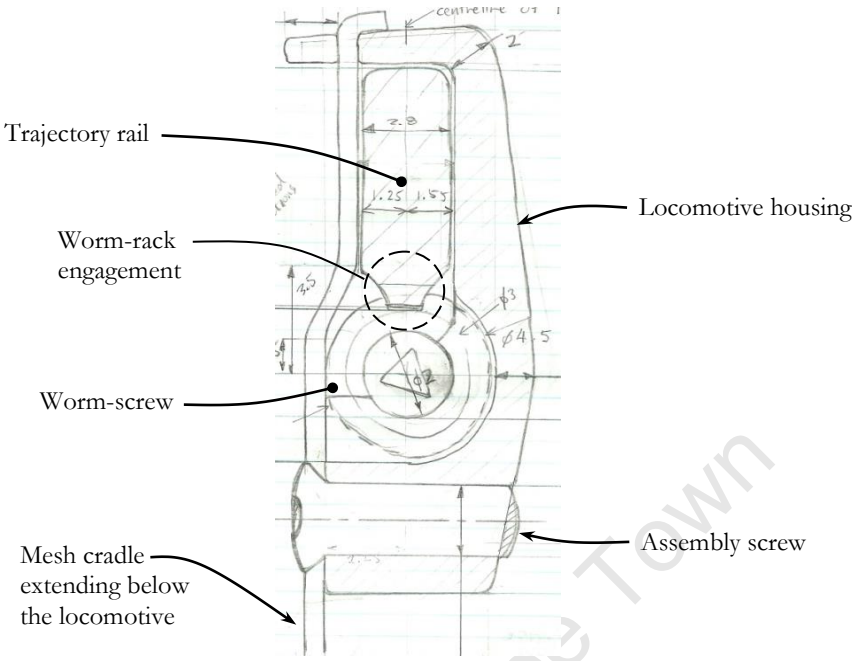

Figure 43: End-view of *V2* locomotive, illustrating the traction mechanism, assembly screws and outer profile (author's sketch).

The plastic traction mechanism was replaced with the metal-on-metal worm-rack traction mechanism described in concept in section 4.2.1. This mechanism is self-locking, provides a large gearing ratio and can easily be scaled according to the application.

Due to the sliding engagement between the worm-screw and rack components, high friction and wear are characteristics of the mechanism, making it inappropriate for most drive applications. However, the mechanical requirements of the TDDO application are relatively undemanding:

- The applied loads are relatively small.
- Energy consumption is irrelevant.
- The device operates at very low speeds.
- The working life of the device involves less than 100 revolutions of the worm-screw.
- Friction, efficiency and wear of the mechanism are therefore insignificant issues.

In worm-rack mechanisms, to compensate for the thread angle the worm-screw is usually orientated with its axis at an angle to that of the rack equal to the thread angle, such that more thread surface is in parallel contact between the worm and rack teeth. However, this adds to the bulk of the device and complexity of manufacturing and complicates access to the worm activation heads. Since the TDDO

application involves low speeds and relatively small loads, there were no clear benefits to justify these clear disadvantages.

The design therefore utilised a much simplified worm-screw arrangement, orientating the worm-screw with its axis parallel to that of the trajectory rail. Ultimately, physical testing has shown that this arrangement performs adequately in practice.

The *V2* locomotive and worm-screw are illustrated in Figure 43 and Figure 44, respectively. The 1mm pitch used in the *V1* distractor was retained in the *V2* device. The worm-screw thread height of 0.65mm provided 0.6mm of engagement with the corresponding toothed rack, with 0.05mm of clearance.

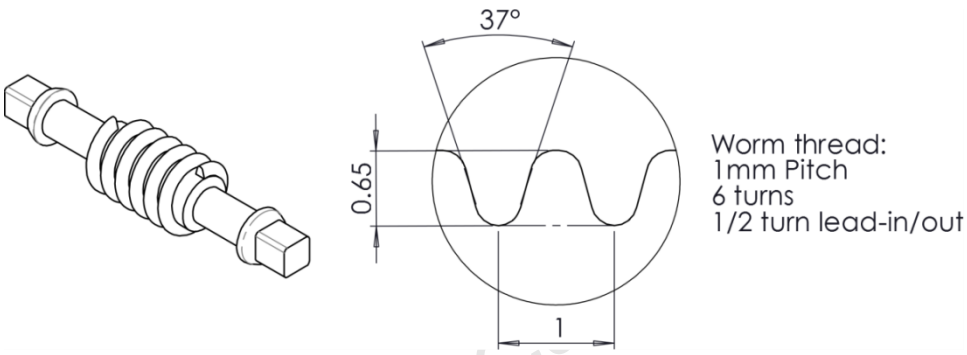

Figure 44: Worm-screw and detail of worm-screw thread.

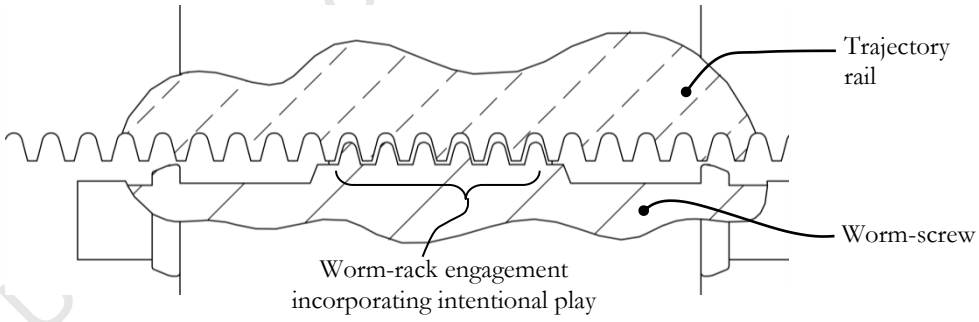

Figure 45: Detail of *V2* traction mechanism, illustrating 'play'.

It was both necessary and intentional to incorporate axial play into the worm-rack engagement (visible in Figure 45) in order to compensate for distortion of the rack feature when the trajectory rail is bent to shape (the pitch of the toothed rack would become wider on the outside of the bend and narrower on the inside). The effects of curvature on the rack teeth were quantified mathematically and it was found that for the minimum expected bend radius of 25mm, 0.3mm of play compensated adequately for distortion of the rack teeth...

Since this type of worm-rack mechanism is not widely used elsewhere, no technical information was found to guide the design of the tooth profiles of the worm or rack. In lieu of such technical information, the design of the traction mechanism was based on basic engineering sense, making use of computer-aided design tools to model and analyse the mechanism.

The manufactured *V2* traction mechanism performed satisfactorily in bench-testing (see section 4.4.2).

4.4.1.2 TRAJECTORY RAIL WITH TOOTHED RACK

The metallic worm-rack traction mechanism incorporated a toothed rack in the trajectory rail component (see Figure 46). While the *V1* case had provided some insight into the requirements of the trajectory rail, the strength and deflection criteria were not yet fully understood. To overcome this uncertainty, the strength and rigidity of the trajectory rail were substantially overdesigned, but were based on the dimensions of the Biomet™ mandibular recon plate, which had provided adequate rigidity in the *V1* clinical case.

The layout of the anchorage holes in the *V2* trajectory rail mimicked those of the Biomet™ mandibular plate. Before manufacturing the final trajectory rail unit, a dummy trajectory rail was manufactured in brass to test the capabilities of the traction mechanism. The final *V2* trajectory rail was manufactured from biocompatible medical grade titanium alloy. Since the trajectory rail was to be submerged in soft tissues for the duration of treatment, the use of a biocompatible material was necessary.

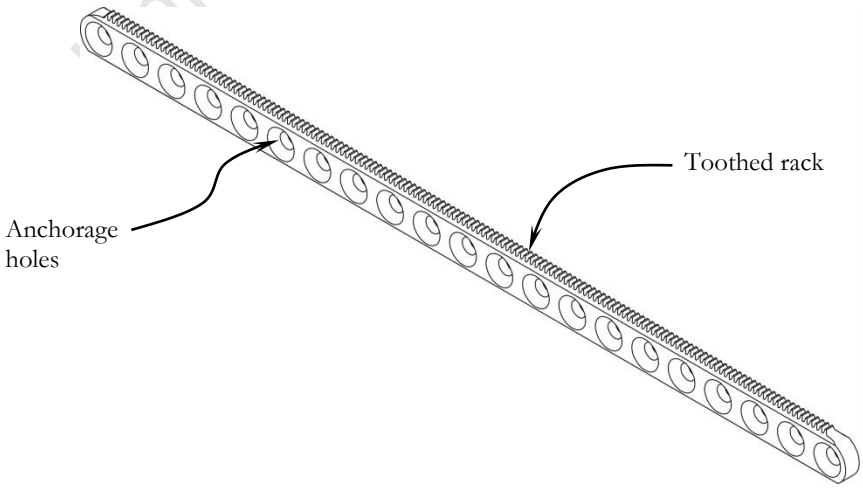

Figure 46: *V2* trajectory rail with serial anchorage holes and integral toothed rack.

4.4.1.3 LOCOMOTIVE REFINEMENTS

The locomotive, which stabilises and propels the bone transport disc, underwent minor ergonomic refinements in the second stage of development. These refinements, directed by observations made during clinical evaluation of the *V1* distractor, included the following:

- The outer profile of the locomotive was improved, introducing smooth contours and removing sharp edges.
- The stability of the locomotive on the trajectory rail was improved by refining the design of the guide channel tab, which constrains the locomotive to the trajectory rail.
- The 0.8mm thick mesh cradle of the *V1* device was found to be too rigid for easy shaping. This was reduced to 0.5mm in the *V2* device, using stainless steel 316 alloy.
- The number of assembly screws was reduced to two, greatly simplifying manufacture and assembly and further reducing the size of the locomotive.

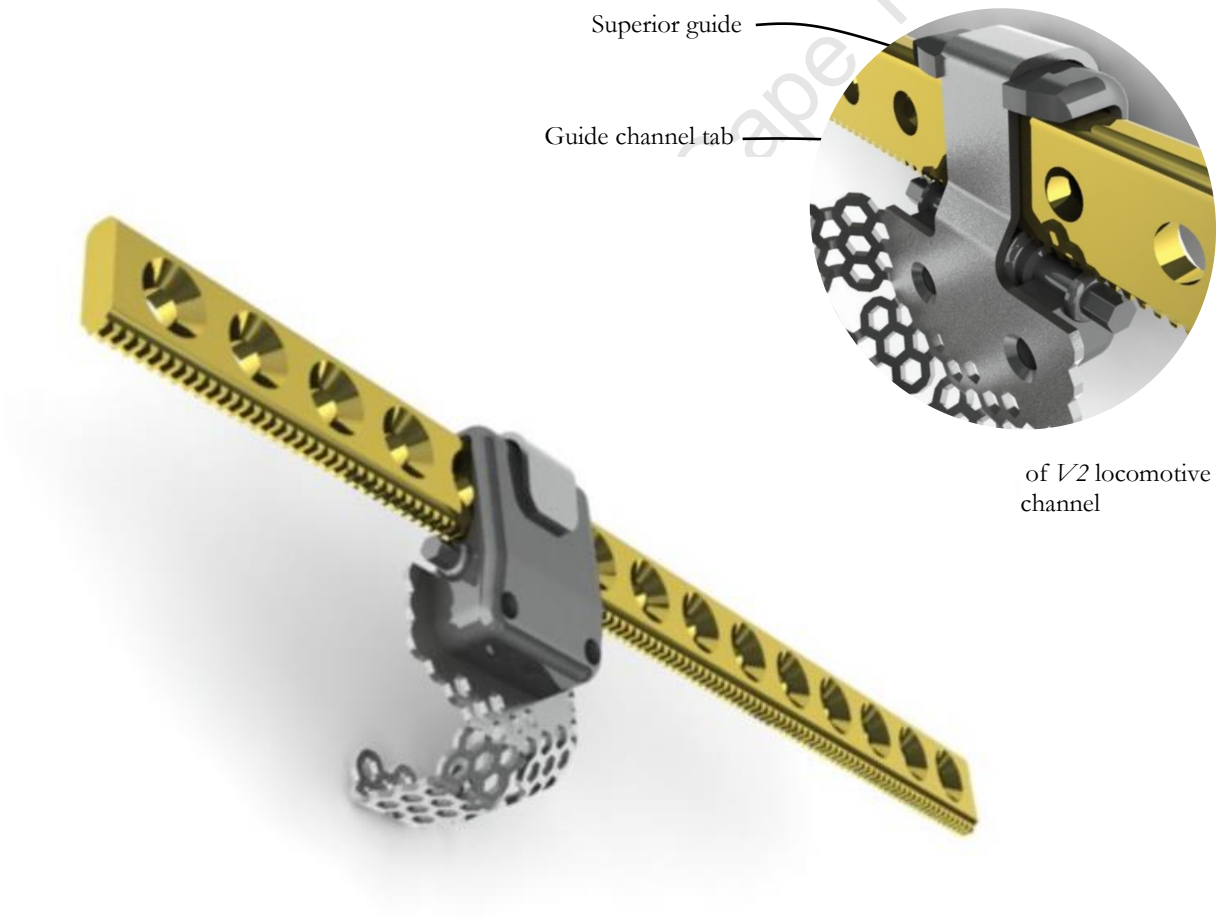

Figure 48: *V2* locomotive refinements

4.4.2 V2: LABORATORY TESTING

Following the failure of the *V1* distractor during clinical treatment, the *V2* device was subjected to more rigorous testing to ensure its reliability in the clinical stage of testing. For the sake of brevity and compactness, full details of these tests are not presented here, but similar tests are described in detail in section 6.1.1, which describes testing of the most recent device version.

4.4.2.1 TEST DISTRACTION ON WORST-CASE TRAJECTORY:

The second prototype underwent a full bench test distraction along a worst-case trajectory (25mm radius of curvature) under a load of 40 N. The device showed no signs of jamming and the worm rotated smoothly. The displacement produced by the device was measured using a vernier caliper and, on average, it was found that 1 rotation produced 1mm of distraction with negligible error, thus providing sufficiently accurate control.

4.4.2.2 LOAD-TEST WITH MAXIMUM EXPECTED LOADS ON LINEAR VECTOR:

A straight distraction of 30mm was carried out under the design load of 100 N, as specified in the PRS, section 3.3. This load incorporated a safety factor of 1.5 over the maximum expected distraction load of 66 N. The 66 N distraction load was based on more recent studies in mandibular distraction (Burstein, Lukas, & Forsthoffer, 2008) elicited subsequent to the *V1* clinical case.

To investigate the strength of the worm-rack interface in isolation, the device was subjected to a static axial load of 200 N continuously for one hour, but without any active distraction.

The device performed adequately under all the tested loading conditions, generating no concerns about the strength, stability, distraction accuracy or reliability of the worm-rack traction mechanism. The results of laboratory testing were thus accepted by the engineering and medical collaborators as satisfactory justification for progression to in vivo testing.

4.4.3 V2: CLINICAL EVALUATION

The second clinical case involved a defect of approximately 80mm of the right side of the maxilla. The defect extended beyond the midline, eliminating more than half of the alveolar ridge, hard palate and much of the nasal floor (see Figure 49). This defect compromised the ability of the patient to speak and eat, and severely affected facial structure and symmetry.

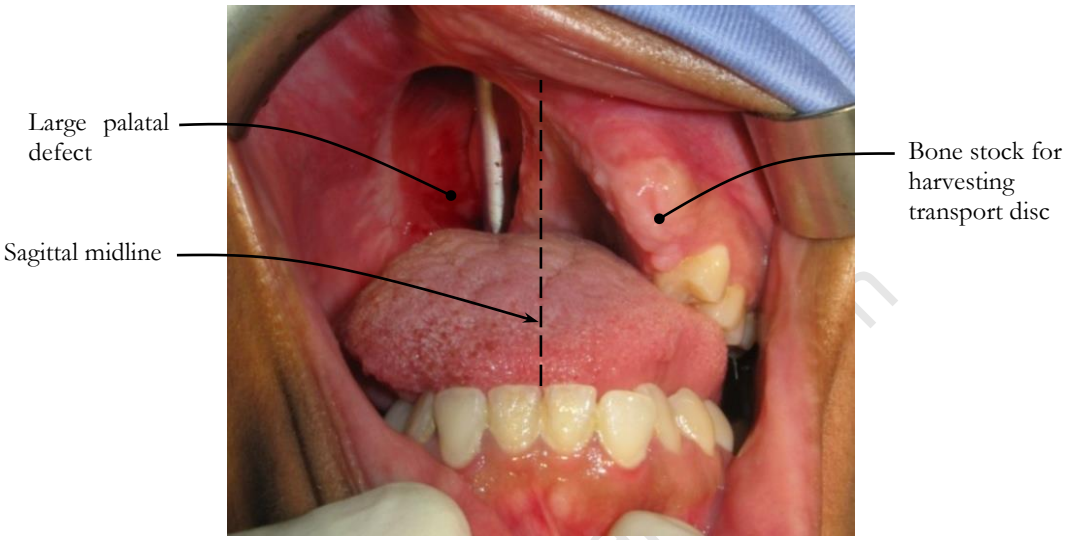

Figure 49: Defect before repair.

The severity of the defect required a TDDO trajectory encompassing an arc of approximately 100°, with a length of 80 mm[19]. It was uncertain how the regenerate would respond to this extreme extent of distraction and there were concerns as to whether the newly-formed bone would conform to the trajectory rail. It was expected that as the transport disc progressed along the arc, the tension in the regenerate would cause the new alveolar ridge to straighten, forming a chord between the initial fracture and the location of the locomotive. This undesirable outcome was termed the '*rubber band effect*'.

[19] A notable aspect of this particular case, associated with the severity of the defect, was explained by the medical collaborator: Besides bone regeneration, TDDO reintroduces the blood supply and cellular immune activity to the area. In the presence of these biological support systems, minor defects remaining after TDDO could be corrected by relatively simple bone grafting and plastic reconstructive surgery.

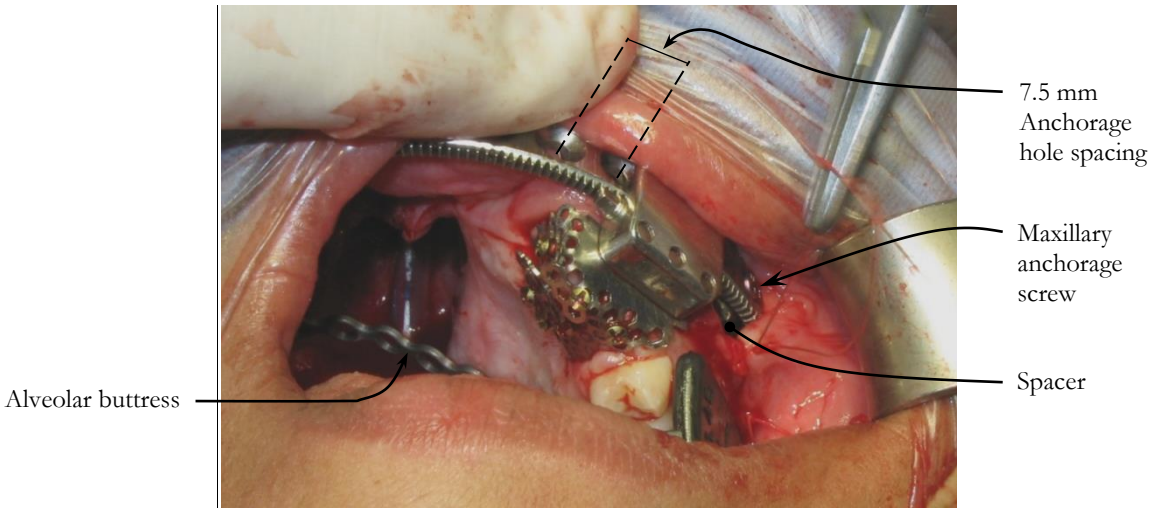

Figure 50: Installed *V2* distractor

Surgical installation of the *V2* prototype took 4½ hours, equal in duration to that of the *V1*. The following problems were encountered (see Figure 50):

- The maxillectomy defect eliminated the entire right side of the maxilla and left only a small segment of the left maxilla intact, posterior to the left canine. Access to this area was hindered by the proximity of the cheek, restricting the angle at which anchorage holes could be drilled and anchorage screws deployed.
- The spacing of the anchorage holes in the trajectory rail prescribed and restricted the anchorage screw spacing to precisely 7.5 mm. This lack of flexibility made it impossible to accommodate all of the desired anchorage screws amongst the dental roots.
- As was the case in the V1 installation, spacers were used to offset the trajectory rail from the maxilla in order to (i) correct the distraction trajectory, (ii) compensate for irregularities in the surface contours of the maxilla and (iii) accommodate the thickness of the gingiva so that the locomotive could bypass the gingiva without injury. Placement of these spacers was cumbersome and they obstructed drilling; prolonging the procedure by approximately 30 minutes.
- As was the case with the V1 device installation, there were geometric discrepancies between the pre-operatively shaped rail and the actual anatomy. The device therefore required time-consuming intra-operative customisation. This issue was partly attributed to discrepancies in the cranial model, due to inadequate resolution of the original CT scan.
- At the request of the surgeon a nut and bolt arrangement was used to secure the ***confluence***. However, this was found to be impractical during both installation and removal of the device, due to the limited access to the ***confluence*** with the necessary tools.

- In order to load the locomotive, the trajectory rail had to be removed entirely, including the anchorage screws, and subsequently re-installed. This was repeated while shaping the mesh cradle, further compromising the integrity of the maxillary anchorage screws.
- The surgeon found that the mesh cradle was too rigid for *in situ* shaping, despite refinements made to the V2 device in this regard (see section 4.4.1.3).
- The locomotive, trajectory rail and buttress plates were pre-assembled outside of the oral cavity once customisation was finalised (see Figure 51). Thus, no difficulties were encountered in the assembly of the bolted *confluence*.
- In the late stages of treatment, the unused trajectory rail anchorage holes were invaded by soft tissue, which became painful. In future versions these holes should be reduced in size, plugged or eliminated entirely.
- As in the V1 case, the screws securing the bone transport disc to the mesh cradle loosened and their orientation shifted under long-term loading.

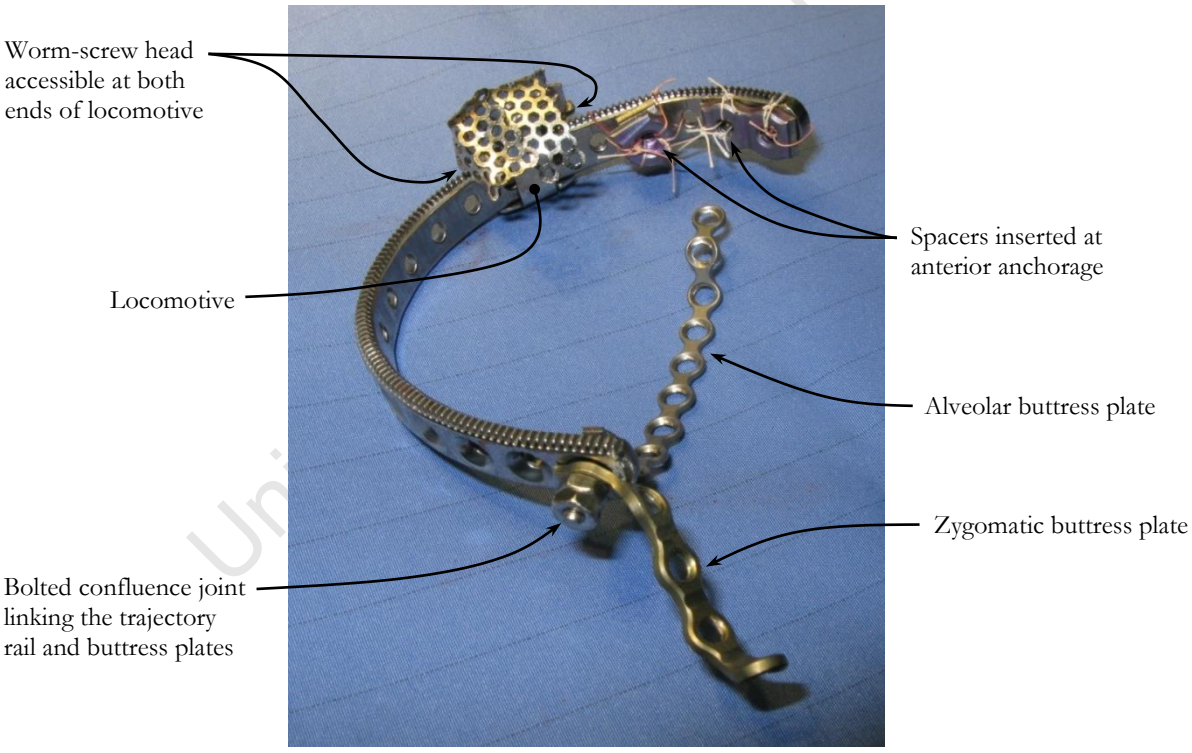

Figure 51: Customised device, ready for final installation.

- After approximately 40 mm of distraction, the regenerate began to form a straight chord between the initial osteotomy and the locomotive, rather than the desired circular arc. Though attempts were made to preserve the curvature of the regenerate using a plastic palatal retainer, this merely resulted in the regenerate thinning out at the points of contact with the retainer. This behaviour suggested the need for an alternative protocol in order to effectively treat such large, curved defects.

Removal of the *V2* prototype exhibited the same difficulties as the *V1*:

- In its final position, the locomotive was confined by the surrounding anatomy. As such, the screw securing the bone transport disc to the cradle could not be accessed with the appropriate screwdriver. In order to remove the device, these screws were unscrewed using surgical tweezers or their heads were ground off with a surgical burr tool.
- The bolted *confluence* joint was significantly more difficult to dismantle than the wired version used in the V1 case. Access to the nut and bolt was especially hindered by soft tissue invasion and trismus of the surrounding muscles, which restricted separation of the jaws.

Despite the ergonomic problems mentioned above, the *V2* distractor successfully performed distraction of the bone transport disc along the entire 80 mm trajectory, with no concerns about the strength or reliability of the traction mechanism. The worm-rack mechanism produced accurate distraction in both the forward and reverse directions and the device demonstrated a satisfactory self-locking action throughout the distraction procedure.

4.4.4 Discussion of V2 Clinical Performance

The *V2* device stably propelled the transport disc along the required 80 mm trajectory. The surgeon reported no difficulty in accessing the worm-screw for daily activation, though it was noted that the resistance to rotation of the worm-screw increased noticeably as distraction progressed. This aligned with reports in the literature that the callus stretching force increases with time.

Nonetheless, having observed the *V2* distractor in practice, the following ergonomic shortcomings of the device were highlighted, directing further enhancements.

4.4.4.1 The Anterior Anchorage

Of particular note in the *V2* clinical case were difficulties associated with repeated installation and removal of the trajectory rail during the initial surgical procedure.

The process of repeatedly removing and re-attaching the trajectory rail not only prolonged the installation procedure, but also compromised the integrity of the bone anchorage screws. Loosening of these screws probably contributed to pain reported in their vicinity.

While the use of spacers at the anterior anchorage provided the correct spatial orientation and fixation of the trajectory rail, manipulation of these spacers was cumbersome and time-consuming and undesirably introduced small, loose components into the oral cavity.

A priority for further refinement was to develop a simple and robust installation interface to overcome these difficulties without adding complexity to the design.

4.4.4.2 Confluence Joint

During removal of the device, disassembly of the bolted ***confluence*** joint was problematic and time-consuming. By the end of treatment, the posterior end of the trajectory rail had become largely obscured by the bone regenerate and encroaching soft tissue. Further hampered by the effects of trismus, access to the nut and bolt arrangement (see Figure 51) with the necessary tooling was significantly restricted. In retrospect, it was found the wired ***confluence*** (as used in the *V1* case) provided a more ergonomic and satisfactory solution.

4.4.4.3 Spacing of the Maxillary Anchorage Screws

The layout of the maxillary anchorage screws was restricted to the set spacing of the anchorage holes in the trajectory rail (see Figure 50). To ensure that the dental roots can be suitably avoided, it was

recommended that future versions of the device offer more flexibility in the layout of anchorage screws.

4.4.5 Reflections on the Second Phase of Development

The *V2* prototype introduced a rigid mechanical traction mechanism to address the reliability issues encountered in the *V1* case. In laboratory tests, the revised device supported the design load of 100 N (Safety Factor = 1.5), and successfully navigated the minimum bend radius of 25 mm. This was reinforced by the clinical success of the device; performing a curvilinear distraction of 80 mm. Ultimately, the *V2* device demonstrated the feasibility of an entirely intra-oral maxillary TDDO device that can be installed, activated and removed with no damage to the facial skin.

5. CULMINATION OF DEVELOPMENT: V3 DISTRACTOR

This project culminated in the design of a fully-functional device for repair of large curvilinear defects in the human maxilla by Transport Disc Distraction Osteogenesis (TDDO). The *V3* distractor, presented in Figure 52, is easily customisable, simple to install and operate and unobtrusive to the patient. It satisfies fully the conditions of the Product Requirement Specification presented in section 3.3.

The *V3* device employs the same worm-rack traction principle as its *V2* predecessor, but it introduces ergonomic improvements that pertain mainly to ease-of-installation, in order to address the various shortcomings of the prior clinical cases described in sections 4.3.5 and 4.4.4.

The installation procedure is arguably the most critical aspect of TDDO as it dictates the outcome of the treatment in crucial areas, namely the stability and integrity of the bone anchorage, the comfort of the patient and the accuracy of the distraction vector, which determines the aesthetic and functional quality of the result.

Section 5.1 provides an overview of the device and its components, a description of its functionality and capabilities, and an explanation of major design decisions. This is followed by numerical justification of critical dimensions in section 5.2.

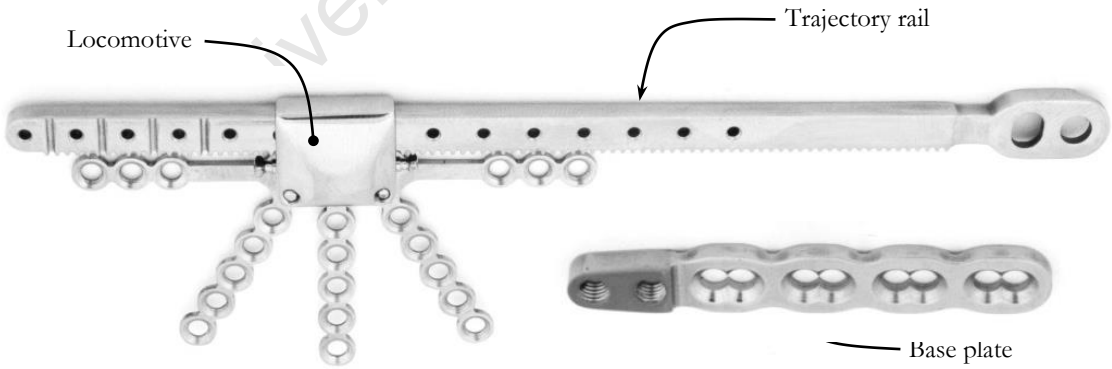

Figure 52: Manufactured final prototype before customisation – trajectory rail, locomotive and base plate.

5.1 DESCRIPTION OF THE HARDWARE

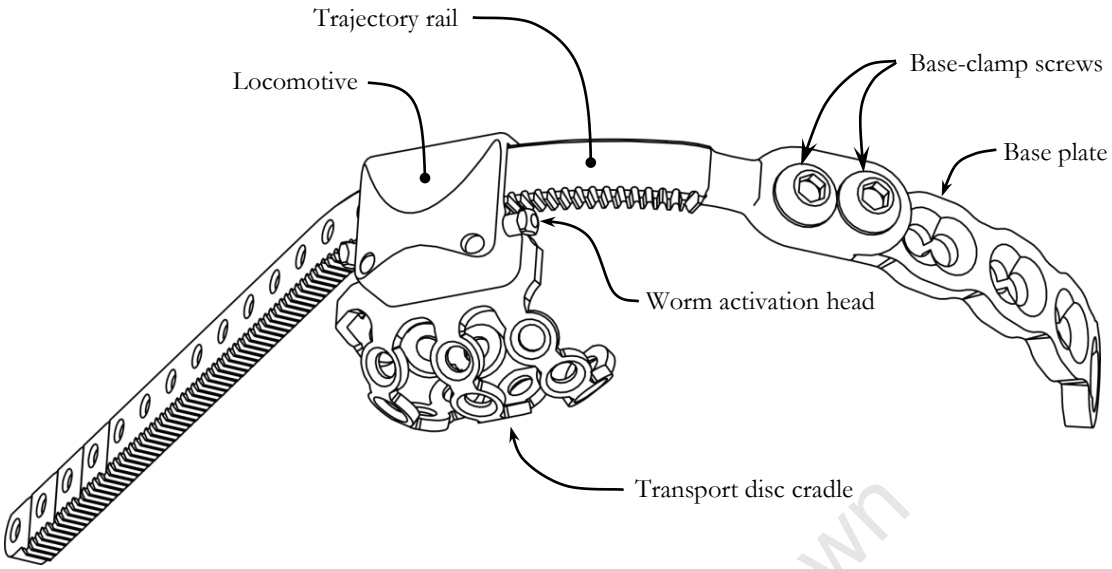

Figure 53: Labelled diagram of the TDDO device after customisation, ready for installation.

The *V3* distractor consists of 3 main components, namely the ***base plate***, ***trajectory rail*** and ***locomotive***, as illustrated by Figure 53. Each component is described below in terms of its structure and functionality.

5.1.1 V3: BASE PLATE

The base plate (see Figure 54) arose from the need to repeatedly attach and remove the trajectory rail during the surgical installation procedure, but without disturbing the bone anchorage.

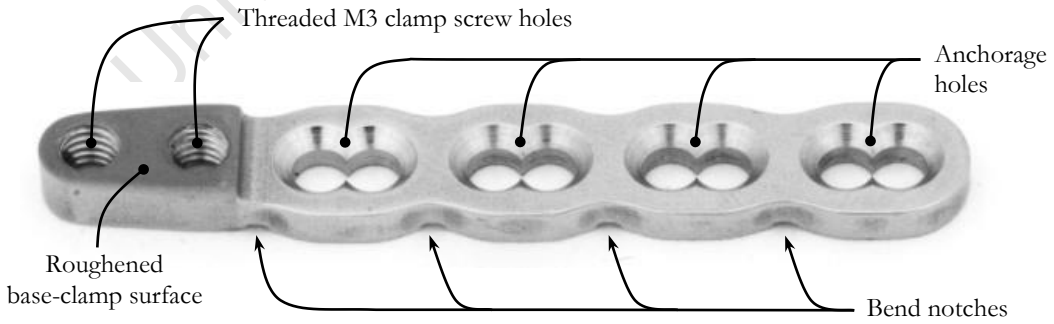

Figure 54: Manufactured base plate – two threaded clamp screw holes to the left and four pairs of anchorage holes to the right

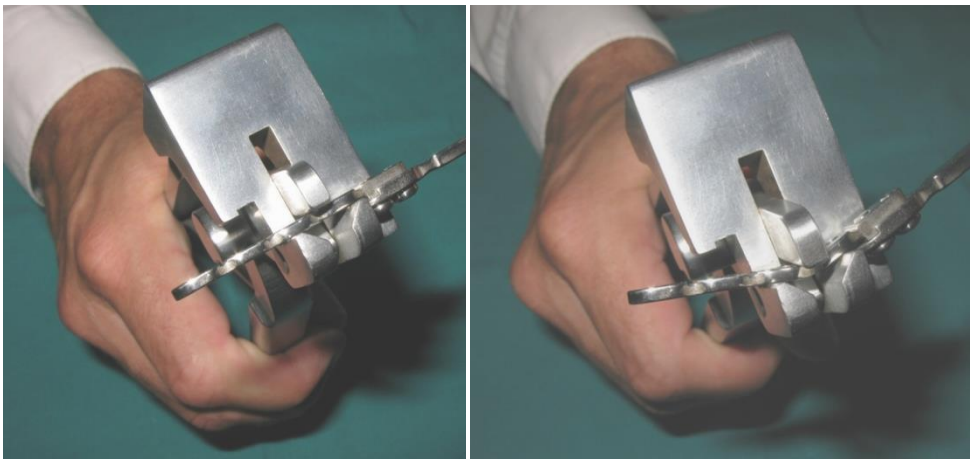

Figure 55: Pre-operative bending of base plate to fit maxillary contour using the Biomet™ plate bender.

The base plate is essentially a 2 mm thick titanium strip, divided into 4 segments by distinct bend notches (see Figure 54). It can be selectively bent to approximate the surface contours of the maxilla (see Figure 55 & Figure 56) and trimmed to the appropriate length. Bending is concentrated at the aforementioned notches, thereby reducing undesirable distortion of the intermediate anchorage holes. All of the tools required for bending and trimming, such as the plate bender in Figure 55, are commonly available in maxillofacial surgical tool-sets.

5.1.1.1 LAYOUT OF THE BASE PLATE ANCHORAGE HOLES

To address the problems raised in section 4.4.4.3, the layout of the base plate anchorage holes accommodates up to four anchorage screws, with enough freedom to avoid intrusion of these screws on the maxillary dental roots.

The length, or pitch, of each of the segments in the base plate emulates the approximate spacing of the anterior teeth in adults (7.5 mm)[20]. Thus, the base plate can be bent and positioned such that the centre of each segment is roughly located between the dental roots where there is adequate bone to receive anchorage screws.

As shown is Figure 54, each segment of the base plate is perforated by a symmetric pair of anchorage holes. The holes in each pair are spaced 2.4 mm apart, providing two options on either side of the 7.5 mm pitch for exact placing of anchorage screws.

[20] Tooth spacing based on measurements of 3 life-size adult stereo-lithographic cranial models, obtained from Dr Rushdi Hendricks, and case studies of existing plating systems.

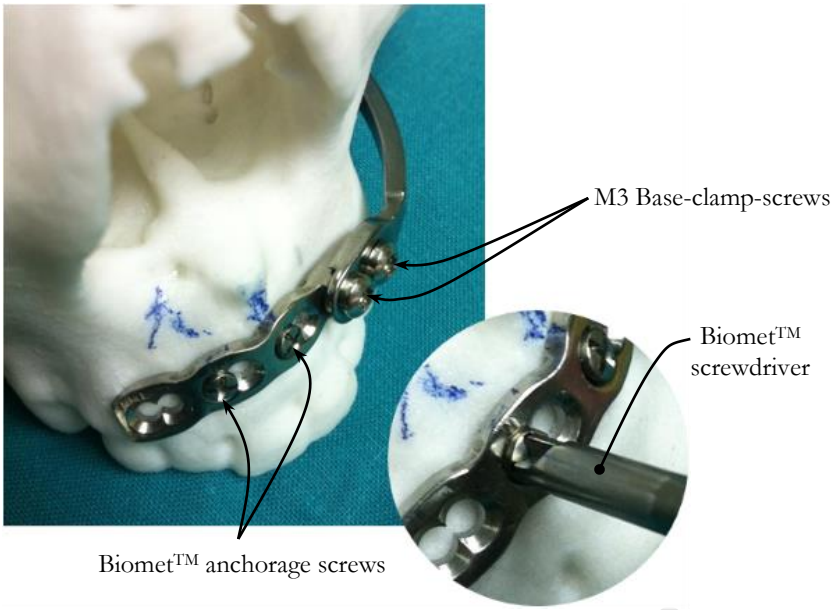

Figure 56: Base plate anchorage to maxilla using 6 mm to 10 mm length mono-cortical anchorage screws.

Each pair of anchorage holes is designed to accept only one screw. This prohibits placement of screws less than 5 mm apart, as two screws placed in such close proximity jeopardize the integrity of the bone. The base plate accommodates up to 4 anchorage screws of up to Ø2.4 mm, each of which can be inserted at an angle of up to 15° to the anchorage hole axis.

Ultimately, it is highly desirable that the base plate anchorage holes should incorporate the ***locking head*** feature found in existing titanium plating systems (see section 4.3.2.1 for a description). However, due to manufacturing constraints the feature was not incorporated into the *V3* distractor and proved unnecessary during clinical implementation.

5.1.1.2 Detachability of the Trajectory Rail

The base plate allows the trajectory rail component to be repeatedly attached and removed during the installation procedure without compromising the base plate anchorage (see section 4.4.4.1).

As shown in Figure 54, the segment at the end of the base plate provides two M3 threaded holes. This is referred to as the ***base-clamp*** segment. These holes are used to attach the trajectory rail once the base plate has been suitably anchored (see Figure 56). The base-clamp segment is 3 mm thick, which accommodates a sufficient threaded length for the M3 clamp-screws and prevents distortion of the base-clamp segment during customisation of the base plate. The opposing clamped surfaces of the base plate and trajectory rail are each roughened by sand-blasting (see Figure 54 & Figure 57) to increase the friction between the clamped surfaces. Further explanation of the base-clamp interface is provided in section 5.1.2.

5.1.2 V3: TRAJECTORY RAIL

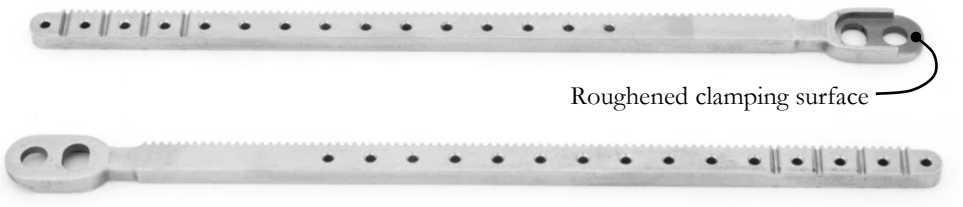

Figure 57: Front and rear views of the manufactured trajectory rail

The trajectory rail, shown in Figure 57, is a 2.5 mm x 4 mm rectangular titanium bar with a toothed rack on the inferior edge. Using standard maxillofacial plate-bending tools, the rail can be bent to the desired curvature and trimmed to the desired length (see Figure 59) to produce the planned distraction path. The device accommodates a minimum bend radius of 25 mm, as prescribed in the PRS.

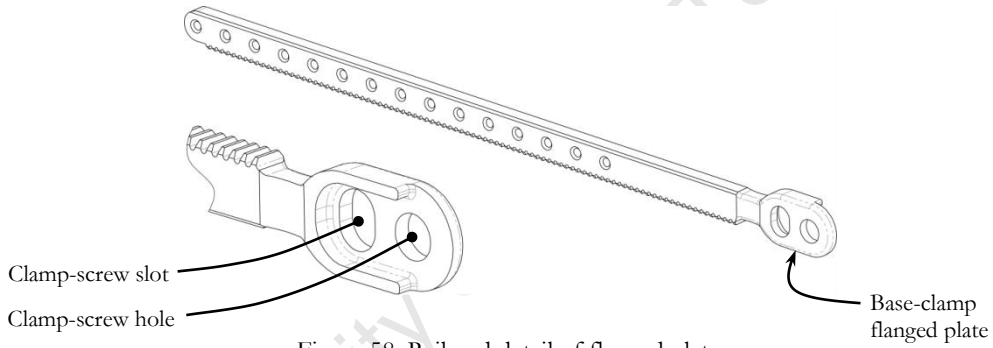

Figure 58: Rail and detail of flanged plate

At one end, the trajectory rail develops into a flanged plate with two perforations (see Figure 58). These perforations match the clamp-screw arrangement in the base plate (as described in section 5.1.1 and illustrated in Figure 54 and Figure 56). This feature allows the trajectory rail to be repeatedly attached and released and permits *in situ* adjustment of the *'exit vector'*, the direction at which the trajectory rail departs from the base-clamp.

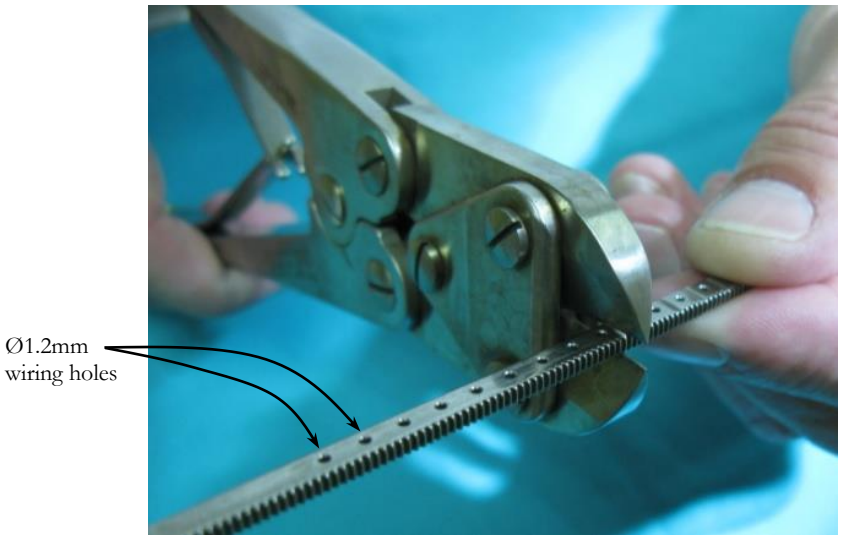

Figure 59: Pre-operative planning – trimming of trajectory rail.

The exit vector can be adjusted in the following three modes:

1. The base-clamp permits adjustment of the trajectory rail over a range of 10° (+5° to -5°) in the vertical/coronal plane (see Figure 60 & Figure 61).
2. By bending and/or twisting the trajectory rail at the neck of the clamp flange the exit vector can be adjusted in two dimensions:
    i. It can be bent sharply to adjust the exit vector direction within the distraction plane[21] (see Figure 62a).
    ii. It can be twisted to adjust the tilt of the distraction plane (see Figure 62b).

These three modes of adjustment allow the surgeon to repeatedly fine-tune the geometry of the distraction trajectory intra-operatively, and since the trajectory rail is detachable this does not disturb the bone anchorage.

The trajectory rail is perforated with a series of Ø1.2 mm holes along its length, spaced 5 mm apart (see Figure 59). The primary purpose of these holes is for connecting the rail to the buttress plates at the *confluence* (see section 5.1.4), but they also provide additional wiring points or locations to place sutures, should the surgeon so require.

[21] The *distraction plane* is a plane parallel to the occlusal plane, at a level specified by the surgeon.

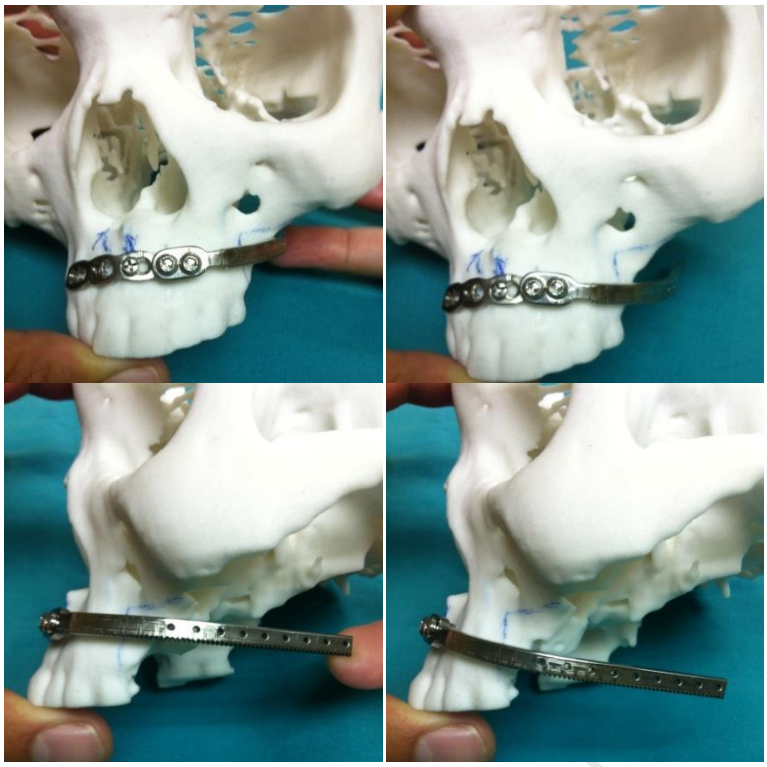

Figure 60: Illustration of base-clamp angle adjustment on cranial model

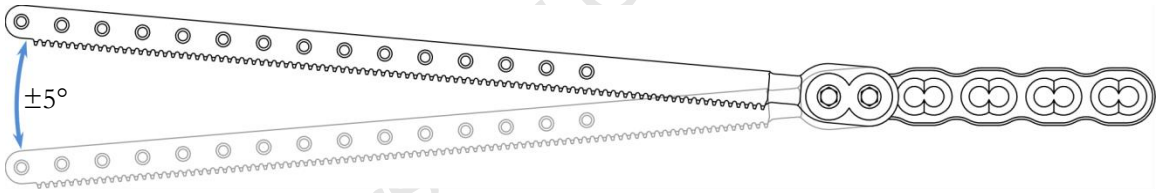

Figure 61: Vertical adjustment of the exit vector.

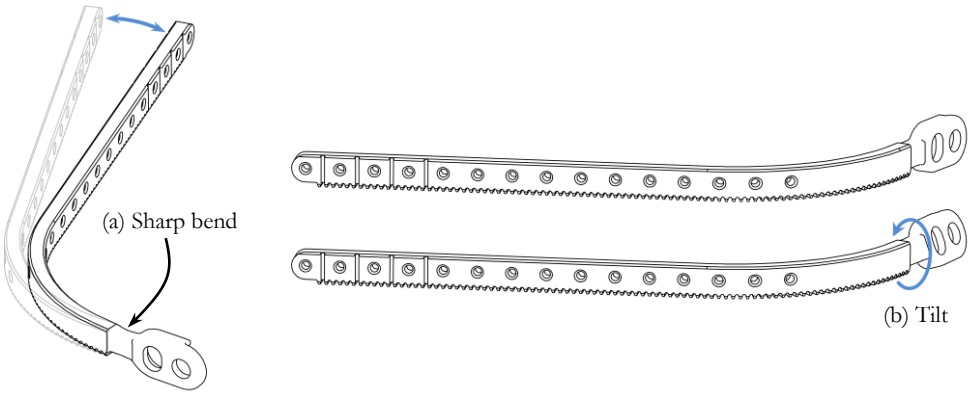

Figure 62: Adjustment of the exit vector and distraction plane tilt.

5.1.3 V3: LOCOMOTIVE

The locomotive supports, stabilises and propels the bone transport disc along the distraction path described by the trajectory rail. It consists of three components: a titanium ***housing***, a titanium ***cradle plate*** and a stainless steel ***worm-screw***. These are held together by two M2 torx-screws threaded into the housing component (see Figure 63).

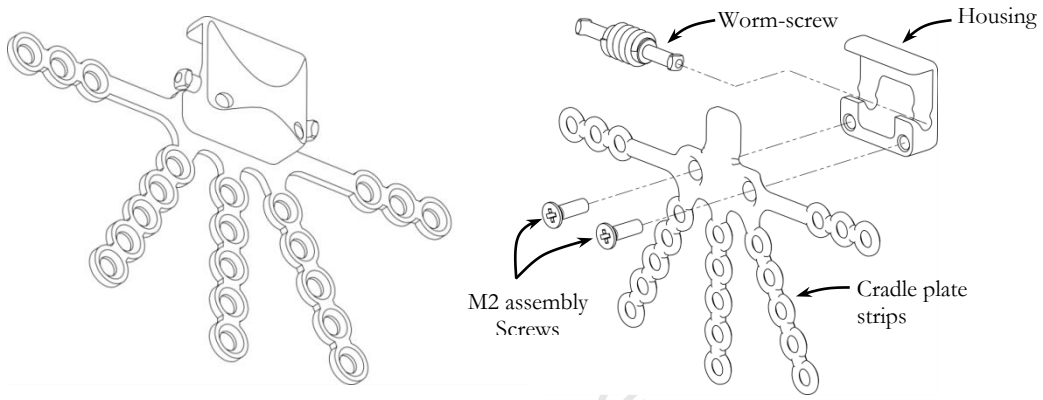

Figure 63: Labelled exploded locomotive assembly

The cradle plate, shown in Figure 63, provides five strips that radiate outwards from the housing. These strips can be bent and trimmed by the surgeon to form a cradle that partially envelops the bone transport disc as shown in Figure 64. A series of countersunk holes in each strip accept mono-cortical bone screws of up to Ø2 mm. These bone screws secure the bone transport disc to the cradle from multiple directions, pinning it securely in place. Figure 64 shows the transport disc cradle in vivo.

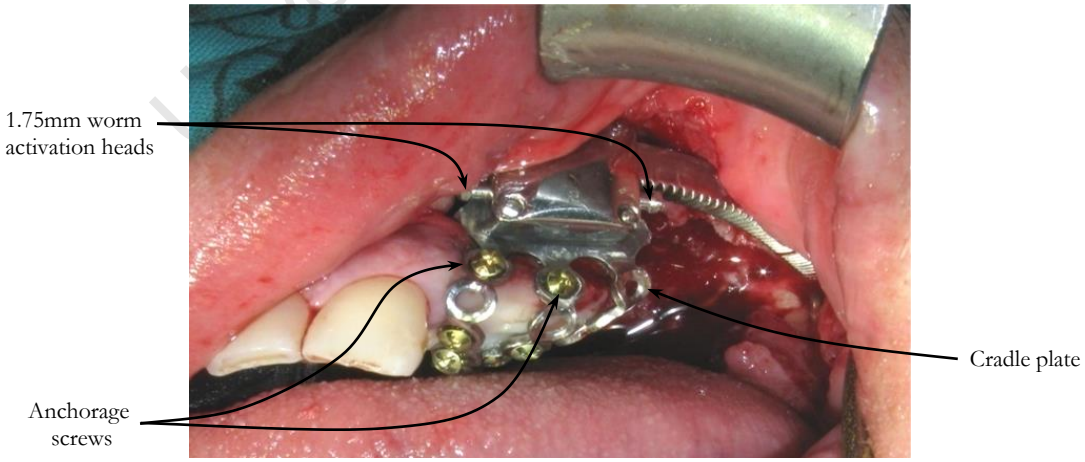

Figure 64: Locomotive in vivo – bone transport disc secured to cradle using anchorage screws.

As shown in Figure 64, the 1.75 mm square heads of the worm-screw protrude from the locomotive at both ends, where they are easily accessible with the standard Biomet™ distraction screwdriver. The

design of the worm-screw head permits axial misalignment between the screwdriver and the worm-screw of up to 15° in all directions (see Figure 65), thus eliminating undesirable bending stresses on the worm-screw and improving accessibility in awkward positions.

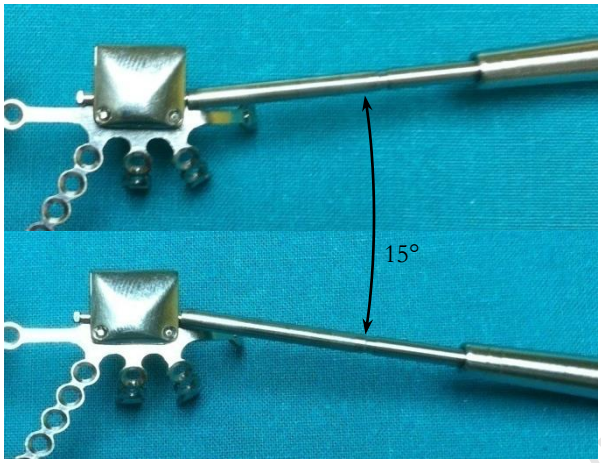

Figure 65: Axial misalignment permitted between the distraction screwdriver and the worm-screw.

In order to navigate curvilinear trajectories and handle irregularities in the trajectory rail a small degree of backlash (0.21 mm) was intentionally incorporated into the worm-rack engagement (see Figure 66). Section 5.2.2 provides a more detailed discussion of this design aspect.

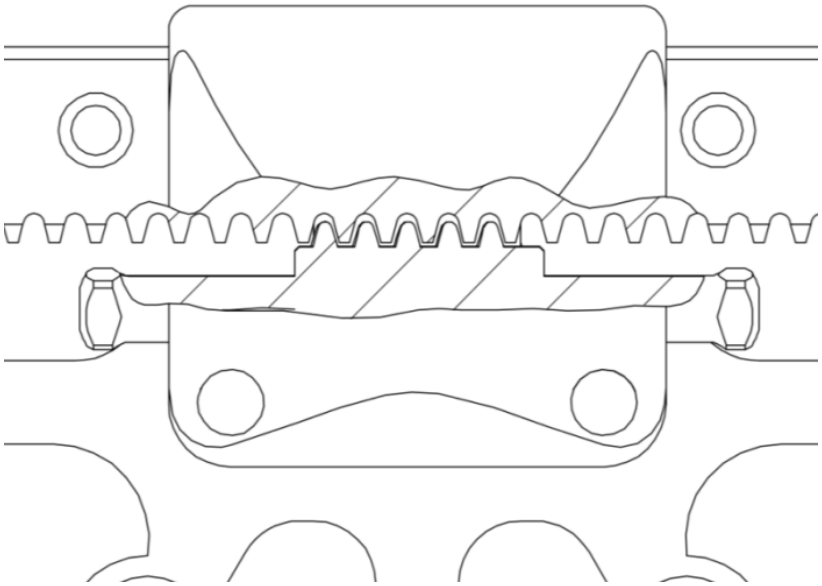

Figure 66: Sectioned view of worm-rack engagement, illustrating intentional backlash.

Activation of the device is achieved intra-orally with no protrusions through the skin as per the recommendations in the literature (see section 2.7). In the *V1* and *V2* clinical cases, intra-oral activation of the device was found to be simple and effective, without any peripheral extension device to assist access. Nevertheless, cases are foreseeable where the device cannot be accessed with the distraction screwdriver directly without painfully disturbing the soft tissues. In anticipation of such cases, the device was made compatible with various commercially available extenders.

A significant refinement between the *V2* and *V3* distractors was the reduction in size of the locomotive, made possible by the smaller *V3* trajectory rail and more compact design of the locomotive assembly. The dimensions of the locomotive were reduced to 61% (height), 86% (length) and 86% (depth) of the *V2* prototype dimensions (see Figure 67). Overall, the *V3* locomotive had a volume of 49% of that of the *V2* prototype, though both versions employ the same traction mechanism. As per the recommendations in the literature, the outer surface of the locomotive was contoured and polished to a matt finish to reduce soft tissue abrasion and thus improve patient comfort, while avoiding glare during surgery.

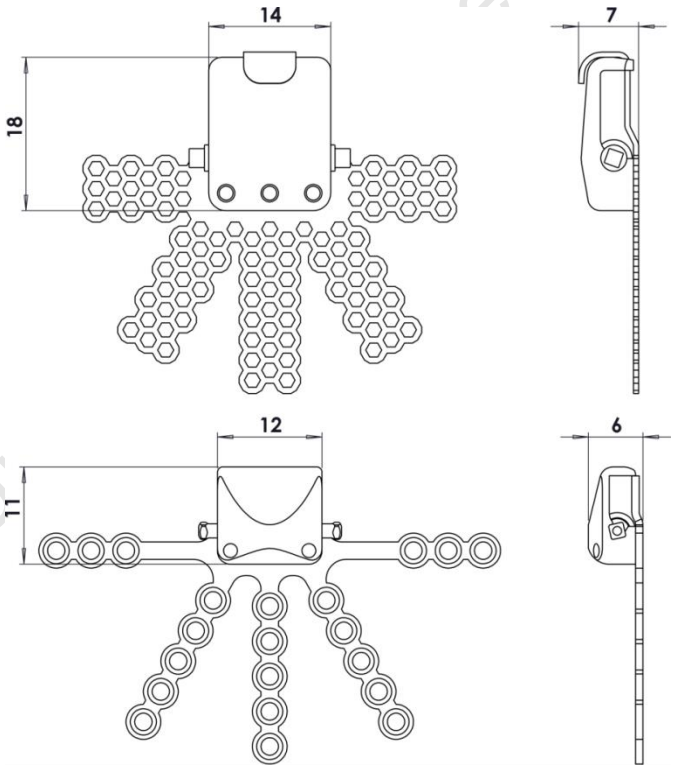

Figure 67: Miniaturisation of the locomotive between the *V2* (top) and *V3* (bottom) prototypes.

5.1.4 V3: BUTTRESS PLATES AND CONFLUENCE

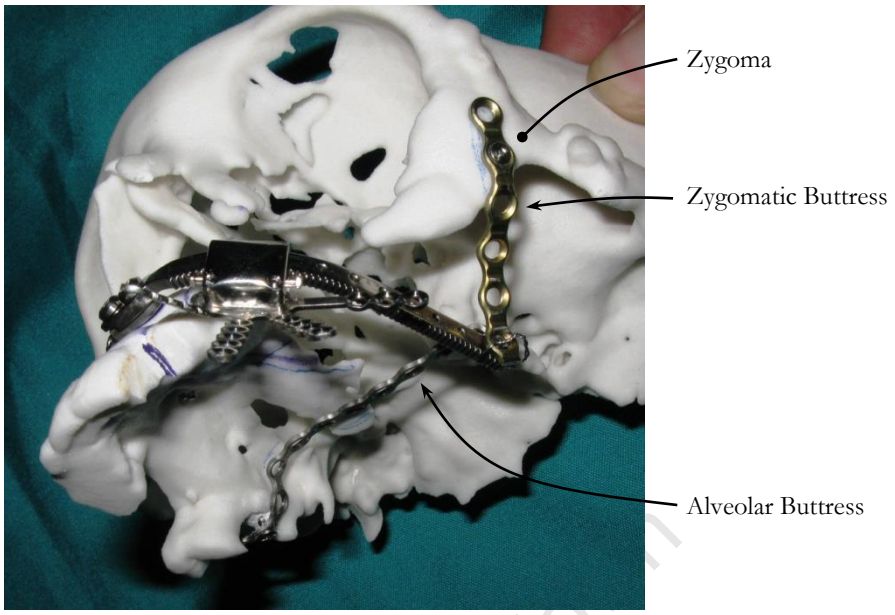

Figure 68: Pre-operative planning – fully customised device installed on cranial model, with zygomatic and palatal buttresses and wired *confluence*.

Figure 68 shows the full *V3* system installed on a cranial model during pre-operative planning. As was the case with the *V1* and *V2* devices, the *V3* distractor utilised buttress plates to stabilise the posterior end of the trajectory rail. The point at which the buttress plates meet the trajectory rail is known as the *confluence*.

The surgeon required a means of securing the *confluence* that was sufficiently rigid, yet easy to assemble and dismantle. Initially, a simple wired *confluence* joint was considered sufficient, but the need for a more aesthetic solution became an ongoing concern. Throughout the development of the *V1*, *V2* and *V3* devices, various alternative concepts were developed in consultation with the surgical and engineering specialists. However, ultimately the design reverted to the wired *confluence* as it offered the following benefits:

- Proven ease-of-implementation and removal in the V1 clinical case.
- Allows flexible, yet secure connection of the trajectory rail and buttress plates.
- Provides a more cost-effective solution than complex alternatives.
- Can be implemented using existing surgical tooling.
- Involves no small or loose parts.

5.2 QUANTITATIVE DESIGN

As discussed at the beginning of section 5, the development of the *V3* distractor was mainly qualitative in approach, owing to the fact that key requirements pertained to the user-interface, patient comfort and similar ergonomic factors. Nevertheless, some calculations were carried out in order to confirm the strength of critical features.

However, these calculations could only be as accurate as the relevant design parameters. Since TDDO in the maxilla finds no precedent elsewhere, many relevant aspects of this procedure were not yet clarified. Thus, many mechanical requirements of the *V3* device were similarly unclear. Accordingly, a number of the design calculations were not based on accurately known parameters; rather they ensured that the size, strength and rigidity capabilities of the device were within reasonable limits.

This section presents the quantitative aspects of design. The details of the pertinent calculations are presented in Appendix B to Appendix F.

5.2.1 RAIL DEFLECTION DUE TO INTRA-ORAL LOADS

The stability provided by the device is a critical aspect of its performance as it dictates to a large extent the quality of the bone formed by TDDO, according to the principles of *micromotion* described in section 2.2.

According to the literature, formation of the healing callus requires a very stable mechanical environment in order to form the desired type of bone. A stable, latent period of callus formation is a necessary stage before active distraction commences. During this period, the literature specifies that *micromotion* of up to 0.3 mm is tolerable. Once the callus formation stage is complete and distraction commences, the stability of the bone fragments becomes less critical. This is for two reasons:

1. Once formed, the cartilaginous healing callus stabilises the fracture surfaces, buffering it against micromotion.
2. After the latent period, the bone transport disc is distracted in the order of 1 mm day, and the relatively minor contribution of micromotion thus becomes irrelevant.

The effects of various tongue forces on the stability of the healing environment were investigated. However, the relatively large forces exerted by the lower jaw were not relevant. Considering their necessarily small size, no intra-oral TDDO devices, nor their anchorage to the surrounding bone,

could realistically withstand normal chewing forces. For this reason the treatment protocol specifies only liquid food and forbids mastication during the active distraction phase.

5.2.1.1 TRAJECTORY RAIL DEFLECTION MODELS

In practice, the anterior base plate and the posterior zygomatic & alveolar buttress plates provide three points of fixation, which constrain and stabilise the trajectory rail in the desired distraction plane.

However, the stabilising contribution of the posterior buttress plates could not be theoretically established. Given the uncertainty of the practical environment, any attempts to do so would be misguided. Therefore, when investigating the deflection characteristics of the trajectory rail, the contribution of the posterior anchorage was neglected, conservatively modelling the trajectory rail as a cantilevered beam that is supported only by the anterior base plate (see Figure 69 to Figure 71).

It was found that even if the contribution of the posterior buttress plates is neglected, the stability of the trajectory rail remains adequate.

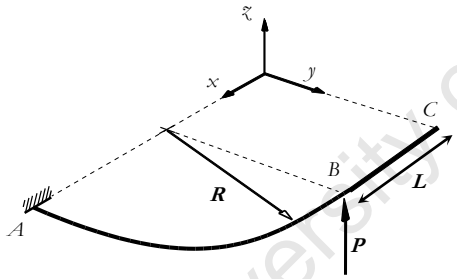

Figure 69: Diagram of bending model of trajectory rail for a vertical load (Nash, 1998)

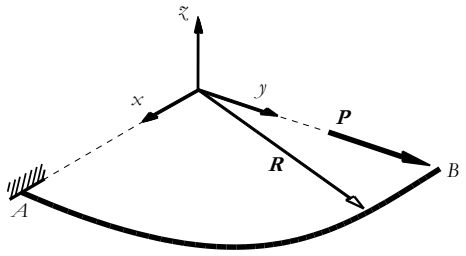

Figure 70: Diagram of lateral deflection model of trajectory rail for a lateral load

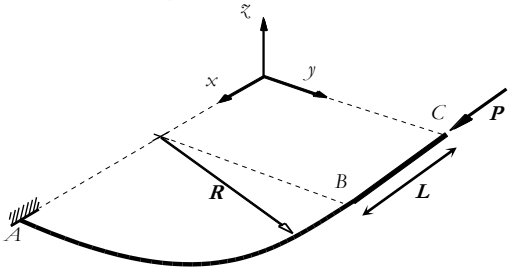

Figure 71: Diagram of bending model of trajectory rail for a tangential distraction load

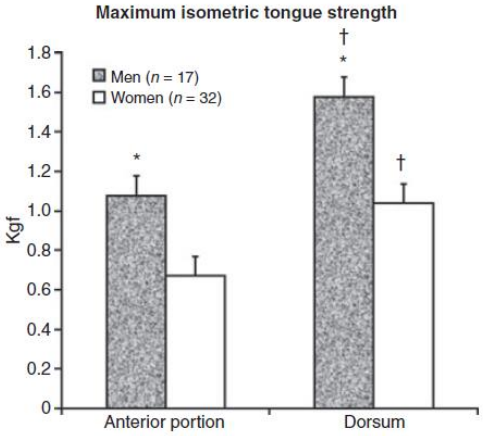

Figure 72: Vertical tongue force in young adults. Of interest was the force exerted by the anterior tip portion of the tongue (Trawitzki, Borges, Giglio, & Silva, 2011)

Based on the configurations illustrated by Figure 69 to Figure 71, Castigliano's second theorem modelled the trajectory rail as a cantilevered curved beam, subjected to two types of loads:

1. Forces exerted by the tongue:

The tongue forces of interest were those in the lateral and vertical direction acting on the posterior segment of the rail (see Figure 69 & Figure 70). Trawitzki et al. present an average maximum vertical tongue force of 12 N in adults from 18 to 32 years of age. A separate study by Dworkin et al. presents an average maximum lateral tongue force of 16 N (see Figure 72), based on a study of tongue force in healthy subjects (Trawitzki, Borges, Giglio, & Silva, 2011).

2. Forces due to callus stretching:

The other loading mode of interest was that of the callus stretching force. In terms of trajectory rail deflection, the worst case involved the maximum expected callus stretching force of 66 N acting on the rear end the rail (see Figure 71).

The cross-sectional dimensions of the trajectory rail (2.5 mm x 4 mm) were guided by the ergonomic requirements of the device and the availability of materials. The aforementioned Castigliano deflection calculations were applied to assess whether this design was adequate. The results were affirmative, as explained below. The relevant calculations are presented in detail in Appendix B.

Only one reference was found in the literature (Sun, Rafferty, Egbert, & Herring, 2007) that described the tolerable limits of micromotion. This study by Sun et al. presented that micromotion as high as 0.3 mm demonstrated no adverse effects on the success of *distraction osteogenesis* treatment. Micromotion is characterised by intermittent and relatively rapid fluctuating strain. However, no

additional evidence could be found to corroborate this data. Therefore, the design specification to limit deflection to the order of 0.5mm, agrees with the 0.3 mm value suggested by Sun et al.

For the chosen cross-sectional dimensions, Castigliano's method returned the following:

1. A vertical force of 12 N produced a deflection of 0.28 mm. A lateral force of 16 N produced a deflection of 0.59 mm.
2. A 66 N callus stretching force produced a total resultant deflection of 1.91 mm at the end of the trajectory rail.

In terms of *micromotion,* the deflection of 1.91 mm at the end of the trajectory rail is not of concern. As shown in Figure 9 of section 2.5.3, the tension in the regenerate fluctuates at low frequency (once per day) and decays exponentially. Furthermore, since the trajectory rail is cantilevered, the transport disc experiences much lesser deflection than its free end.

This exercise confirmed that in theory, even under the most severe loading conditions, with the trajectory rail acting in cantilever and neglecting the contribution of the posterior buttress plates, the device is capable of maintaining adequate stability of the fracture site.

5.2.2 WORM-RACK DESIGN TO ACCOMMODATE RAIL CURVATURE

In order to accommodate the distorting effects of bending on the trajectory rail, the worm-rack traction mechanism intentionally incorporated a small amount of ***backlash***.

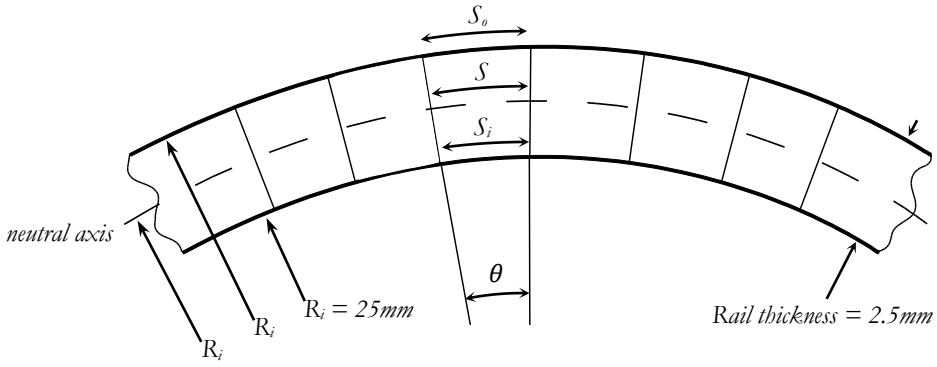

Figure 73: Extract from Appendix C: Geometry of curved rail – plan view.

Bending distorts the teeth of the trajectory rail rack, causing the rack pitch to narrow on the inside of the curve and to widen on the outside (see Figure 73). This distortion was investigated geometrically (see Figure 74) to determine the amount of play required to avoid jamming of the traction mechanism over the 5 engaged turns of the worm-screw. It was calculated that 0.2mm of play was sufficient to accommodate the distortion effects of the minimum expected bend radius of 25mm. The relevant calculations are presented in Appendix C.

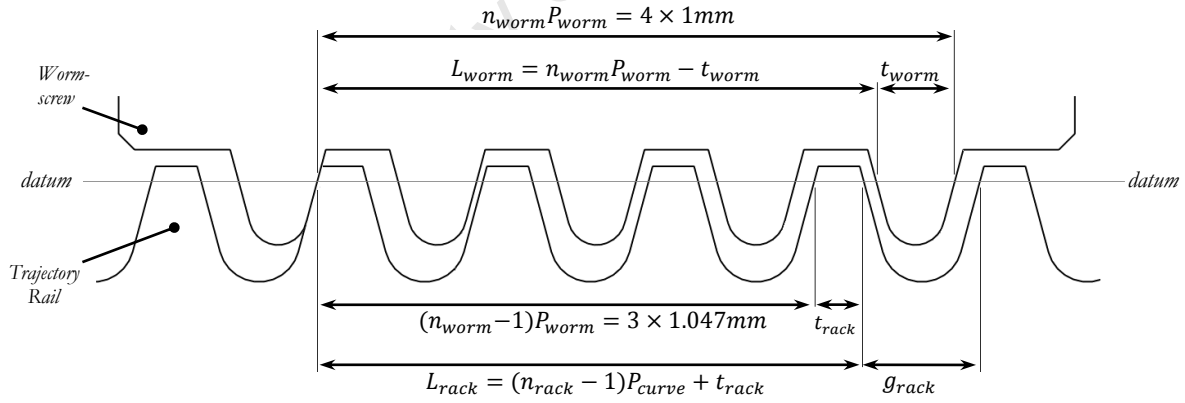

Figure 74: Geometric investigation of traction mechanism.

Tension in the healing callus provides a residual force on the locomotive, keeping it settled at one extreme. Therefore, introduction of this ***backlash*** into the traction mechanism is not a compromise on stability as it never translates into actual movement.

5.2.3 WORM TORSION STRENGTH

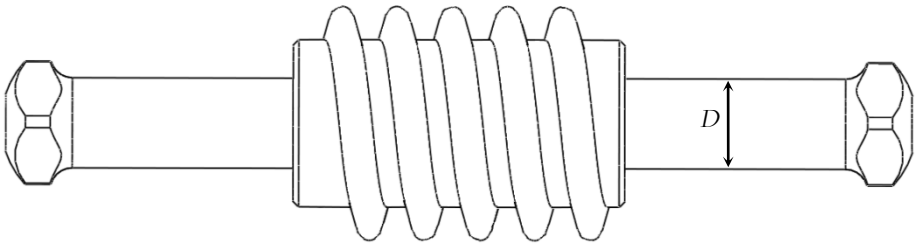

Figure 75: Worm-screw torsion strength – critical shaft diameter, D.

The torsion strength of the worm-screw was investigated using principles of solid mechanics to ensure that it could sustain a benchmark activation torque of 12 Ncm; an estimate based on information in the literature. Detailed calculations are provided in Appendix D.

It was concluded that the shaft can withstand a load of 18 Ncm, thereby providing a safety factor of 1.5 over the maximum expected load of 12 Ncm.

Subsequent laboratory strength testing of the worm-screw revealed a torque-carrying capacity of 30 Ncm. Thus, in practice a safety factor of 2.5 was demonstrated.

The initial benchmark torsion load specified in the PRS (section 3.3) of 12 Ncm was upheld by in vivo measurements during clinical implementation of the device, where the maximum distraction torque was 8 Ncm.

5.2.4 BASE-CLAMP SLIPPAGE

The base-clamp joint rigidly connects the trajectory rail to the base plate. The strength of this connection was investigated to ensure that a moment could be sustained without relative slippage of the clamped surfaces.

In theory, the maximum moment on the base-clamp in practice is 1.2 Nm; due to a vertical tongue force of 12 N (see section 2.5.4) acting at the end of a 100mm long rail. This upper limit estimate provided a bench-mark.

The calculations in Appendix F estimate that the base-clamp joint withstands a maximum moment of 2.72 Nm before slippage occurs, providing a safety factor of more than 2 over the benchmark load of 1.2 Nm.

5.3 MATERIAL SPECIFICATION

The material specification for each component (see Table 2) was based primarily on the bio-compatibility and strength requirements of the device. Grade 5 titanium 6Al4V alloy was specified for all components, with the exception of the worm-screw, the M3 base-clamp screws and the M2 locomotive assembly screws. Grade 5 titanium is most commonly used, due to its high biocompatibility and fracture resistance.

Titanium's poor shear strength makes it unsuitable for components subjected to torsion, such as the worm and assembly screws. Also, titanium alloy has a high co-efficient of friction, especially when in sliding contact with other titanium components. Thus, cold-drawn and annealed stainless steel 316 was specified for the worm-screw for its relatively high shear strength, good corrosion resistance and lower friction against the titanium alloy housing component.

Standard medical grade stainless steel 316 alloy was specified for the base-clamp screws and the locomotive assembly screws for its shear strength.

Table 2: Material specification for *V3* device.

Component Name	**Material**	**Yield Strength (MPa)**	**Shear strength (MPa)**	**Implantability**
Base plate	Ti 6Al4V	880	NA	✓
Trajectory rail	Ti 6Al4V	880	NA	✓
Locomotive housing	Ti 6Al4V	880	NA	✓
Locomotive cradle plate	Ti 6Al4V	880	NA	✓
Worm-screw	SST 316	415	236	✓

6. TESTING OF THE V3 PROTOTYPE

The performance of the *V3* device was evaluated in two stages:

1. Laboratory testing assessed whether the traction mechanism and other critical features met the requirements of the PRS in section 3.3.
2. Subsequent clinical implementation provided an opportunity to observe and evaluate the ergonomic performance aspects of the device.

Laboratory testing of the *V3* device was more rigorous than in previous versions and the results of testing are presented in more detail. In the interests of repeatability of these tests, more extensive reports are included in Appendix G.

6.1 LABORATORY TESTING

Guided by the product requirement specifications, the aims of laboratory testing were to assess whether the:

1. Device as a whole could achieve TDDO along the 25mm minimum-radius trajectory, against the design load of 100 N.
2. Worm-rack interface could safely withstand the design load of 100 N.
3. Worm-screw could withstand the torque corresponding to a 100 N distraction force.
4. Base-clamp joint could withstand the effects of a 12 N vertical tongue force.
5. Self-locking action of the worm-screw was satisfactory.

While every attempt was made to create laboratory loading scenarios that mimic the worst expected case, they did not reproduce the exact operating conditions of the device in practice. Recommendations for more accurate and detailed study of the mechanics of the device are presented in section 9.

6.1.1 Distraction Force Capabilities

6.1.1.1 Linear Trajectory with a Longitudinal Load

TDDO involves overcoming a tensile resistive force within the healing callus, which is a maximum at the time of distraction and decays exponentially (Romanyk, Lagravere, Toogood, Major, & Carey, 2012). A test rig was constructed to evaluate the behaviour of the device under load and the magnitude of the worm-screw activation torque under various loading conditions.

The device was tested dry, as well as wetted with a water/detergent solution to produce an aqueous film on the meshing surfaces. This basic lubrication was an effort to more closely mimic the mucoid intra-oral environment.

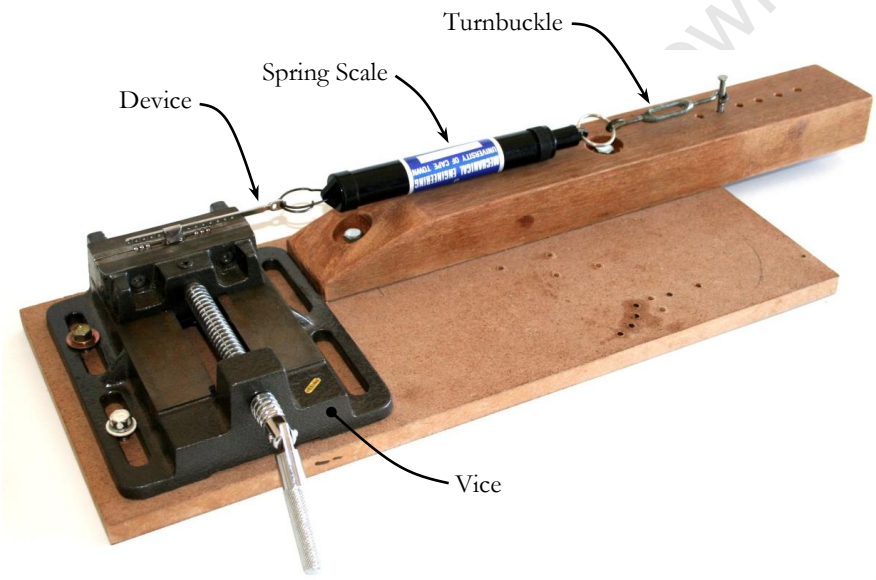

Figure 76: Test rig for longitudinal load tests

As shown in Figure 76, the test apparatus employed a spring-scale to provide resistance (representing the tension in the healing callus) as well as a means of measuring the load on the distractor. A turnbuckle in series with the spring-scale was used to adjust this load. The distractor was subjected to loads up to 100 N, acting purely axially, i.e. producing no tipping moment on the locomotive. The 100 N design load was provided by a spring-scale.

For each load, the device was activated by one full rotation in four quarter-turn increments. Using a highly sensitive electronic torque-measuring screwdriver[22] (see Figure 79), the activation torque was

[22] The BMS MS050S electronic torque screwdriver has a resolution of 0.02 Ncm and range of 5-50 Ncm.

successively measured and recorded. From each set of four quarter-turn measurements, the mean value was calculated.

RESULTS – LINEAR TRAJECTORY WITH A LONGITUDINAL LOAD

The device successfully produced the required maximum distraction load of 100 N. The maximum activation torque measured was 18.56 Ncm in the dry case and 8.82 Ncm in the wetted case, both of which fall within the 20 Ncm limit specified in the PRS (see section 3.3). The dry test provided a measure of the absolute worst case, but for all practical purposes the 8.82 Ncm reading is more relevant.

The relationship between activation torque and distraction load was found to be exponential over the tested range. The device performed consistently, and the graphical results were closely approximated by an exponential trendline, as shown in Figure 77 & Figure 78. These graphs illustrate the maximum, minimum and mean activation torque required to generate distraction forces up to 100 N.

The exponential trendline functions for distraction under load on a straight trajectory were as follows:

Dry trajectory rail: $[\, y = 2.552e^{0.020x} \,]$ (Eqn. 1)

$[\, y = 2.359e^{0.021x} \,]$ (Eqn. 2)

Wetted trajectory rail: $[\, y = 2.370e^{0.013x} \,]$ (Eqn. 3)

$[\, y = 2.719e^{0.011x} \,]$ (Eqn. 4)

Where y is the torque required (Ncm), and x is the distraction force generated (N).

Equations 1 and 3 are the trendlines depicted in Figure 77 and Figure 78. Similar plots produced trendlines corresponding to equations 2 and 4.

Each of the trendline functions presented above is based on an independent test. Comparing the co-efficients of equations 1 to 4, it is evident that for each set of loading conditions (*dry* and *wet*), the behaviour of the device was consistent and predictable. The close proximity of the maximum and minimum curves in Figure 77 and Figure 78 demonstrates this consistent behaviour graphically.

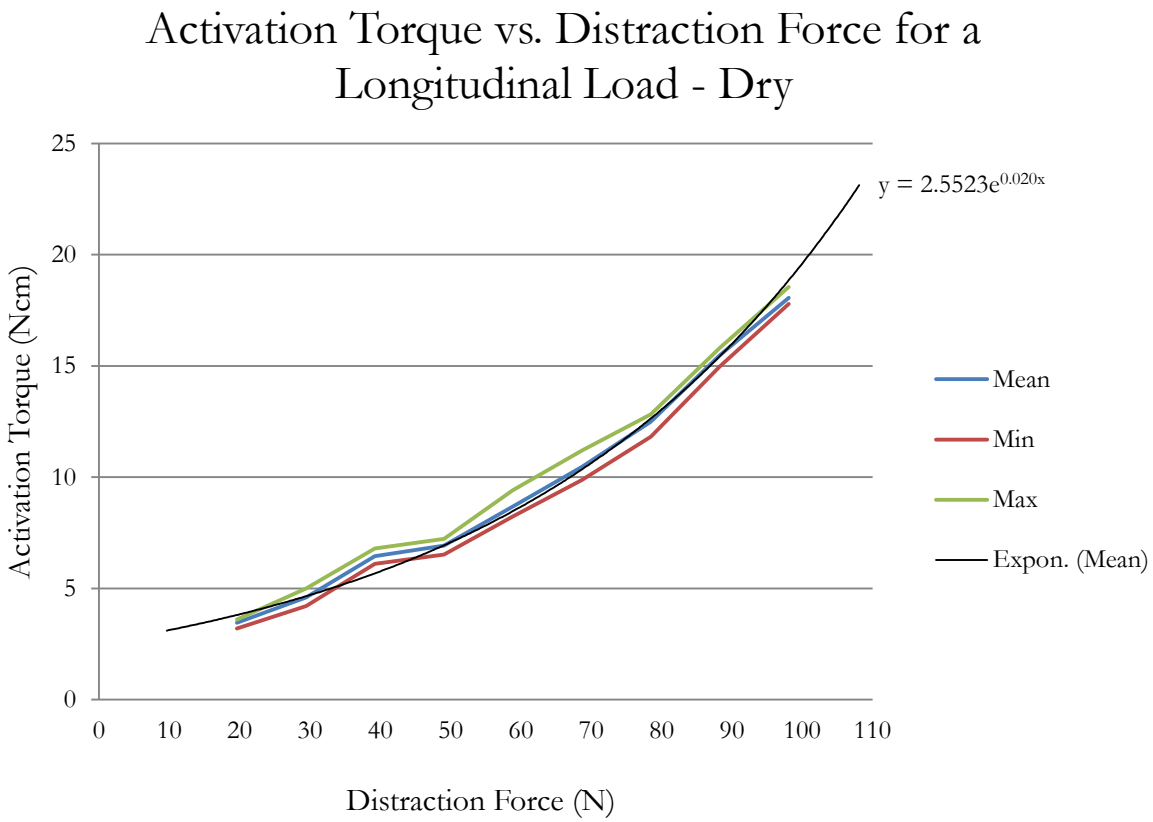

Figure 77: Activation torque vs. distraction force on a straight trajectory, dry.

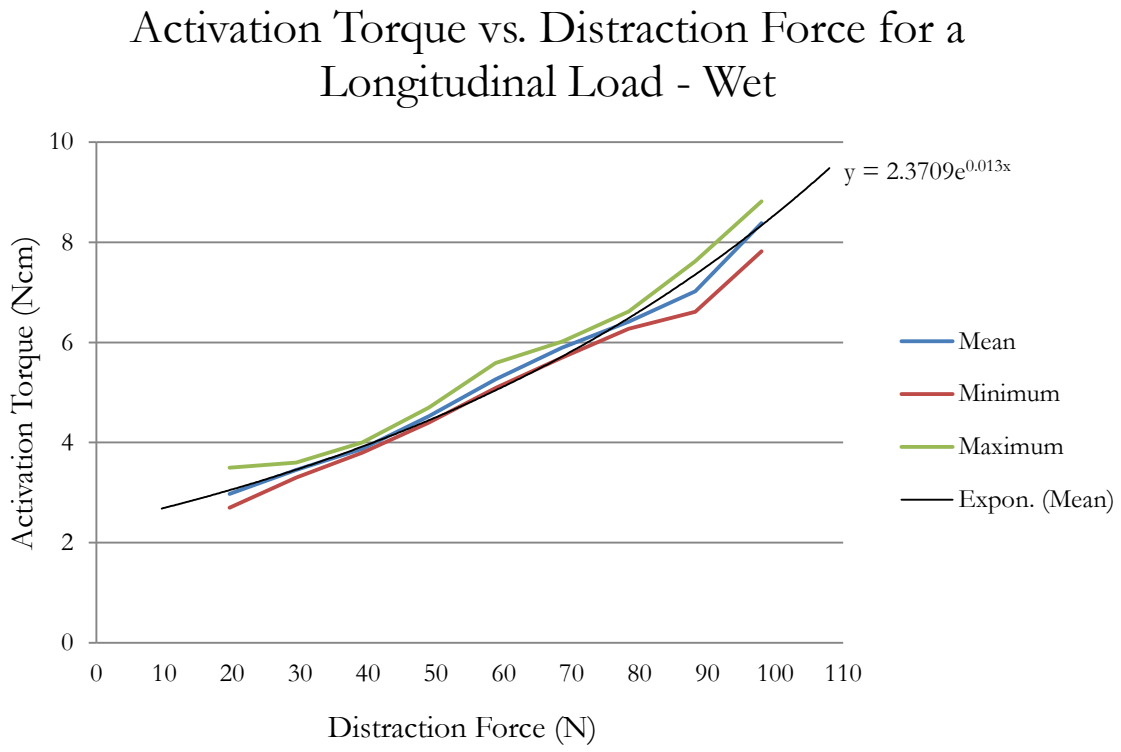

Figure 78: Activation torque vs. distraction force on a straight trajectory, wetted with a detergent solution.

6.1.1.2 TIPPING MOMENT: LINEAR TRAJECTORY WITH AN OFFSET LOAD

In the clinical situation, the callus stretching force acts at a distance of up to 10mm from the worm-rack engagement, which generates a net tipping moment on the locomotive. In order to investigate these effects, the procedure described in section 6.1.1.1 was repeated under *wet* conditions, however with the load acting on the locomotive over a moment arm of 4mm and 10mm, measured from the worm-rack (Figure 80).

Figure 79: BMS MS050S electronic torque screwdriver

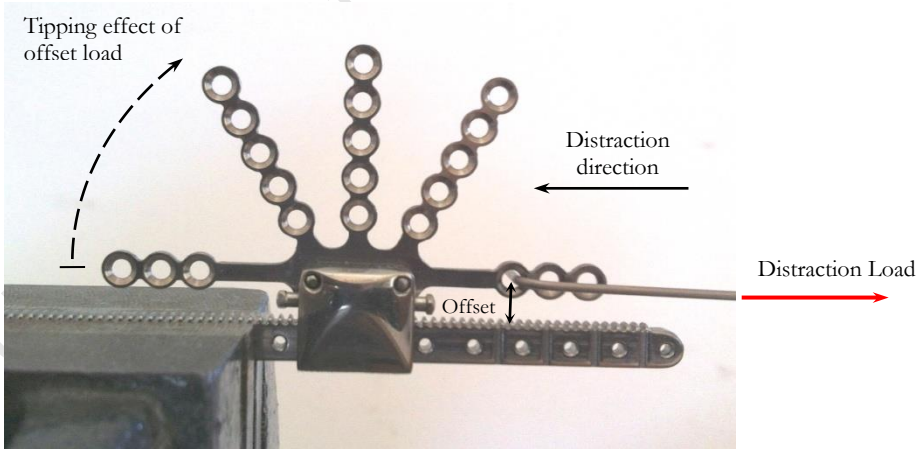

Figure 80: Locomotive testing with 4mm offset load, indicating tipping effect.

RESULTS – LINEAR TRAJECTORY WITH AN OFFSET LOAD

Under a distraction load of 100 N, offset by 4mm, the device required a maximum activation torque of 7.48 Ncm and 7.71 Ncm in two separate tests. For an offset of 10mm the torque measurements were 11.32 Ncm and 12.03 Ncm.

It was expected that the leverage of the offset load and its tipping effect on the locomotive (see Figure 80) would produce greater frictional resistance within the traction mechanism. This was the case for the 10mm offset load. However, it was found that the 4mm offset load required a lower activation torque than the purely axial load tested in section 6.1.1.1. This behaviour was explained as follows. The offset load caused the locomotive to tip away from the direction of motion (see Figure 80). On close analysis, it was found that with the worm-screw proceeding at this tipped angle, the worm thread was eased gradually into each successive tooth of the rack. By contrast, without this tipping effect the worm thread was forced to engage each successive rack tooth more rapidly.

The exponential trendline functions for distraction with an offset load on a straight trajectory were as follows:

4mm offset load: $[\, y = 2.637e^{0.011x} \,]$ (Eqn. 5)

$[\, y = 2.760e^{0.010x} \,]$ (Eqn. 6)

10mm offset load: $[\, y = 2.097e^{0.017x} \,]$ (Eqn. 7)

$[\, y = 2.133e^{0.017x} \,]$ (Eqn. 8)

Where y is the torque required (Ncm), and x is the distraction force generated (N).

Once again, equations 5 and 7 are depicted in Figure 81 and Figure 82.

Each of the trendline functions presented above is based on a completely independent data set. Once again, the similarity of the coefficients within each pair of functions demonstrated consistent behaviour of the device for a given set of loading conditions. For example, in the case of the 10mm offset load, the base co-efficients were *2.097* and *2.133* and the exponent co-efficients were identically *0.017* and *0.017* in two independent tests. Once again, the proximity of the maximum and minimum curves in Figure 81 & Figure 82 demonstrates the consistent behaviour of the device.

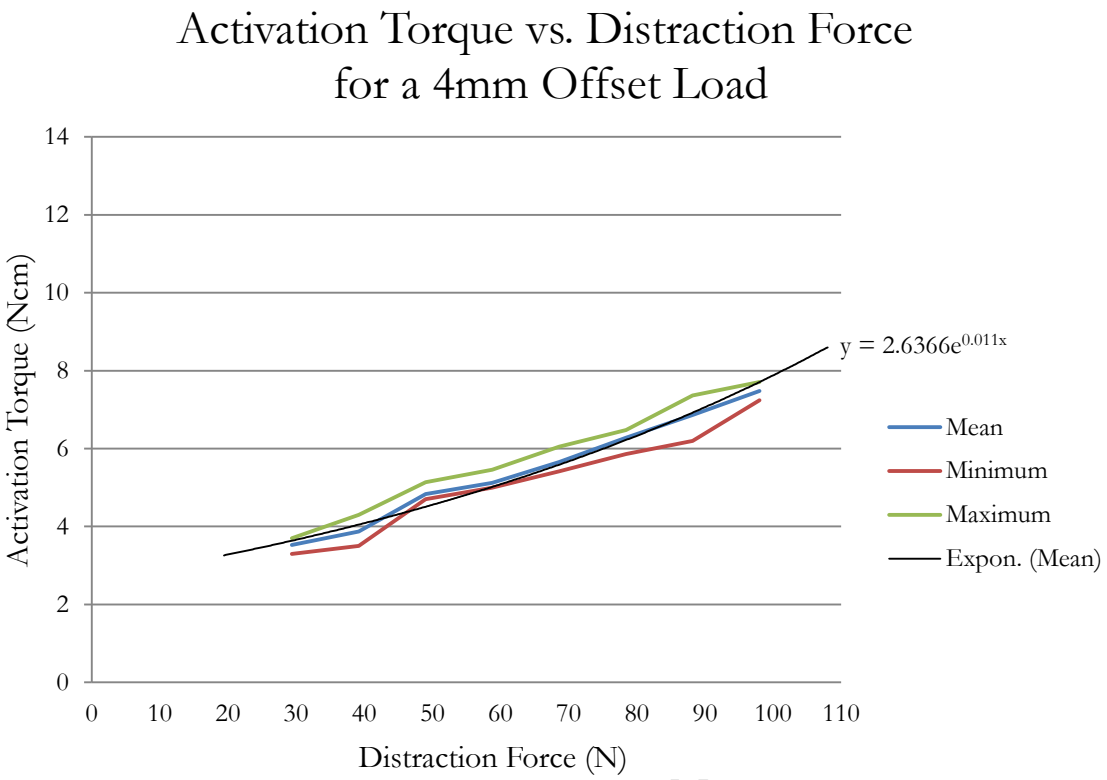

Figure 81: Activation torque vs. distraction force on a straight trajectory with a 4mm offset load, wetted with a detergent solution.

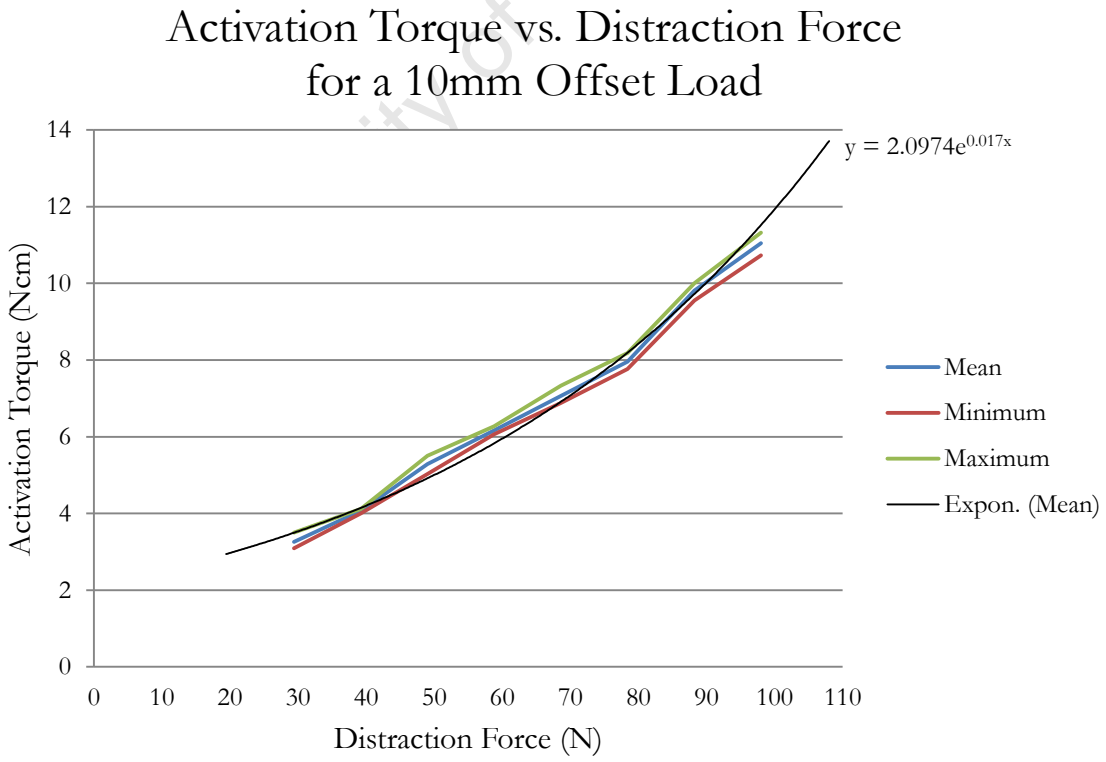

Figure 82: Activation torque vs. distraction force on a straight trajectory with a 10mm offset load, wetted with a detergent solution.

6.1.1.3 CURVILINEAR DISTRACTION UNDER LOAD

In order to assess the reliability of the device before progressing to clinical implementation, a simulated distraction was conducted on a curvilinear trajectory with the device subjected to incrementally increasing distraction loads up to 100 N. A test rig was constructed whereby the locomotive could be loaded approximately tangentially with the desired force (Figure 83). Mass pieces provided the load and a spring-scale provided a reading of the applied force.

The curved trajectory rail mimicked the worst expected case, with a bend radius of 25mm. During this test the device was wetted with a water-detergent solution applied directly to the traction mechanism. The distraction load on the locomotive was applied at a distance of 4mm from the worm-rack.

For each load, the locomotive was activated by 4 quarter-turn increments and the maximum torque for each increment was recorded with an electronic torque-measuring driver[22], as shown in Figure 79. Thus, for each load a set of four readings was taken.

Figure 83: (a) Test rig for simulated curvilinear distraction, (b) spring-scale and mass-pieces connected to cable in (a).

The torque measurements were recorded and the minimum, maximum and mean values were found for each set of four readings. The results are displayed graphically in Figure 84 & Figure 85, with an exponential trendline fitted to the data points.

For these worst-case loading conditions, the following exponential trendlines were found:

$$[y = 1.817e^{0.020x}] \qquad \text{(Eqn. 9)}$$

$$[y = 1.927e^{0.019x}] \qquad \text{(Eqn. 10)}$$

Where y is the torque required (Ncm), and x is the distraction force generated (N).

As discussed in section 6.1.1.2, comparing the coefficients in each equation gives an indication of how consistently the device behaves for the given set of operating conditions. While the mean

trendlines in two independent tests were consistent (compare equations 9 and 10), within each of these tests the activation torque varied greatly for a given distraction force, as can be seen in Figure 84. It was noted that, while the worm-screw rotated smoothly in general, an intermittent 'click' was palpable. These observations indicate irregularities in the traction mechanism, causing the large variations in activation torque measurements, and suggest that the lead-in of the worm-screw thread requires further refinement.

Nonetheless, the activation torque for the maximum distraction load was 16.2 Ncm. Thus, demonstrating the ability of the device to deliver the required distraction force with an activation torque within the 20 Ncm range prescribed in the PRS.

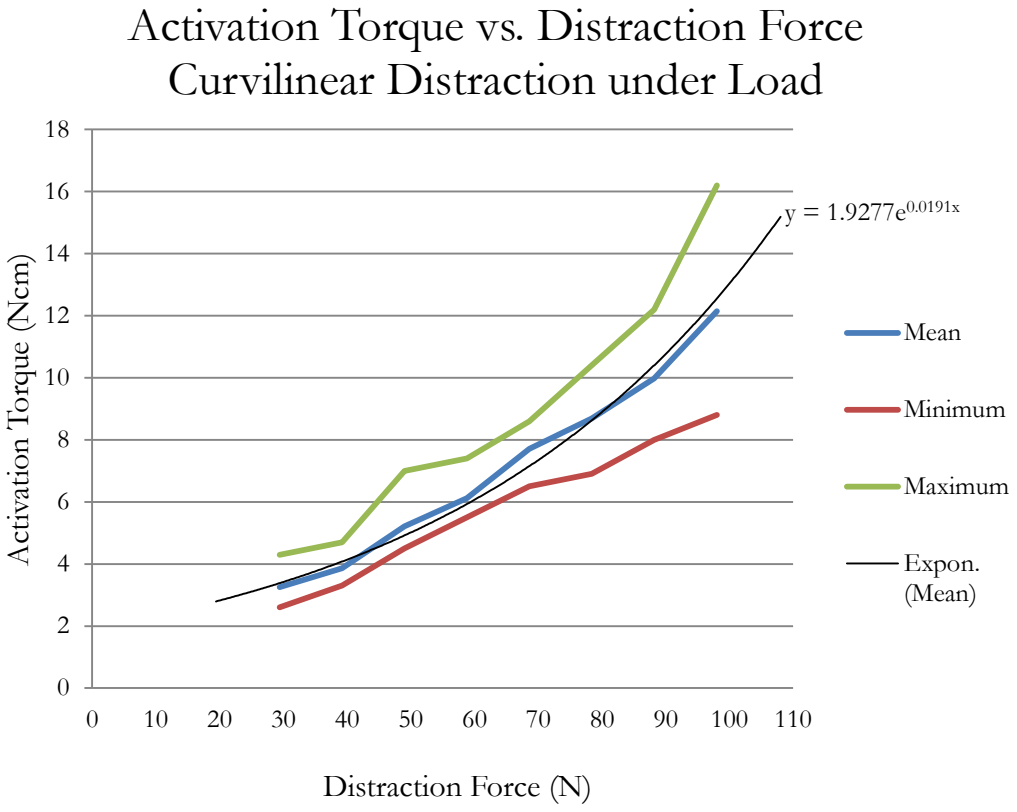

Figure 84: Activation torque vs. distraction force with an offset load on a curved trajectory, wetted with a detergent solution.

Out of all of the tests, the steepest gradient between activation torque and distraction force was observed in the curvilinear distraction test. The flattest gradient was observed for a straight trajectory combined with a 4mm offset load. Figure 85 compares the torque vs. distraction force relationship graphically for these two cases.

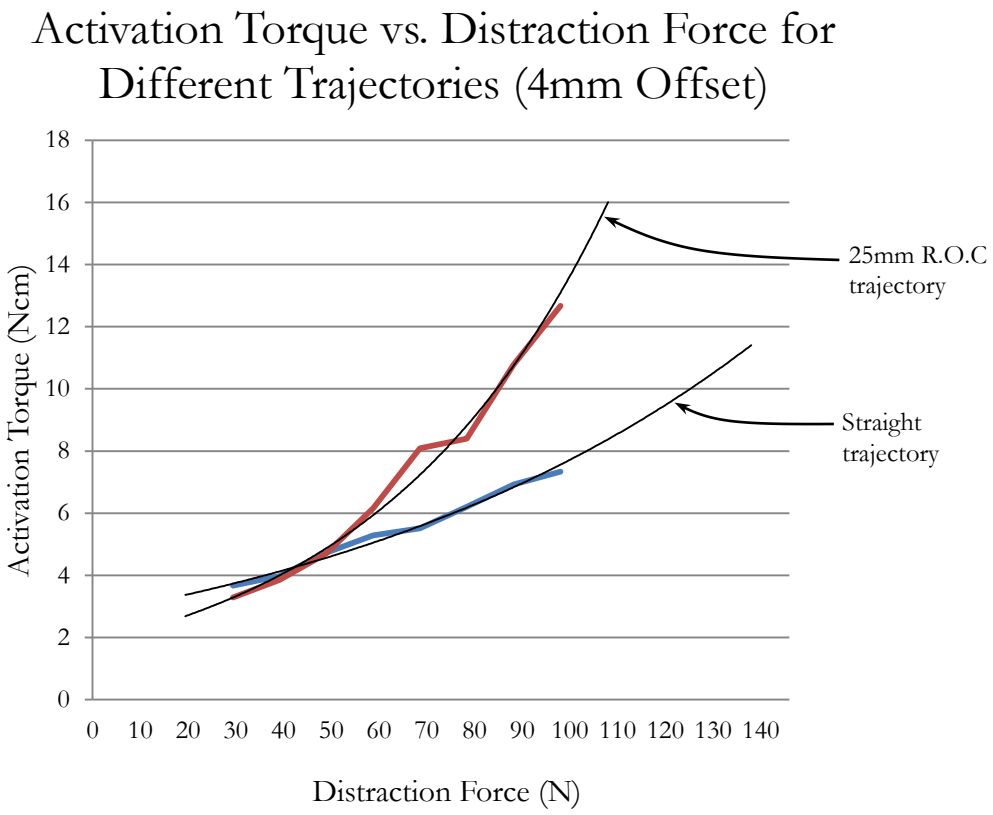

Figure 85: Activation torque vs. distraction force, 4mm offset load on a curved vs. straight trajectory, both wetted with a water-detergent solution.

6.1.2 WORM-RACK: SELF-LOCKING ACTION

The device relies on the self-locking action of the worm-rack interface to stop the locomotive from retracting between activations. In theory, the small thread angle, coupled with friction in the presence of a residual load prevents rotation of the worm, and thus prevents retraction. In TDDO, the significant residual load on the mechanism, in the order of 50 N, produces substantial friction within the mechanism.

In order to evaluate the self-locking action of the traction mechanism, tests were carried out to investigate the amount of retraction caused by the following disturbances:

- Under a constant load of 66 N, the locomotive was 'rocked' fore and aft in the vertical plane to simulate agitation due to intra-oral activity.
- The device was subjected to a cyclic load, fluctuating between 10-66 N, to mimic the cyclic distraction load.

In both tests, the position of the locomotive was measured relative to a fixed datum on the rail before and after manipulation, using a Vernier calliper. Table 3 presents the results:

Table 3: Retraction of the *V3* device in response to cyclic disturbance.

Cyclic Rocking under 66 N Load	Reading (mm)	Δ (mm)
Initial	24.54	0
10 Cycles	24.54	0
20 Cycles	24.54	0
30 Cycles	24.54	0
40 Cycles	24.56	0.02
50 Cycles	24.60	0.06
60 Cycles	24.58	0.04
70 Cycles	24.62	0.08
80 Cycles	24.64	0.1
90 Cycles	24.66	0.12
100 Cycles	24.66	0.12
200 Cycles	24.80	0.26

Cyclic Load (10-66 N)	Reading (mm)	Δ (mm)
Initial	11.52	0
10 cycles	11.52	0
20 cycles	11.53	0.01
30 cycles	11.54	0.02
40 cycles	11.55	0.03
50 cycles	11.55	0.03
150 cycles	11.60	0.08
300 cycles	11.63	0.15
500 cycles	11.80	0.28

The conditions investigated in this test were extreme. Nevertheless, the device exhibited less than 0.3mm of retraction. Given that distraction rates between 0.5mm and 1.5mm per day produce good results, retraction of 0.3mm in the worst case was deemed acceptable.

6.1.3 BASE-CLAMP INTERFACE: SLIPPAGE

The base-clamp feature of the *V3* device permits *in situ* adjustment of the distraction trajectory. The base-clamp is controlled via two M3 torx-headed screws. A simple test was conducted to assess whether the base-clamp joint could withstand the leverage of the tongue on the rear end of the trajectory rail, which produces a moment at the base-clamp joint.

A known force was applied on the trajectory rail, 36mm from the pivot. As per the PRS, the device must cater for a vertical tongue force of 12 N.

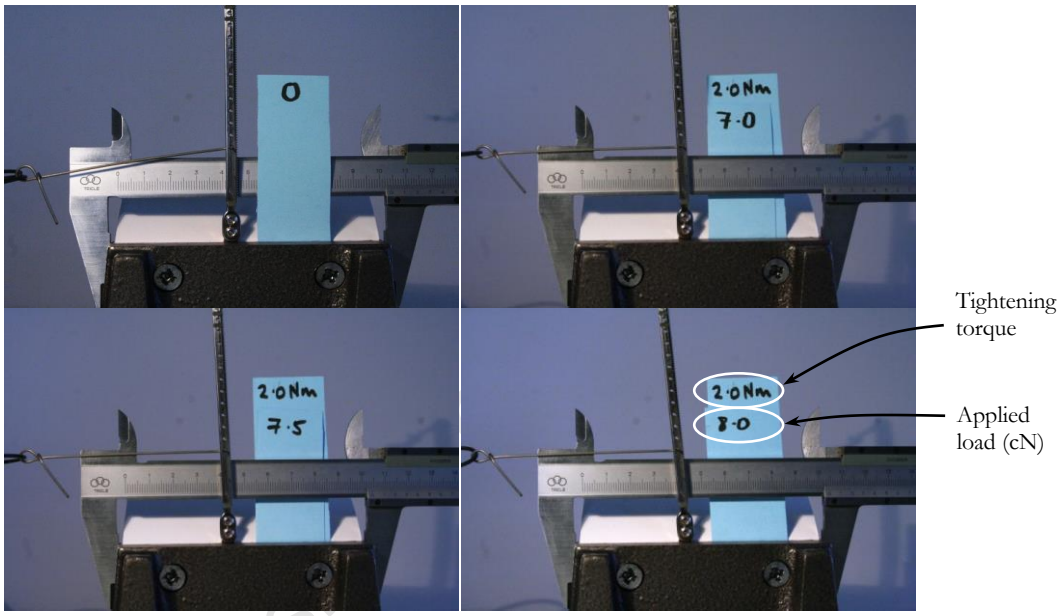

Figure 86: Sequence of photographs from base-clamp slippage test[23].

The clamp screws were tightened to 1.0 Nm, 1.5 Nm and 2.0 Nm, using a torque-limiting screw-driver. With the specimen clamped in a vice, the initial position of the joint was recorded photographically (see Figure 86). For each tightening torque case, a force was then applied and increased incrementally until slippage was observed. Intermediate photographs of the test apparatus were reviewed to determine the maximum load that was sustained by the joint before slippage.

For a clamp screw tightening torque of 2.0 Nm, within the rated torque range[24] for the specified M3 screw, the joint sustained a moment of more than 2.47 Nm before slippage. The original design

[23] The 7.0, 7.5, and 8.0 values correspond to the load (in cN) applied at a distance of 36mm from the base-clamp. The 2.0Nm value represents the tightening torque.
[24] M3 tightening torque rating for stainless steel 316 ranges from 0.4-3Nm.

calculations estimated a maximum loading capacity of 2.72 Nm; 10% higher than the 2.47 Nm found in testing.

In practice, the maximum conceivable moment that must be withstood by the joint is 1.2 Nm, produced by a vertical tongue force of 12 N acting over a moment arm of 100mm, which is the total length of the trajectory rail. Thus, by withstanding a moment of 2.47 Nm, the base-clamp joint provides a safety factor of 2.1.

6.1.4 Ultimate Strength Testing of Critical Features

Features of the device with critical strength requirements were tested to establish their maximum strength capabilities and the relevant factors of safety. Each of these features was submitted to incrementally increasing loads, either until failure occurred or until the specified upper limit was reached.

Testing assessed the following critical features:

- **Axial loading capabilities of the worm-rack mechanism**. The worm-rack traction mechanism was subjected to an axial load up to a maximum of 200 N.

Results: The device sustained 200 N, providing a safety factor of 2.9 over the 66 N design load.

- **Torque-carrying capabilities of the worm-screw.** The worm-screw was subjected to torsional load up to 50 Ncm. Figure 87, and Figure 88 present the test apparatus.

Results: The worm withstood a maximum torsional load of 35.35 Ncm before plastic deformation was observed, thus providing a safety factor of 2.18 over the maximum activation torque of 16.2 Ncm (see section 6.1.1.3, page 92).

- **Tightening torque of the torx base-clamp screws**. A 2 Nm tightening torque was specified for the base-clamp screws, based on laboratory slippage tests described in section 6.1.3. To ensure that these screws would not fail due to over-tightening in the clinical setting, a safety factor of 2 was desirable. The base-clamp screws were over-tightened to a torque of 4 Nm using a torque-limiting screwdriver and inspected for signs of failure. Failure was defined as thread stripping, shear failure of the bolt shank or stripping of the torx-socket.

Results: The base-clamp screws sustained a tightening torque of 4 Nm, with no signs of failure.

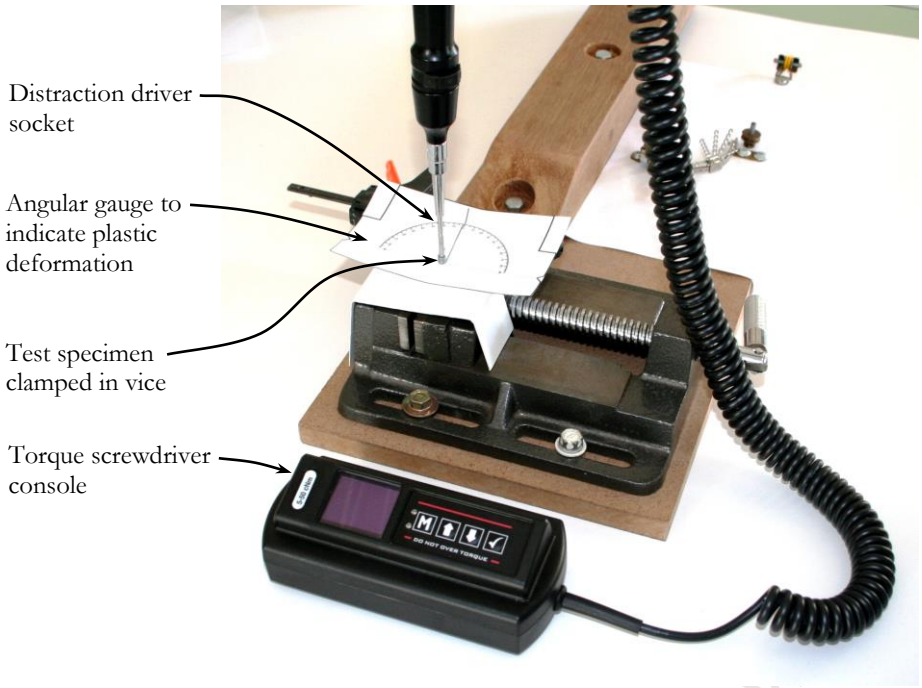

Figure 87: Worm torsion strength test apparatus

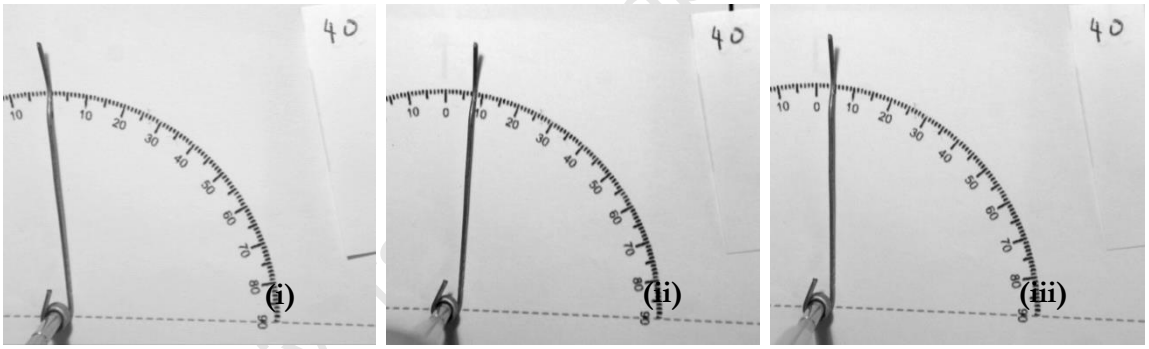

Figure 88: Sequence of photographs of angular gauge from worm torsion testing. (i) Unloaded; (ii) loaded to 40 Ncm; (iii) after torque was released. Plastic deformation is evident between (i) and (iii).

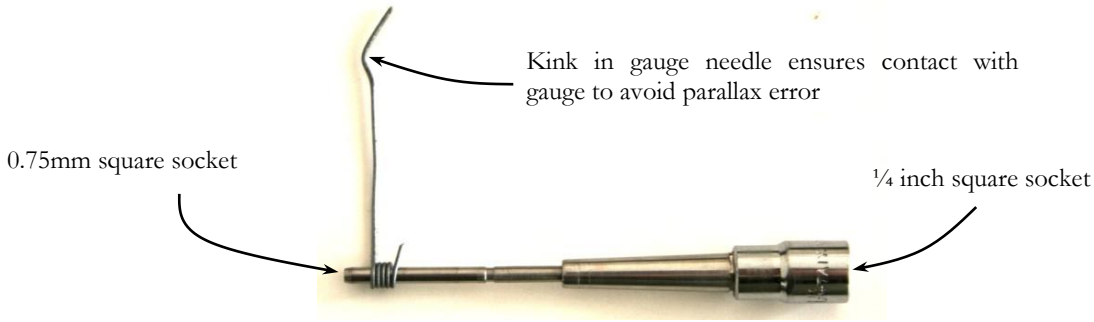

Figure 89: Distraction driver socket for electronic torque screwdriver

6.1.5 RESULTS OF LABORATORY TESTING

The purpose of laboratory testing was to assess whether the device could perform its function in the most extreme conceivable conditions, and to determine the ultimate strength capabilities of the device. The conclusions of testing are presented below, arranged according to the aims outlined in section 6.1.

1. **The *V3* device navigated the minimum-radius trajectory under a load of 100 N:**

The device successfully performed satisfactorily on both a straight trajectory and the minimum 25mm bend radius; in both cases subjected to loads up to 100 N.

2. **The worm-rack interface withstood a load of 200 N; double the maximum expected distraction force of 100 N.**

3. **The worm-screw provides a safety factor of 2.18 over the maximum expected activation torque:**

The maximum conceivable activation torque, determined by practical testing, was 16.2 Ncm. Strength-testing of the worm-screw revealed a torque-carrying capacity of 35 Ncm, thus providing a safety factor of 2.18.

4. **The base-clamp joint withstood the effects of the maximum tongue force:**

The base-clamp joint sustained a moment of 2.47 Nm, providing a safety factor of 2.1 over the maximum foreseeable load of 1.2 Nm. In a separate test, the base-clamp screws sustained a tightening torque of 4 Nm without failure; double the specified tightening torque of 2 Nm. Thus, a large margin of over-tightening is accommodated.

5. **The self-locking action of the worm-rack mechanism limited retraction of the locomotive to tolerable levels:**

The device exhibited retraction of less than 0.3mm under extreme test conditions. These conditions mimicked disturbance by the tongue and the fluctuating distraction load. Given that distraction rates of 0.5 to 1.5mm per day lead to successful bone formation, the 0.3mm of retraction exhibited by the device was deemed acceptable.

6.2 V3 CLINICAL PERFORMANCE

The following observations were made during the third and fourth clinical cases, which employed the *V3* distractor:

1. **The functionality of the base plate-trajectory rail interface was a highly beneficial development.**

By enabling the surgeon to attach and detach the trajectory rail repeatedly, without disturbing the anchorage to the maxilla, the base-clamp feature improved the efficiency of the installation procedure.

2. **The ease-of-deployment of the base-clamp screws demands improvement.**

While the broad functionality of the base plate was found to be beneficial, the surgeon encountered difficulty with the base-clamp screws. These screws were difficult to align with their respective threaded holes in the base plate. It was suggested that the design of these screws be refined with an unthreaded lead-in to aid alignment and that tooling be developed to improve the grip on the screw head for more controlled placement.

3. **Shaping of the cradle plate remained difficult.**

The cradle plate supports and secures the mobile bone transport disc. The *V3* distractor employed a 0.8mm thick titanium cradle plate. The surgical protocol requires that the cradle plate be formed such that it envelopes the bone transport disc, to ensure that it is adequately supported. The surgeon found that in the *V3* format the cradle plate was excessively rigid. In addition, work hardening of the material produced visible cracks in the cradle plate, and led to breakage of one plate. This was partly attributed to the need for tight bend radii (<1mm) on a relatively thick plate (0.8mm).

The surgeon suggested that the formability of the *V2* cradle plate (0.5mm stainless steel) was preferred.

4. **Repetitive removal of the trajectory rail in order to adjust the cradle plate geometry was time-consuming and cumbersome.**

In order to accurately shape the locomotive cradle plate, it was necessary to remove it from the mouth entirely. The *V3* distractor facilitated this with the detachable base-clamp feature. However, for the reasons mentioned in point 2 above, placement of the base-clamp screws was cumbersome. It was suggested the in future versions, the cradle plate should be designed to be detachable from the locomotive so that it can be quickly and efficiently removed and re-attached *in situ*.

5. **Patients reported only minor discomfort.**

Feedback from the patients treated with the *V3* distractor indicated that the device was generally unobtrusive. The most noticeable sources of discomfort and irritation were the accumulation of food in the cradle plate and the palpability of the alveolar buttress plate in the roof of the mouth.

6. **Clinical measurements of activation torque suggested only minor resistance from the healing callus at a distraction rate of between 1mm and 1.5mm per day.**

The distraction activation torque was measured clinically using an electronic torque meter (see section 6.1.1.1 and Figure 79). These in vivo measurements were consistently less than 4 Ncm.

Consulting laboratory data in the graphs in Figure 78 to Figure 85, a 4 Ncm activation torque corresponds to a distraction force of approximately 40 N. This is well within the 100 N loading capabilities of the *V3* device, as described in the entirety of section 6.1.1.

7. DISCUSSION

The objectives of this project, as stated in the introduction to this report were discussed on page 2.

Due to the fledgling nature of TDDO in the maxilla, no precedent existed on which to base or compare the new device. The design process demanded much fundamental study of the distraction osteogenesis technique and its underlying physiological and mechanical principles. In general, this information was not available. In particular, the literature lacked definitive data on the forces involved in TDDO; the only available information pertaining to the mandible, rather than the maxilla. In light of this information shortage initial estimates were made, based on the limited information available at the time.

Based on available information, the aforementioned estimates and in consultation with specialists, a Product Requirement Specification was compiled, which prescribed benchmarks for the capabilities of the new device. Based on these requirements, a novel traction mechanism was developed, utilising a sharp-threaded worm-screw that progressively cut its own 'rack' into a corresponding plastic track. The device performed adequately in bench testing, where it successfully provided a 50 N distraction force, which was at the time thought to be adequate. However, in practice, the actual in vivo forces turned out to be considerably higher than the expected maximum of 36 N, and in the late stages of the first clinical case the *V1* traction mechanism failed due to stripping of the plastic track.

This plastic track was in the form of a low density polyethylene (LDPE) tube, fitted tightly around a Biomet™ mandibular recon plate, providing a rigid, plastic-encased trajectory rail. The following were cited as the major reasons for failure:

The V1 device specifications were based on a single study of mandibular distraction force, which was not confirmed with additional evidence. However subsequent to the first clinical case, further research elicited more information on the magnitude of these forces. This information presented mandibular distraction force measurements of up to 60 N, significantly higher than the previously specified 36 N.

The fact that the device failed only towards the end of treatment supports assertions in the literature that the resistance offered by the healing callus increases over time.

Under prolonged loading, the load-bearing notches in the plastic track failed gradually, due to the combined effects of creep and plastic flow. As these notches failed, the distraction load became

concentrated on a smaller area of the track, thus increasing the load on each notch, further speeding up the rate at which successive notches failed.

Due to the deformable nature of the LDPE track material, there was some slippage between the worm-screw and the trajectory rail. As a result, the notches formed by the leading turns of the worm-screw did not always mesh precisely with successive turns. Instead there was destructive interference between the sharp metallic thread and the relatively delicate plastic notches.

Ultimately, the shortcomings of the plastic track concept were not related to the specific LDPE plastic material, but rather to the nature of plastic materials themselves. To be compatible with the self-cutting concept, the track material must be suitably ductile and pliable. By definition, materials with these characteristics are prone to damage, especially in conditions of prolonged loading. In short, the plastic track concept was found to be fundamentally incompatible with the uncertain aspects of maxillary TDDO, the surgical environment and the long treatment process.

In spite of the failure of the *V1* device, the first clinical case was nevertheless an encouraging success, culminating in full oral rehabilitation: reconstruction of the facial bone structure and the surrounding soft tissues and placement of permanent dental implants. In addition, the first case provided essential insights into the mechanical and ergonomic requirements of the TDDO device and the medical procedure and the distraction healing process and its limitations.

Figure 90: The first clinical case – (a) The defect before treatment, (b) after repair using the *V1* distractor and (c) after dental restoration with permanent implants.

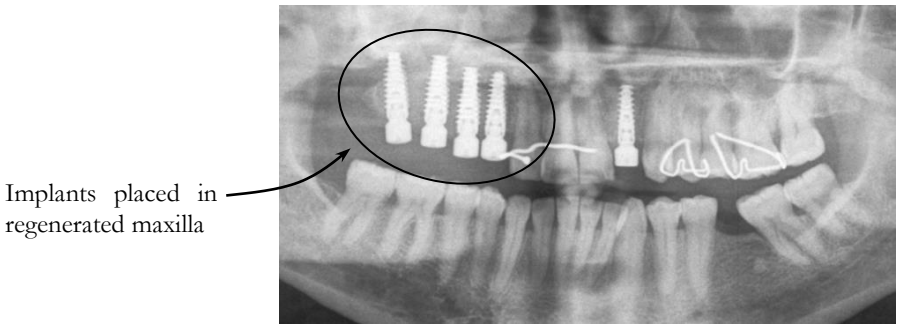

Figure 91: X-ray image of dental implants in regenerate

The *V2* device introduced a metal-on-metal traction mechanism wherein the worm-screw engaged with a toothed rack in the trajectory rail. The main concern with this type of rigid mechanical engagement was the fact that bending would be likely to distort the trajectory rail, leading to jamming of the mechanism. To overcome this, a small amount of backlash was incorporated into the mechanism design. The *V2* distractor satisfied the mechanical requirements in bench testing and facilitated the clinical repair of a major maxillary defect of approximately 80 mm, spanning the midline of the jaw.

Having satisfied the basic functional requirements, the design was refined ergonomically to better cater for intra-operative needs and to improve the broad patient experience. These final refinements included a unique and versatile method of anchoring the device which considerably simplified the initial surgical procedure and reduced operating time. The *V2* locomotive was also reduced to less than half the volume of the first version and the outer profile was smoothed for improved comfort.

The current *V3* device has been implemented in two clinical maxillary reconstruction cases. Although treatment of these patients has not yet reached completion, feedback from patients and the surgeon has endorsed the device for its functionality, ease-of-installation and operation and comfort. Regarding the ergonomics of the device, opportunities for further enhancement were highlighted. These enhancements generally pertained to the interface between the base plate and trajectory rail, the format of the bone transport cradle plate and the attachment interface between the cradle plate and the locomotive.

Although the design process was iterative, it was nonetheless systematic and focused – first addressing the basic functional requirements and gradually moving attention to higher-level ergonomic refinements. This approach ensured that design variables were always limited to a manageable number and that the behaviour of the device could be closely studied and refined.

The recommendations for further development, presented in section 9 will form the basis of the next generation distractor, the *V4,* which is beyond the scope of this work.

8. CONCLUSIONS

In conclusion, this project culminated in a device that successfully performs curvilinear TDDO in the human maxilla. The final version of the device aligns with both qualitative and quantitative recommendations in the literature, which are summarised in the PRS, section 3.3:

8.1 GENERATES THE REQUIRED DISTRACTION FORCE

In functional bench-tests the *V3* distractor actively provided the required distraction force of 100 N. The maximum expected distraction load, according to multiple sources in the literature, is approximately 60 N. Thus, the device provides a safety factor of more than 1.5.

The worm-screw demonstrated practically its ability to transmit the required activation torque. The worm safely sustained a torque of 30 Ncm, providing a safety factor of 1.5 over the maximum distraction torque of 16 Ncm, determined by physical testing.

8.2 PROVIDES THE REQUIRED CONTROL AND STABILITY

Distraction can be controlled to an accuracy of ±0.05mm. This is based on the assumption that the user is capable of rotating the worm-screw to within ±18° of a set-point.

The literature cited the potentially adverse effects of excessive micromotion on the TDDO healing process. Accordingly, the device was designed according to the principles of solid mechanics to limit deflection to the order of 0.5mm, which were deemed tolerable by the medical collaborator.

8.3 INTRA-ORAL

The device is housed entirely within the natural confines of the mouth and never requires protrusions though the skin. Where there is contact with the oral soft tissues, the outer surfaces of the device, particularly those of the mobile elements, were smoothly contoured and highly polished to minimise abrasion and the associated discomfort.

With the traction mechanism located below the trajectory rail the activation mechanism is not obscured by the soft tissues and thus is always accessible intra-orally. To compensate for the confinement of the mouth, the distraction screwdriver can be engaged with the worm activation head

misaligned by up to 10°. This universal-type joint accommodates misalignment without transferring undesirable bending stresses onto the worm-screw.

8.4 Size of the Device

By incorporating the traction mechanism into the trajectory rail and locomotive, the size of the device has been substantially reduced without compromising on either strength or reliability. Furthermore, by situating the traction mechanism inferior to the trajectory rail, the locomotive protrudes less than 2.5mm beyond the outer surface of the rail, crucially minimising the extent to which the device intrudes on the soft tissues of the cheek. This refinement greatly reduces the discomfort experienced by the patient during the lengthy treatment process, which can extend to 6 months in some cases.

8.5 Easily Customisable Geometry

The device supports customisation in various ways:

1. The ***trajectory rail*** can be curved to a minimum radius of 25mm, to mimic the desired maxillary arch geometry, and it can be trimmed to the appropriate length.
2. The maxillary ***base plate*** can be accurately adapted to accurately match the surface contours of the maxilla, and dental roots can be easily avoided due to the accommodating layout of the base plate anchorage holes. The base plate caters for up to four Ø2.4mm anchorage screws, which can be angled by up to 15° off-axis.
3. The versatile ***clamp-screw*** connection between the base plate and trajectory rail allows the surgeon to externally fine-tune the distraction vector in three dimensions during the installation procedure; without compromising the anchorage of the base plate to the native maxilla.
4. The ***transport disc cradle*** can be shaped according to case-specific geometry to form an enveloping 'basket' to rigidly support the bone transport disc. This is, however, an area where further refinement is suggested.

8.6 General Performance and Expectations of the Device

In all areas of the design the worst-case scenario was considered, in terms of the loads applied to the device and to safety, and in terms of the desired customisation.

While the research team endeavoured to foresee all possible eventualities, in practice it is likely that further issues will arise regarding the operational ergonomics and/or the reliability of the device. Four cases of TDDO treatment were initiated during the project, using three versions of the device. The first case has reached completion, with successful dental implantation. During these case studies, emerging shortcomings of the devices were addressed with successive refinements. Likewise, in the course of ongoing experience, further opportunities for added refinements of the design will undoubtedly arise.

9. RECOMMENDATIONS

The following recommendations aim to direct future design refinements. These pertain mainly to the ease-of-installation aspects of the device.

9.1 BASE-CLAMP SCREW INTERFACE: SCREW HOLDING & LOCATING FEATURES

While the base plate-trajectory rail clamp interface proved highly beneficial, the surgeon found deployment of the base plate clamp-screws awkward and frustrating. To remedy this, it was recommended that:

- The design of the base-clamp screw threads should incorporate a narrower lead-in, slightly less than the minor diameter of the M3 thread to easily align the clamp screws in their respective holes.
- A specialised screwdriver-screw gripping system should be developed, which allows the base clamp screws to be captively latched onto the driver. Such a feature would improve the dexterity in inserting the screws and mitigate the dangers of handling small, loose components within the oral cavity.

9.2 CRADLE PLATE RIGIDITY: PROFILE, THICKNESS & MATERIAL CHOICE

Aside from the difficulties encountered with the base clamp, the most challenging aspect of *V3* installation involved shaping of the transport disc cradle plate. The *V3* cradle plate, cut from 0.8mm titanium alloy sheet, was found to be too rigid and showed signs of cracking due to work hardening when bent sharply and/or repeatedly. The surgeon reported that, in terms of its formability of the cradle plate, the *V2* device had been preferred. The *V2* cradle plate was cut from 0.5mm sheet stainless steel 316 alloy.

Based on this feedback, it is recommended that future versions employ a medical grade stainless steel cradle plate, since stainless steel alloys are generally more resilient against work hardening than titanium alloys. The surgeon requested that in future versions the rigidity of the cradle plate should mimic that of the *V2* device.

9.3 DETACHABILITY OF THE TRANSPORT DISC CRADLE

Clinical implementation of the *V3* device highlighted an opportunity to greatly simplify the surgical installation procedure, involving the ***transport disc cradle plate*** subsystem. In order to provide adequate support of the bone transport disc, the cradle plate must be formed by the surgeon such that it envelopes the ***bone transport disc*** (see Figure 64, page 73). This requires that the plate be carefully and iteratively manually shaped. Ideally, this shaping should be done outside of the mouth, rather than ***in situ***. However, during this shaping process, in order to extract to cradle plate from the mouth, the locomotive and trajectory rail had to be removed as well[25]. This unnecessary removal the trajectory rail caused frustrating delays during surgery, and was exacerbated by issues with the base clamp screws, as discussed in section 9.1.

A simple remedy to this problem is to make the cradle plate detachable from the locomotive ***in situ***, allowing the cradle plate to be extracted without disturbing the locomotive or trajectory rail. Thus, the trajectory rail can be installed with the locomotive pre-loaded, independent of the cradle plate, which can then be shaped freely before final attachment to the locomotive.

The major benefits of this modification are as follows:

- The cradle plate can be shaped outside of the mouth where it is more easily manoeuvrable and accessible with bending and trimming tools.
- The cradle plate can be replaced if it becomes damaged or needs major reshaping.
- A range of cradle plates can be provided in kit form with varying geometries, from which an appropriate plate can be chosen according to the specific requirements of the individual case.

This added functionality had been considered previously, but at that stage the benefits did not seem to justify the added complexity and cost. Locomotive and cradle plate detachability is discussed further in Appendix H.

[25] The *V3* device the locomotive and cradle plate form a single, pre-assembled unit, and removal of the locomotive requires removal of the trajectory rail.

9.4 MULTISTAGE DISTRACTION

In the *V2* clinical case, which involved distraction along a particularly long arc, the regenerate formed a straight chord between the initial osteotomy and the locomotive, rather than the desired curved arc defined by the trajectory rail. This was termed the *'rubber band effect'*. It was suggested by the surgeon that multi-stage distraction might be applied to compensate for the rubber band effect.

Multi-stage distraction has been successfully applied in mandibular distraction. Rather than a single bone transport disc, two distinct discs are created by way of two osteotomies; a leading disc and a trailing disc. This technique provides two healing interfaces, thereby producing bone at double the rate of a single interface.

This same concept might be applied to curvilinear distraction in such a way that the trailing bone transport disc could be halted midway through distraction and rigidly secured to the trajectory rail, which might stabilise the regenerate near the centre of the curved arc. The leading disc would continue on its trajectory, repairing the remaining defect. By stabilising the regenerate near the centre of the arc, the trailing disc might reduce the tendency of the regenerate to straighten, facilitating the repair of larger curvilinear defects than otherwise possible.

Future versions of the device should consider the potential for multi-stage TDDO.

9.5 STUDY OF THE DISTRACTION FORCE

This project opened up opportunities for detailed study of the forces involved in callus stretching. The literature provided limited data on the magnitude of distraction forces in the craniofacial complex, due largely to the fledgling nature of craniofacial TDDO. Nonetheless, some studies were found, which measured the mandibular distraction force. Since existing distraction devices generally utilise a power-screw mechanism to generate the distraction effect, several of these studies involved laboratory correlation of activation torque with the distraction force produced. By measuring the activation torque in vivo and comparing these measurements with correlative laboratory data, the in vivo distraction force can be inferred.

Since the maxillary TDDO cases presented in this document are the first of their kind in humans, such a study would contribute greatly to the understanding of the mechanics of TDDO bone formation, by providing data on the:

- Changes in the callus stretching force as treatment progresses.
- Relationship between distraction rate and callus stretching force.
- Relationship between callus stretching force and the properties of, and rate of bone generation.

During testing of the *V3* distractor the feasibility of such a correlation was investigated. In controlled laboratory conditions the activation torque and distraction force were correlated. The data is presented in Appendix G.

The results showed clear trends in the relationship between the applied load and the activation torque, which could be used to infer the distraction load in vivo. However, for the *V3* device there were large variations in the torque-force relationship for different test conditions, such as trajectory rail bend radius. The correlation experiment is presented in detail in Appendix G.

At this stage, minor inconsistencies in the performance of the current version of the device do not lend themselves to such a study. However, as the device is refined further such a study may become viable.

BIBLIOGRAPHY

Akay, M. C. (2011). Distraction Osteogenesis of the Maxillofacial Skeleton: Clinical and Radiological Evaluation. In K. Subburaj, *CT Scanning - Techniques and Applications*. InTech.

Bhatt, K. A., Chang, E. I., Warren, S. M., Lin, S., Bastidas, N., Ghali, S., . . . Gurtner, G. C. (2007). Uniaxial Mechanical Strain: An In Vitro Correlate to Distraction Osteogenesis. *Journal of Surgical Research*, 329–336.

Burstein, F. D., & Williams, K. J. (2004). Resorbable bone distraction: current status and future directions. *Clinical Plastic Surgery*, 407–414.

Burstein, F. D., Lukas, S., & Forsthoffer, D. (2008). Measurement of Torque During Mandibular Distraction. *The Journal of Craniofacial Surgery*, 644-647.

Chen, J., Liu, Y., Ping, F., Zhao, S., Xu, X., & Yan, F. (2010). Two-step transport-disk distraction osteogenesis in reconstruction of mandibular defect involving body and ramus. *International Journal of Oral & Maxillofacial Surgery*, 573–579.

Cheung, L., Chow, L. K., & Chiu, W. K. (2004). A randomized controlled trial of resorbable versus titanium fixation. *Oral Surgery, Oral Medicine, Oral Pathology, and Endodontology*, 386-397.

Dahlberg, T. (2004). Procedure to calculate deflections of curved beams. *International Journal of Engineering*, 503-513.

Elias, C., Lima, J., Valiev, R., & Meyers, M. (2008). Biomedical Applications of Titanium and its Alloys. *Journal of the Minerals, metals, and Materials Society*, 46-49.

Elsalanty, M., Zakhary, E., Akeel, S., Benson, B., Mulone, T., Triplett, G. R., & Opperman, L. Y. (2009). Reconstruction of Canine Mandibular Bone Defects Using a Bone Transport Reconstruction Plate. *Annals of Plastic Surgery*, 441–448.

Gray, H., & Banniser, L. (1995). Gray's Anatomy: The Anatomical Basis of Medicine and Surgery. Oxford: Elsevier Books.

Hendricks, R., & Vicatos, G. (2011-2012). Dr. (J. Boonzaier, Interviewer)

Kulak, K. L., Fisher, J. W., & Struik, J. H. (1974). *Guide to Design Criteria for Bolted and Riveted Joints*. Chicago: American Institute of Steel Construction.

Lambrechts, H., De Baets, E., Fieuws, S., & Willems, G. (2010). Lip and tongue pressure in orthodontic patients. *European Journal of Orthodontics*, 466-471.

Meyer, U., Kleinheinz, J., & Joos, U. (2004). Biomechanical and clinical implications of distraction osteogenesis in craniofacial surgery. *Journal of Cranio-Maxillofacial Surgery*, 140–149.

Nash, W. A. (1998). Schaum's Outline of theory and problems of strength of materials, Fourth Edition. McGraw-Hill.

Newson, T. (2002). Stainless Steel – A Family of Medical Device Materials. *Business Briefing: Medical Device Manufacturing & Technology*.

Robinson, R., O'Neal, P., & Robinson, G. (2001). Mandibular distraction force: laboratory data and clinical correlation. *Journal of Oral & Maxillofac Surgery*, 539-545.

Romanyk, D. L., Lagravere, M. O., Toogood, R., Major, P., & Carey, J. P. (2012). Review of Maxillary Expansion Appliance ActivationMethods: Engineering and Clinical Perspectives. *Journal of Dental Biomechanics*.

Saunders, M. M., & Lee, J. S. (2008). The Influence of Mechanical Environment on Bone Healing and Distraction Osteogenesis. *Atlas of Oral & Maxillofacial Surgery Clinic of North America*, 147–158.

Serhan, H., Slivka, M., Albert, T., & Kwak, S. D. (2004). Is galvanic corrosion between titanium alloy and stainless steel spinal implants . *The Spine Journal*, 379–387.

Sun, Z., Rafferty, K. L., Egbert, M., & Herring, S. (2006). Mandibular Mechanics Following Osteotomy and Distraction Appliance Placement: I. *Mandibular Mechanics Following Osteotomy and Distraction Appliance Placement: I. Postoperative Mobility of the Osteotomy Site*, 610–619.

Sun, Z., Rafferty, K. L., Egbert, M., & Herring, S. (2007). Masticatory Mechanics of a Mandibular Distraction Osteogenesis Site: Interfragmentary Micromovement. *Bone*, 188–196.

Suzuki, E. Y., & Suzuki, B. (2011). Chapter 2: Assessment of Maxillary Distraction Forces in Cleft Lip and Palate Patients. In V. Klika, *Biomechanics in Applications*. InTech.

Trawitzki, L. V., Borges, C. G., Giglio, L. D., & Silva, J. B. (2011). Tongue strength of healthy young adults. *Journal of Oral Rehabilitation*, 482–486.

Valentim, A. F., Furlan, R. M., de Castro Perilo, T. V., Motta, A. R., Berbert, M. C., Barroso, M. F., . . . de Las Casas, E. B. (2012). Development and Clinical Application of Instruments to Measure Orofacial Structures. *Applied Biological Engineering – Principles and Practice*, 365-390.

Wang, J. J., Chen, J., Ping, F. Y., & Yan, F. G. (2012). Double-step transport distraction osteogenesis in the reconstruction of unilateral largemandibular defects after tumour resection using internal distraction devices. *International Journal of Oral and Maxillofacial Surgery*, 587-595.

Young, W. C., & Budynas, R. G. (2002). Roark's Formulas for Stress and Strain, Seventh Edition. McGraw-Hill.

Zapata, U., Elsalanty, M. E., Dechow, P., & Opperman, L. A. (2010). Biomechanical Configurations of Mandibular Transport Distraction Osteogenesis. *TISSUE ENGINEERING: Part B*, 273-283.

APPENDIX A: WORKING DRAWINGS OF V3 DISTRACTOR

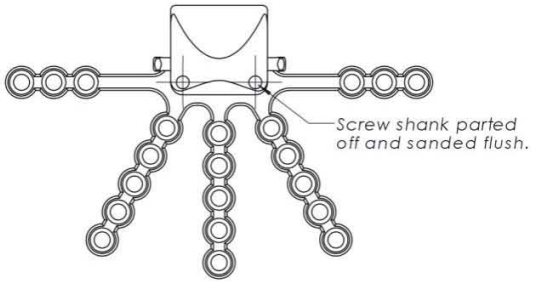

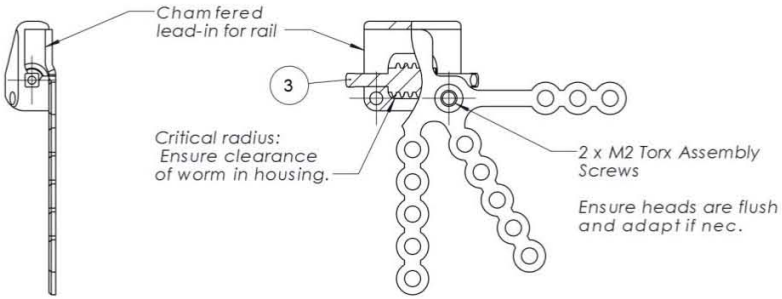

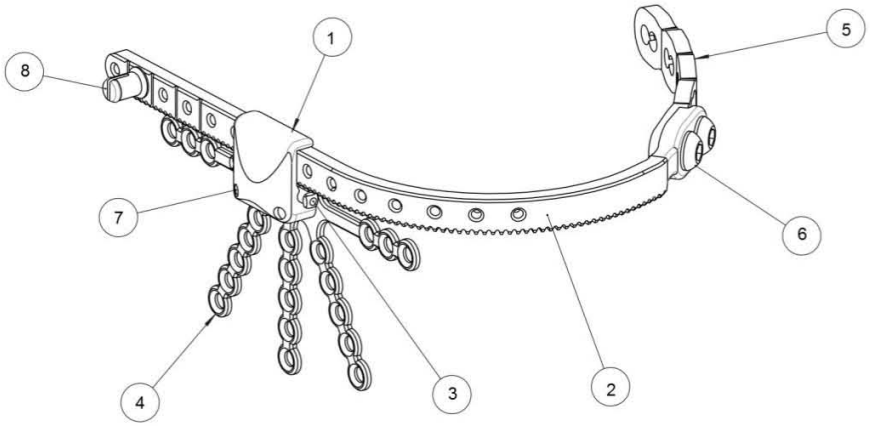

Note: Polished finish on all components.

ITEM NO.	PART NUMBER	QTY.
1	Housing	1
2	Trajectory Rail	1
3	Worm	1
4	Cradle Plate	1
5	Base Plate	1
6	M3 Base Clamp Screws	2
7	M2 Locomotive Assembly Screws	2
8	Confluence Grommet	1

A3 Landscape	University of Cape Town Department of Mechanical Engineering			
	Title: V3 Distractor Assembly			
Assembly Drawing	Scale: 2:1	Date: 2012/12/20	Sheet 1	of 1
	Drawn By: J A Boonzaier		Drawing Number 1 of 7	

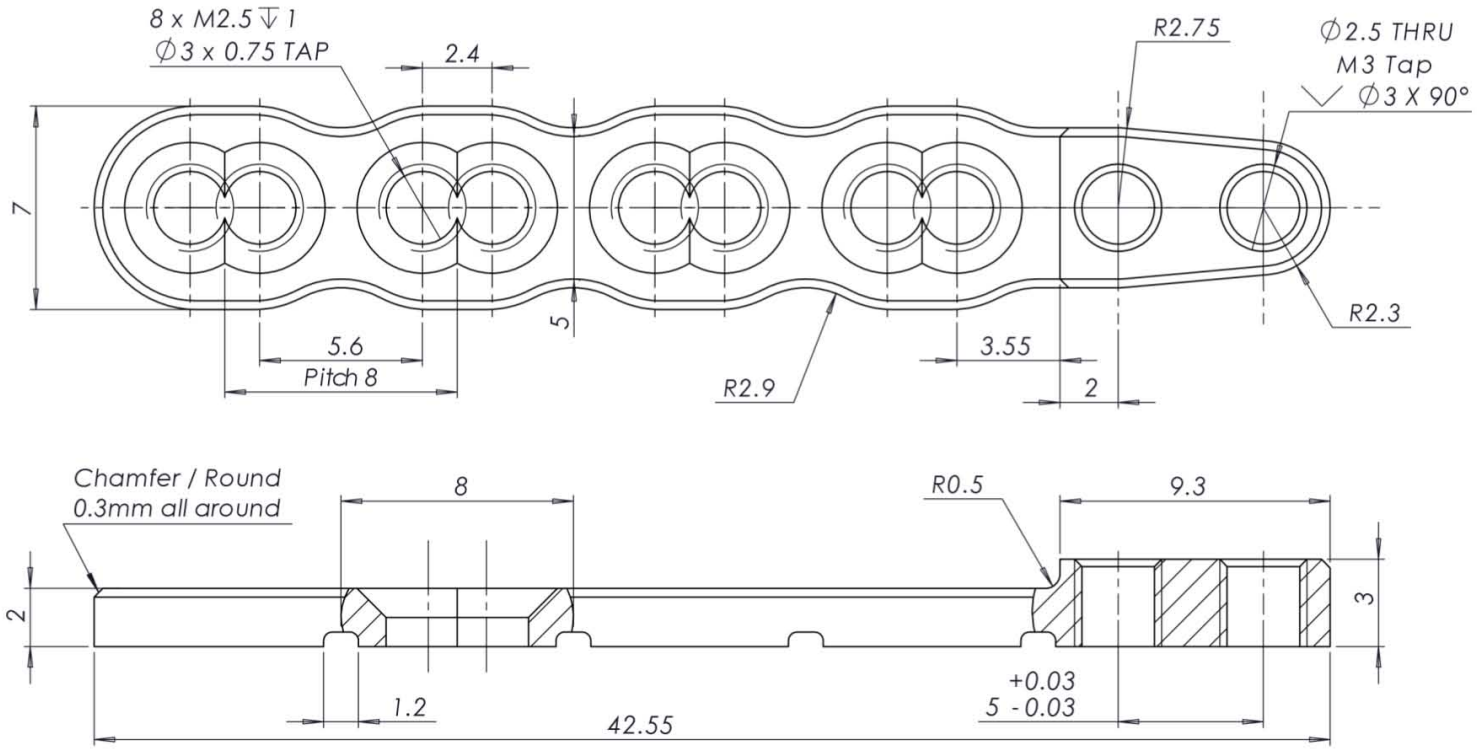

A4 Landscape	University of Cape Town Department of Mechanical Engineering				
	Title: Base Plate				
Quantity:	Part Finish	Date: 2012/12/20	Scale: 5:1	Sheet 1	of 1
Material: Ti (Med. Grade)	Drawn By: J A Boonzaier			Drawing Number 2 of 7	

Note: All sharp edges to be deburred and buffed.

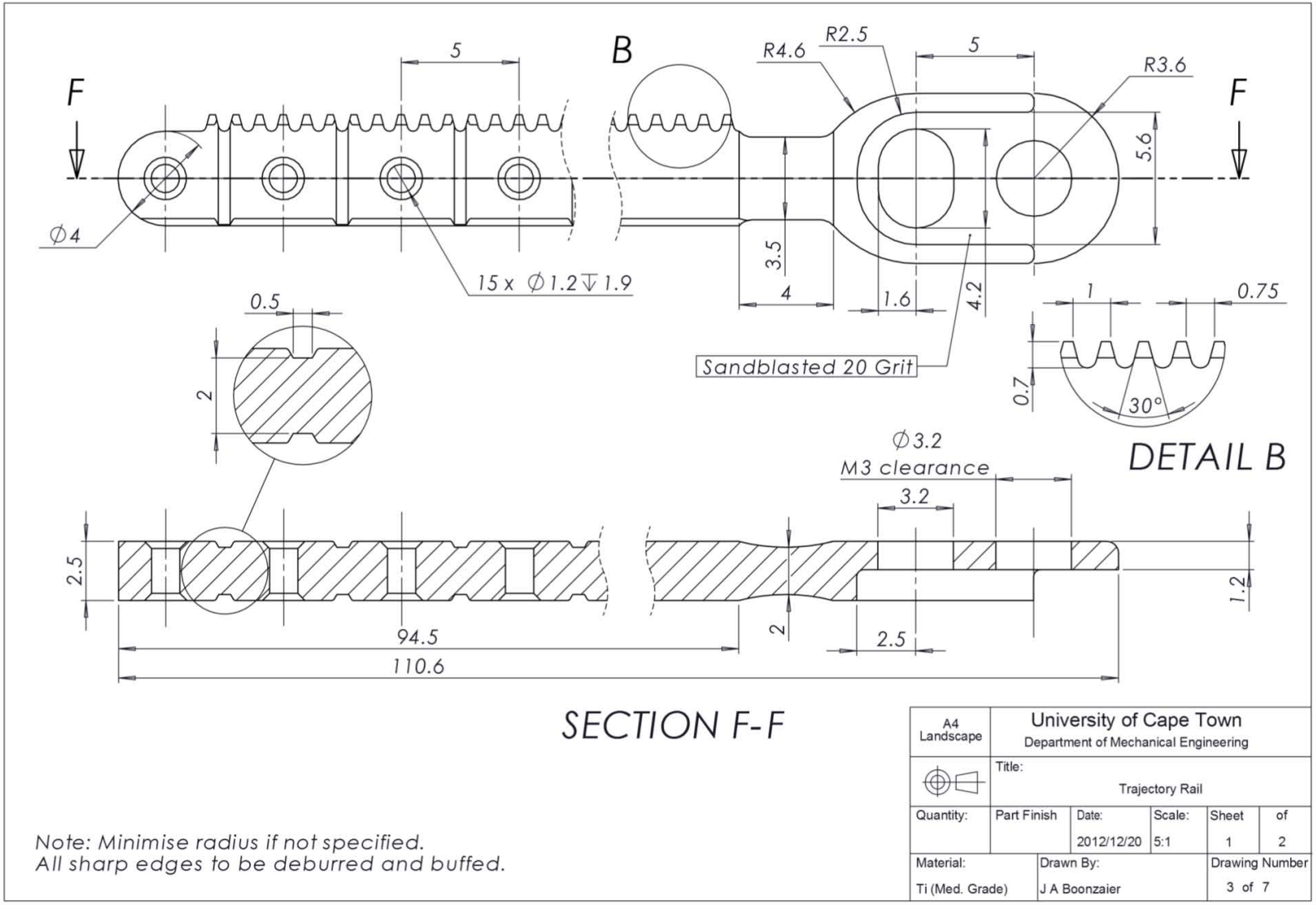

A4 Landscape	University of Cape Town Department of Mechanical Engineering				
	Title: Trajectory Rail				
Quantity:	Part Finish	Date: 2012/12/20	Scale: 5:1	Sheet 1	of 2
Material: Ti (Med. Grade)	Drawn By: J A Boonzaier			Drawing Number 3 of 7	

Note: Minimise radius if not specified.
All sharp edges to be deburred and buffed.

View for outer profile wire cutting

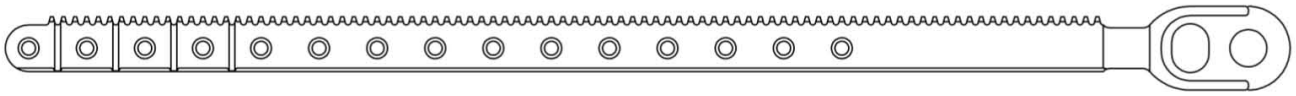

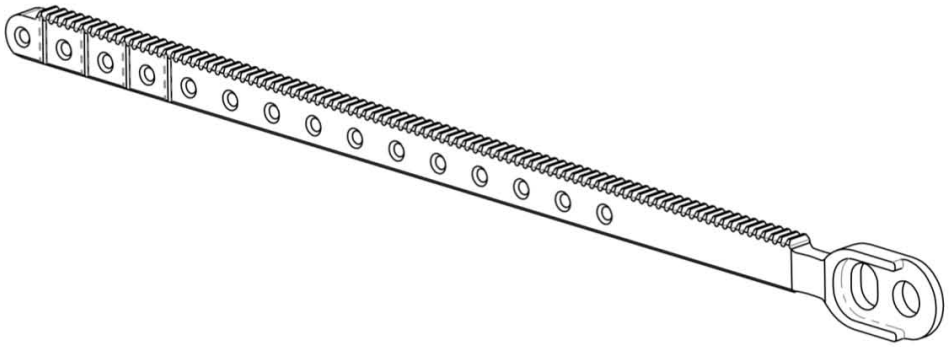

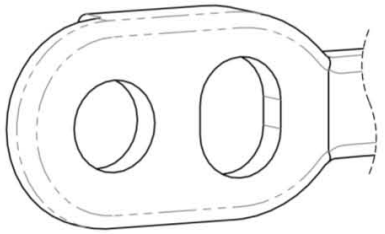

Head Feature Detail

A4 Landscape	University of Cape Town Department of Mechanical Engineering				
	Title: Trajectory Rail				
Quantity:	Part Finish	Date: 2012/12/20	Scale: 2:1	Sheet 2	of 2
Material: Ti (Med. Grade)	Drawn By: J A Boonzaier			Drawing Number 3 of 7	

Note: Deburr and buff all external edges.

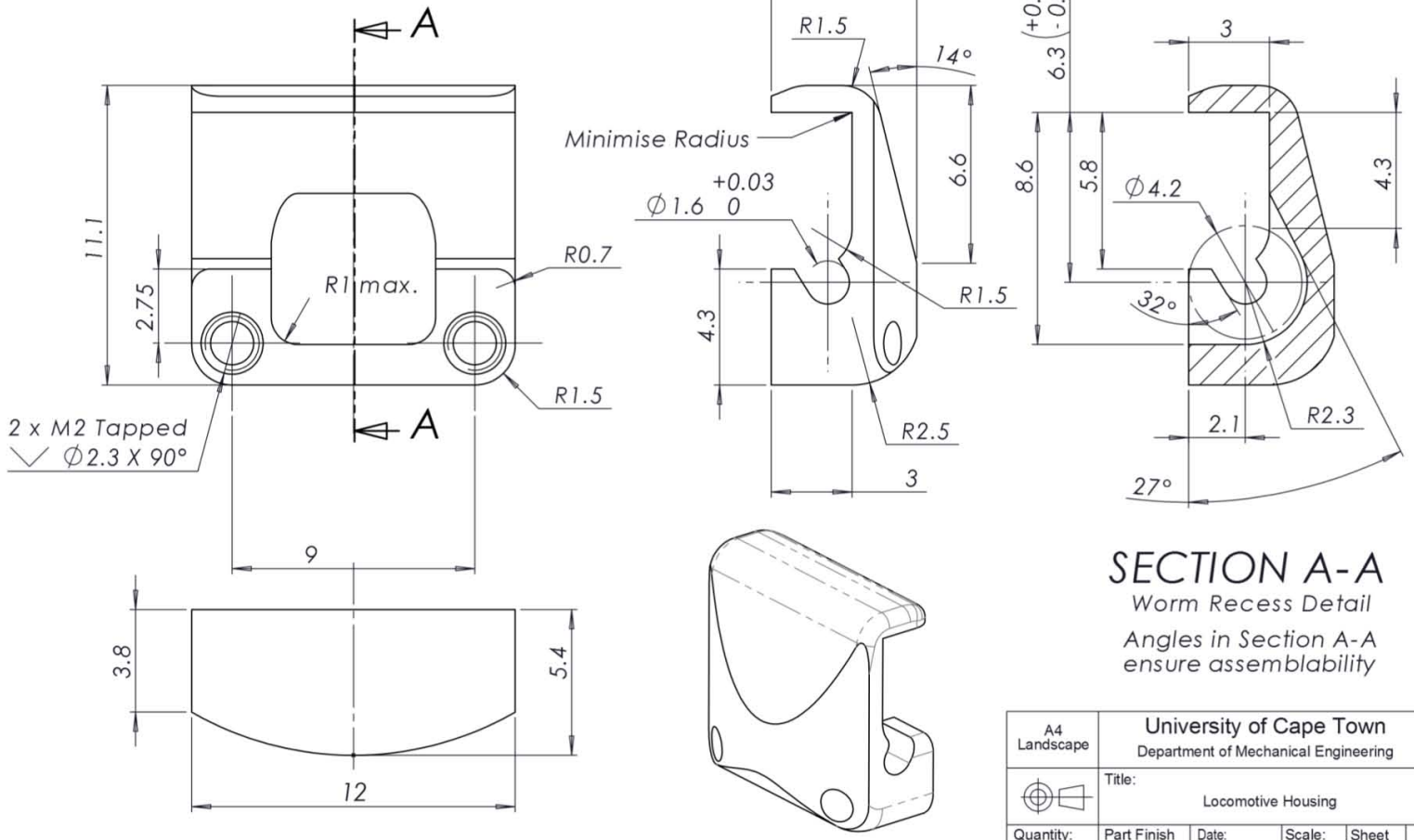

SECTION A-A

Worm Recess Detail

Angles in Section A-A ensure assemblability

A4 Landscape	University of Cape Town Department of Mechanical Engineering				
	Title: Locomotive Housing				
Quantity:	Part Finish	Date: 2012/12/20	Scale: 5:1	Sheet 1	of 1
Material: Stainless Steel 316	Drawn By: J A Boonzaier			Drawing Number 4 of 7	

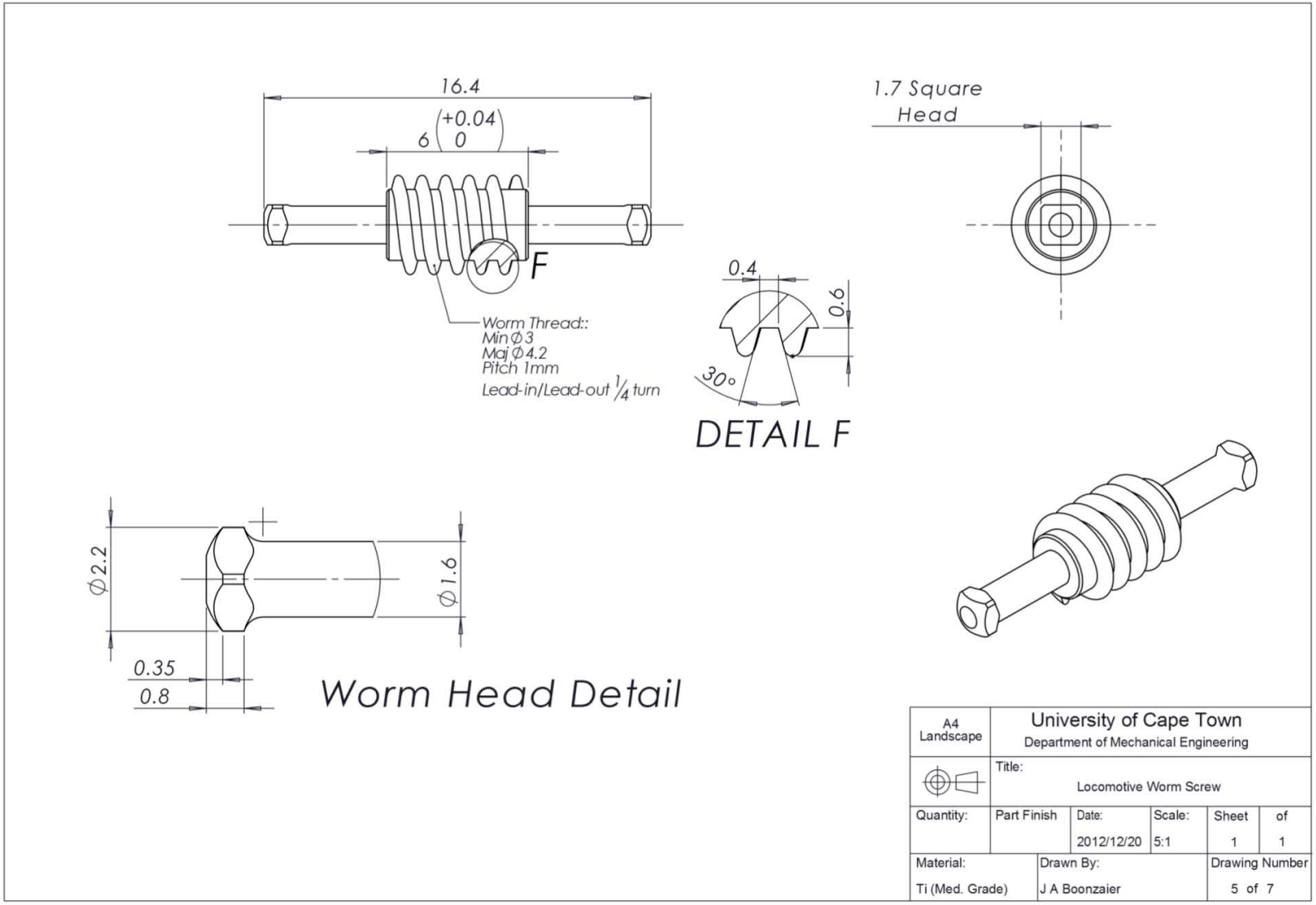
16.4
6 (+0.04 0)
F
Worm Thread::
Min Ø3
Maj Ø4.2
Pitch 1mm
Lead-in/Lead-out 1/4 turn
1.7 Square
Head
0.4
0.6
30°
DETAIL F
Ø2.2
Ø1.6
0.35
0.8
Worm Head Detail
A4
Landscape
University of Cape Town
Department of Mechanical Engineering
Title:
Locomotive Worm Screw
Quantity:
Part Finish
Date:
2012/12/20
Scale:
5:1
Sheet
1
of
1
Material:
Ti (Med. Grade)
Drawn By:
J A Boonzaier
Drawing Number
5 of 7

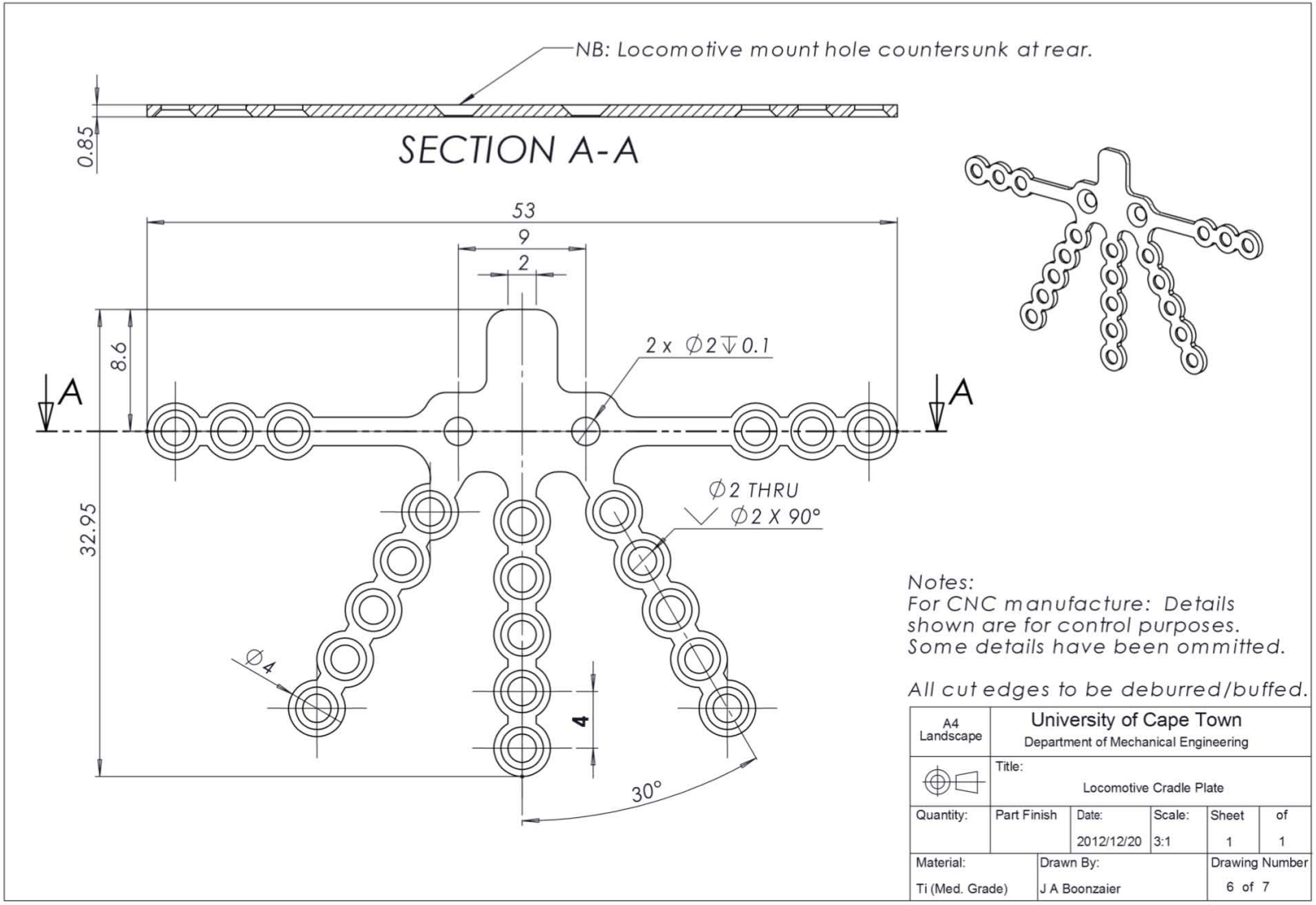
NB: Locomotive mount hole countersunk at rear.
0.85
SECTION A-A
53
9
2
8.6
2 x ⌀2↧0.1
A
A
32.95
⌀2 THRU
⌀2 X 90°
⌀4
4
30°
Notes:
For CNC manufacture: Details shown are for control purposes.
Some details have been ommitted.
All cut edges to be deburred/buffed.
A4 Landscape
University of Cape Town
Department of Mechanical Engineering
Title:
Locomotive Cradle Plate
Quantity:
Part Finish
Date: 2012/12/20
Scale: 3:1
Sheet 1
of 1
Material: Ti (Med. Grade)
Drawn By: J A Boonzaier
Drawing Number 6 of 7

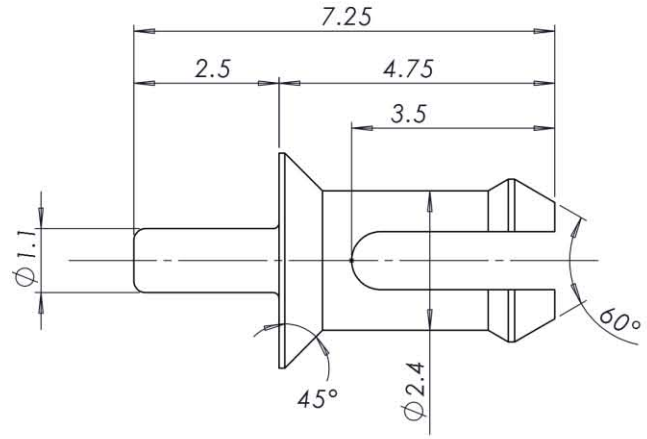

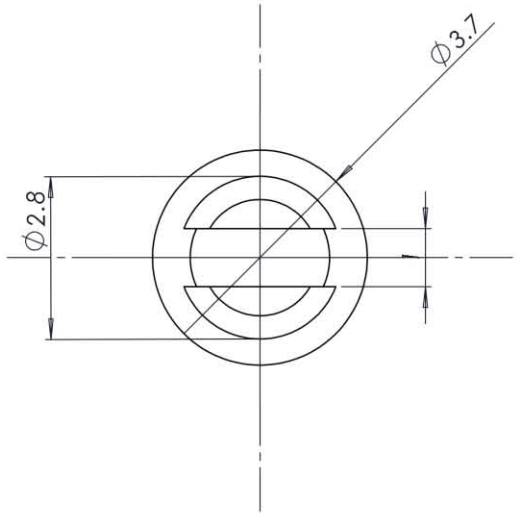

A4 Landscape	University of Cape Town Department of Mechanical Engineering				
	Title: Confluence Grommet				
Quantity:	Part Finish	Date: 2012/12/20	Scale: 10:1	Sheet 1	of 1
Material: Stainless Steel 316	Drawn By: J A Boonzaier			Drawing Number 7 of 7	

APPENDIX B: TRAJECTORY RAIL DESIGN – DEFLECTION DUE TO INTRA-ORAL FORCES

The calculations below investigate the rigidity of the trajectory rail under various intra-oral loads. Their relevance is explained in section 5.2.1.

As stated at the beginning of section 5.2.1, the trajectory rail was designed to provide adequate rigidity to limit micromotion. Therefore, the calculations that follow do not investigate strength or failure characteristics of the trajectory rail, but rather ensure that the deflection characteristics are within acceptable limits.

Applying Castigliano's second theorem, the trajectory rail was modelled as a quarter-circular curved beam, cantilevered at one end and loaded at the other end in three modes: a vertical load of 12 N, a lateral load of 16 N or an axial load of 66 N. [26] For the vertical and lateral loading scenarios, formulae were found in the literature. The axial deflection was derived from first principles.

B. 1. VERTICAL LOADING

For the vertical load, the trajectory rail was modelled as a cantilevered curved beam, as shown in Figure 69. The maximum vertical tongue force (12 N) acting at the point where the rail trajectory straightens, point B, mimics the tongue pushing on the rail in the region adjacent to the second premolar. Due to physiological constraints the tongue is unable to apply a force posterior to point B. Thus the maximum deflection was found at the rear of the rail, point C, given by the equation:

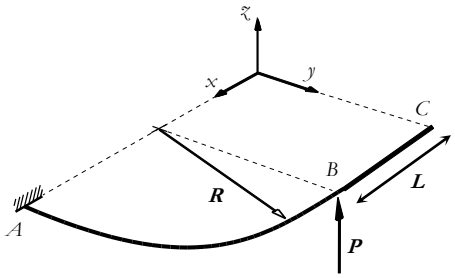

Figure 92: Diagram of vertical bending model of trajectory rail for a vertical load, ***P*** (Nash 1998)

$$\delta_{vertical} = \frac{1}{EI}\left[\frac{\pi}{4}PR^3 + \frac{1}{2}PR^3L\right] + \frac{1}{GJ}\left[\left(\frac{3\pi}{4} - 2\right)PR^3 - \frac{1}{2}PR^2L\right]$$

(Nash, 1998)

[26] 12N and 16N values are based on studies on tongue force in adults presented in section 2.5.4

B. 2. LATERAL LOADING

For the lateral load, the trajectory rail was modelled as a cantilevered curved beam, as shown in Figure 70, with the maximum lateral tongue force acting at the same point as in the vertical case described above, point B. However, since the regenerate forms on the inside of the trajectory rail, between the rail and the tongue, it would not be possible for the tongue to apply a lateral force on the trajectory rail anterior to the locomotive, as the trajectory rail is obscured by the regenerate tissue.

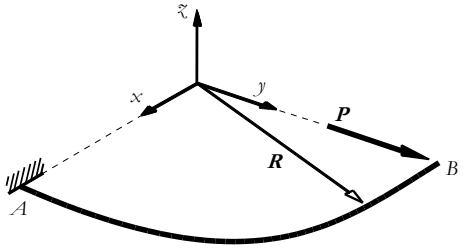

Figure 93: Diagram of lateral deflection model of trajectory rail for a lateral load, ***P***

As such, the critical deflection was taken to be that at the point where the tongue exerts a maximum force, i.e. adjacent to the second premolar. This evaluates to:

$$\delta_{lateral} = \frac{PR^3}{EI} \cdot \frac{\pi}{4}$$

(Young & Budynas, 2002)

B. 3. AXIAL LOADING

Finally, for the load due to the distraction force acting axially, the trajectory rail was modelled identically to that in the vertical deflection case, except with the load acting in line with the straight portion of the rail, at the rear end, point C. The deflection, as calculated by Castigliano's method, evaluated to:

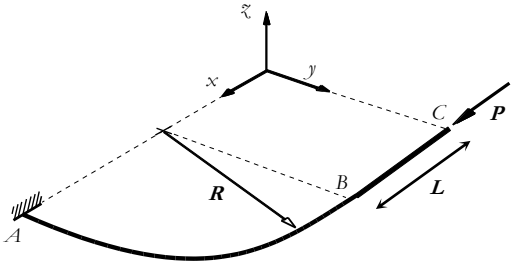

Figure 94: Diagram of bending model of trajectory rail for an axial distraction load, ***P***

$$\delta_{axial,y} = \frac{PR^3}{EI}\left[\frac{3\pi}{4} - 2sin\frac{\pi}{2} + \frac{sin\pi}{4}\right] \quad \text{and}$$

$$\delta_{axial,x} = \frac{PR^3}{EI}$$

The derivation of the axial loading deflection equations is presented overleaf.

B. 4. AXIAL LOADING DEFLECTION DERIVATION

Modelling the trajectory rail as shown in the diagram at right, the deflection at point C in the x- and y-directions can be calculated by Castigliano's method.

For deflection in the x-direction, an expression is found for the bending moment due to $\boldsymbol{P}$ in terms of $\boldsymbol{x}$ an $\boldsymbol{y}$, which is differentiated w.r.t. $\boldsymbol{P}$ to find $\boldsymbol{\frac{\partial M_P}{\partial P}}$.

For deflection in the y-direction, an expression is found for the bending moment due to $\boldsymbol{P}$ and the virtual force, $\boldsymbol{Q}$, in terms of $\boldsymbol{x}$ and $\boldsymbol{y}$, which is differentiated w.r.t. $\boldsymbol{Q}$, to find $\boldsymbol{\frac{\partial M_{P,Q}}{\partial Q}}$.

Each expression is then substituted into Castigliano's definition of deflection, shown below:

$$\delta = \int \frac{M(\frac{\partial M}{\partial Q})}{EI} ds = \int \frac{M(\frac{\partial M}{\partial Q})}{EI} R d\theta$$

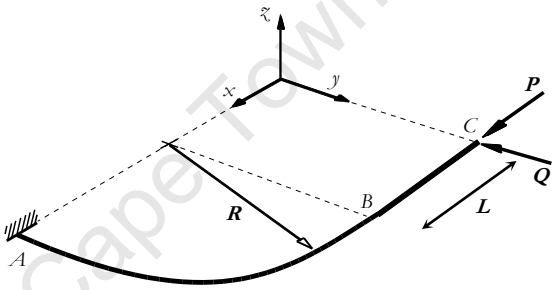

$x = Rsin\theta + L \qquad y = R - Rcos\theta$
$I = 52 \cdot 10^{-12} m^4 \qquad E_{titanium} = 110GPa$
$P = 66N$

$$M_P = Py = P(R - Rcos\theta) \qquad \frac{\partial M_P}{\partial P} = R - Rcos\theta$$

$$\delta_x = \int_0^{\frac{\pi}{2}} \frac{M_P(\frac{\partial M}{\partial P})R}{EI} d\theta = \frac{R^3 P}{EI} \int_0^{\frac{\pi}{2}} (R - Rcos\theta)^2$$

$$= \frac{R^3 P}{EI} \int_0^{\frac{\pi}{2}} \left[1 - 2cos\theta + cos^2\theta\right] d\theta$$

$$= \frac{R^3 P}{EI} \left[\frac{\pi}{2} - 2sin\frac{\pi}{2} + \frac{\pi}{4} + \frac{sin\pi}{4}\right] = 0.64mm$$

$$M_{P,Q} = Py + Qx = P(R - Rcos\theta) + Q(Rsin\theta + L) \qquad \frac{\partial M_{P,Q}}{\partial P} = Rsin\theta + L$$

$$\delta_y = \int_0^{\frac{\pi}{2}} \frac{M_{P,Q}(\frac{\partial M_{P,Q}}{\partial Q})R}{EI} d\theta = \frac{R}{EI} \int_0^{\frac{\pi}{2}} \left[PR^2(sin\theta - sin\theta cos\theta) + QR^2 sin^2\theta + PRL(1 - cos\theta)\right] d\theta$$

$$= \frac{R}{EI} \left[PR^2 \left(-cos\theta + \frac{2cos2\theta}{2}\right) + QR^2 \left(\frac{\theta}{4} - \frac{sin2\theta}{4}\right) + PRL(1 - sin\theta)\right] d\theta$$

$Setting\ the\ virtual\ force,\ Q = 0:$

$$\delta_y = \frac{R}{EI} \left[PR^2 \left(-cos\frac{\pi}{2} + cos\pi\right) + PRL\left(1 - sin\frac{\pi}{2}\right)\right] = \frac{PR^3}{EI} = 1.8mm$$

By Pythagorus' theorem, the resultant deflection at point C is 1.91mm.

APPENDIX C: TRAJECTORY RAIL DESIGN – DISTORTION OF RACK TEETH DUE TO BENDING

The calculations below investigate the effects of bending on the pitch of the trajectory rail rack teeth. Their relevance is explained in section 5.2.2.

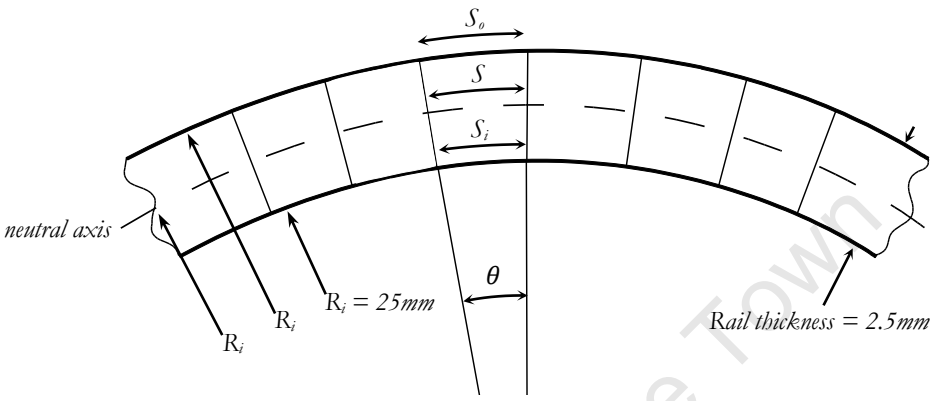

Figure 95: Geometry of curved rail – plan view.

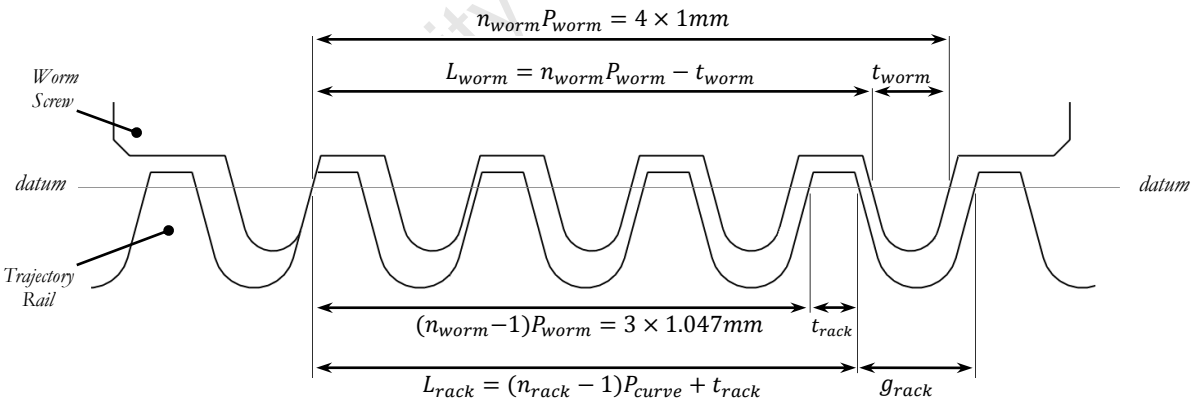

Figure 96: Geometric investigation of traction mechanism.

The worm engages with the rack with a bias towards the outside of the curve, thus the analysis focused on the deformation of the rail's outer edge. Assuming a symmetric neutral bending axis (i.e. equal strain in tension and compression), bending the rail to a 25mm radius of curvature causes a pitch change of ±4.7% on the fringes of the rack. The outside of the curve sees the pitch change from 1.00mm to P_{curve} = 1.047mm. Referring to Figure 74, the following approach was taken:

$$L_{rack} = (n_{rack} - 1)P_{curve} + t_{rack}$$

$$L_{worm} = n_{worm}P_{worm} - t_{worm}$$

$$t_{rack} = P_{curve} - g_{rack}$$

where L_{rack} *is the outer measurement across the rack teeth within the worm envelope;*
L_{worm} *is the inner measurement between the first and last turns of the worm thread;*
n_{rack} *is the number of rack teeth within the worm thread envelope;*
n_{worm} *is the number of turns of the worm;*
P_{bend} *is the pitch of the rack on the outside of the curve;*
P_{worm} *is the pitch of the worm thread;*
t_{rack} *is the width of the peak of the rack teeth;*
t_{worm} *is the worm tooth width in line with the peaks of the rack;*
and g_{rack} *is the gap between the peaks of the rack teeth.*

To avoid interference between the worm and rack:

$$L_{rack} < L_{worm}$$

$$(n_{rack} - 1)P_{curve} + t_{rack} < n_{worm}P_{worm} - t_{worm}$$

$$3 \times 1.047mm + t_{rack} < 4 \times 1mm - t_{worm}$$

$$t_{rack} + t_{worm} < 0.859mm$$

$$Since\ t_{rack} = P_{curve} - g_{rack} = 1.047mm - g_{rack}$$

$$g_{rack} - t_{worm} > 0.141mm$$

APPENDIX D: WORM-SCREW DESIGN – TORSION STRENGTH

The calculations below evaluate the torsion strength of the worms screw shaft at its narrowest point, to ensure that an adequate safety factor is provided. The maximum torsional load expected in practice was approximately 12 Ncm based on studies in the literature on mandibular distraction force.

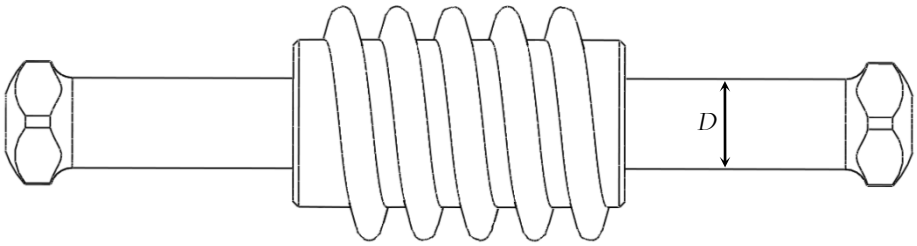

Figure 97: Worm-screw torsion strength – critical shaft diameter, D.

The maximum shear stress induced in the 1.6mm diameter worm-screw shaft was found using the formula:

$$\tau_{max} = \frac{16M_T}{\pi D^3}$$

where M_T is the torque applied to the shaft; and D is the minimum diameter of the shaft.

For an applied torque of 18 Ncm (Safety factor = 1.5) a maximum shear stress of 223.81MPa was calculated. For alloy steels the yield strength in shear, S_{SY}, can be approximated as:

$$S_{SY} = 0.58S_Y$$

where S_Y is the tensile yield strength.

The specified material, cold-drawn and annealed stainless steel 316, has a tensile yield strength of 415MPa, which according to the above relationship, provides a shear yield strength of 240MPa, which is greater than the induced shear stress of 223.81MPa.

Subsequent strength testing of the manufactured worm-screw demonstrated an actual torque-carrying capacity of 30 Ncm, corresponding to a shear strength of 373.02MPa in the worm-screw. This represents an actual safety factor of 2.5 over the expected torque of 12 Ncm.

APPENDIX E: HOUSING DESIGN - DEFLECTION DUE TO DISTRACTION FORCE

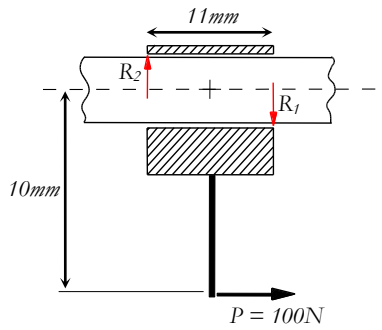

Figure 98: Reaction forces on guide channel due to locomotive tipping moment.

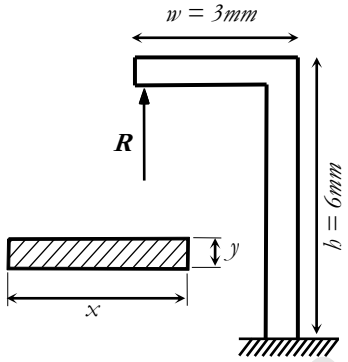

Figure 99: Deflection of housing guide channel.

The offset distraction force (see Figure 98) produces a tipping moment on the locomotive, which in turn produces forces on the guide channel within the locomotive housing. The deflection of the housing caused by these forces was investigated using Castigliano's theorem. The housing was modelled as an inverted L-shaped column, cantilevered at its base and subjected to a vertical force at its far end (see Figure 99). The force, ***R***, applied to the end of the beam represents the reaction of the rail on the housing that balances the moment due by the offset distraction load from the rail. The 100 N distraction force incorporates a safety factor of 1.5 over the maximum expected distraction load of 66 N. The reaction force, ***R***, was found to be 90.91 N. Applying Castigliano's method, the deflection was found to be:

$$\delta = \frac{R^2}{3EI} w^3 + \frac{R^2 h}{EA} = 0.052mm$$

where R is the reaction force from the rail; h is the vertical height of the column; w is the horizontal dimension of the column; E is the Young's modulus of the housing; I is the second moment of area of the cross section; and A is the area of the cross section.

This deflection is negligible, as was the case with similar structural analyses of the housing, rack teeth, base plate and base-clamp features.

APPENDIX F: BASE-CLAMP SLIPPAGE CALCULATIONS

The strength of the connection between the base plate and trajectory rail was investigated, to ensure that it could withstand intra-oral tongue forces. The base-clamp employs two M3 screws that clamp the trajectory rail against the base plate, producing a frictional interface between the two.

The clamping force due to each of the clamp-screws was found by calculating the bolt pretension, F_i, from (Kulak, Fisher, & Struik, 1974):

$$F_i = K_i \cdot A_t \cdot S_p = 1810N$$

where K_i *is a constant* $= 0.9$; A_t *is the tensile stress area of the bolt* $= 5.03mm^4$ *for M3;*
and S_p *is the proof strength of the bolt material* $= 400Mpa$ *for 316 stainless steel.*

The force required to cause slippage, P_{slip}, can then be found from (Kulak, Fisher, & Struik, 1974):

$$P_{slip} = K_s \cdot F_i \cdot m \cdot n$$

where K_s *is the slip coefficient;* F_i *is the initial bolt tension;*
m *is the number of clamped surfaces; and* n *is the number of bolts.*

The maximum moment that could be resisted by friction was then found by modelling the frictional force due to clamping of the surfaces, P_{slip}, as a point load acting at the centre of area of the clamped surfaces. That is:

$$M_{slip} = P_{slip} \cdot s = K_s \cdot F_i \cdot m \cdot n \cdot s \qquad (1)$$

Using Solidworks' cross-section analysis tool, the centre of area was found to be $s = 1.88mm$ from the pivot.

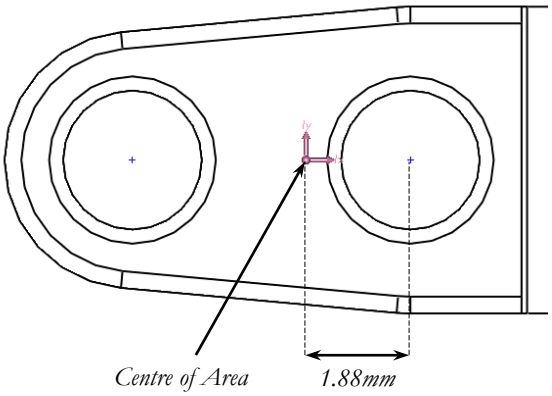

Figure 100: Distance to centre of area of clamped contact surface

The maximum moment load expected in practice was M = 1.2 Nm. For a safety factor of 1.5, M = 1.8 Nm, the minimum slip coefficient, K_s, was found by setting M_{slip} = 1.8 Nm and rearranging (1) thus:

$$K_s = \frac{M}{F_i \cdot m \cdot n \cdot s} = 0.264$$

where $M = 1.2Nm$ *is the applied moment;* $F_i = 1810N$ *is the initial bolt tension;* $m = 1$ *is the number of clamped surfaces;* $n = 2$ *is the number of bolts and* $s = 2.07mm$ *is the distance from the pivot to the centre of area of the clamped surfaces.*

A grit-blasted surface was specified with a grit size of 20, which provides a slippage coefficient, K_s, of at least 0.4 (Kulak, Fisher, & Struik, 1974). Substituting back into (1), the maximum moment before slippage occurs is 2.72 Nm, providing a safety factor of 2.27 over the maximum expected moment of 1.2 Nm.

APPENDIX G: DETAILED REPORT OF V3 BENCH TESTING

G. 1. TEST: AXIAL LOADING CAPABILITIES AND CORRELATION OF ACTIVATION TORQUE WITH APPLIED LOAD

Aims: To test the performance of the *V3* distractor under a range of distraction loads up 100 N on a straight trajectory rail. To evaluate whether the behaviour of the device is consistent, and whether the correlation of distraction activation torque (the torque required to rotate the worm screw) might be useful for determining the in vivo distraction force in forthcoming clinical cases.

Apparatus:

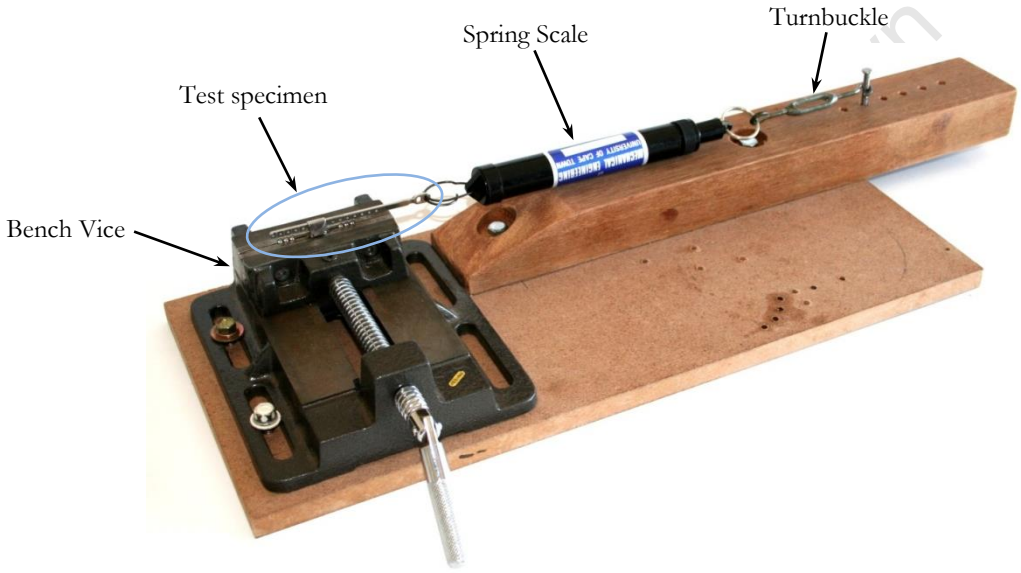

- Test specimen: V3 distractor with straight trajectory rail.
- 16mm medium-density fibreboard base
- 45 x 70mm meranti wooden beam
- Bench vice
- Turnbuckle: 500 N; 80mm – 110mm
- Spring scale: 200 N x 2 N, k_{spring}=250kg/m
- BMS MS050S torque screwdriver:
  - Range: 5-50 Ncm
  - Resolution: 0.01 Ncm
  - Accuracy: +-0.25%
- Distraction driver adapter: ¼" square (male) to 1.75mm square (female)
- Water/detergent solution

Method:

The device was cleaned with a toothbrush in a warm detergent solution to ensure that it was free of any debris or oily residue.

A test rig was constructed that allowed the assembled device to be clamped in the vice by the locomotive and a tensile force applied to the straight rail using the spring scale. The locomotive was clamped with its orientation fixed, to ensure that there was no tipping moment on the traction mechanism. The spring-scale was connected directly to the trajectory rail at one of the base-clamp holes. The turnbuckle in series with the spring scale allowed the preload tension to be adjusted.

The device was preloaded to tensile forces from 0-100 N in increments of 10 N. For each load, the device was activated by four quarter turns amounting to one full rotation of the worm screw. The maximum torque for each quarter turn was recorded using the PEAK function of the torque screwdriver and tabulated in Microsoft Excel. The device was retracted by one rotation after each set of four readings, thereby returning it to its starting point. Thus, each of the test distractions was carried out over the same portion of the trajectory rail.

Using Microsoft Excel, the average, maximum and minimum of each set of four readings was calculated. These were then plotted against the corresponding distraction force and a straight line trendline was added (not force through the origin). An exponential trend-line was also added for each case.

This process was carried out a total of four times; twice without lubrication and twice wetted with a solution of detergent in water.

Results:

The relationship between distraction force and activation torque is demonstrated graphically in Figure 101 to Figure 104.

1. Dry mechanism:

The torque-measuring screwdriver was unable to measure torque values of less than 2.5 Ncm. Accordingly, the lowest recorded torque readings were between 3 to 4 Ncm. For the maximum load of 100 N, the device required an activation torque of 18.05 Ncm and 18.56 Ncm for the two non-lubricated tests.

The relationship between activation torque and distraction load was approximately linear over the range of interest, however in general the relationship appeared to be exponential.

2. Mechanism wetted with detergent solution:

The activation torque vs. distraction force in the lubricated test behaved similarly to the non-lubricated case, but with a shallower slope and a closer approximation to a straight line. The results show a clear dip below the linear trend-line in the central region, suggesting an exponential relationship between activation torque and distraction force. This 'dip' was consistent across all four tests (lubricated and non-lubricated).

For the maximum load of 100 N the device required 8.39 Ncm and 8.82 Ncm, less than half of the required torque for the non-lubricated case.

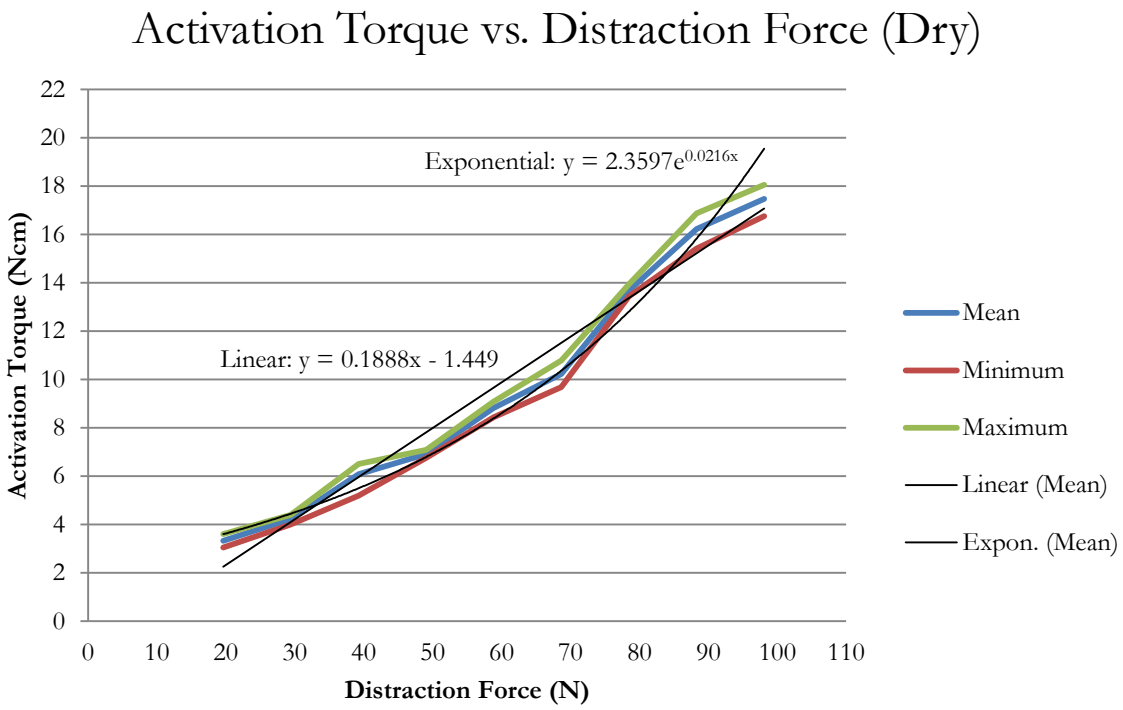

Figure 101: Activation Torque vs. Distraction Force, straight trajectory, dry.

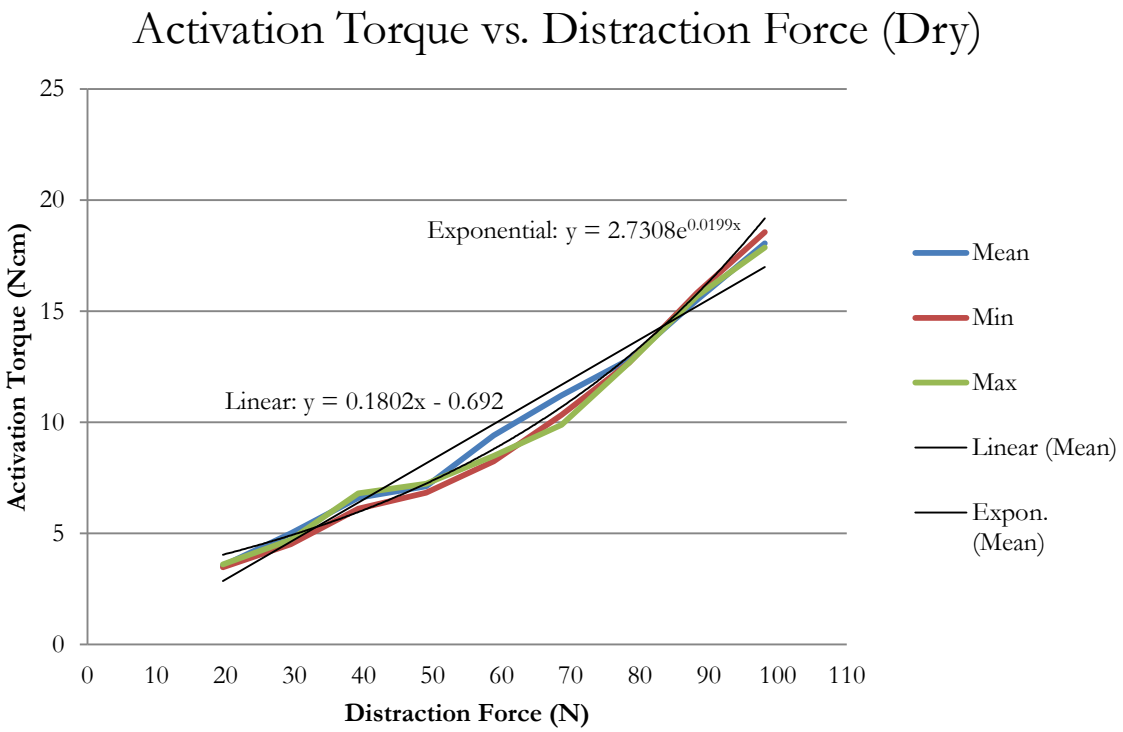

Figure 102: Activation Torque vs. Distraction Force, straight trajectory, dry.

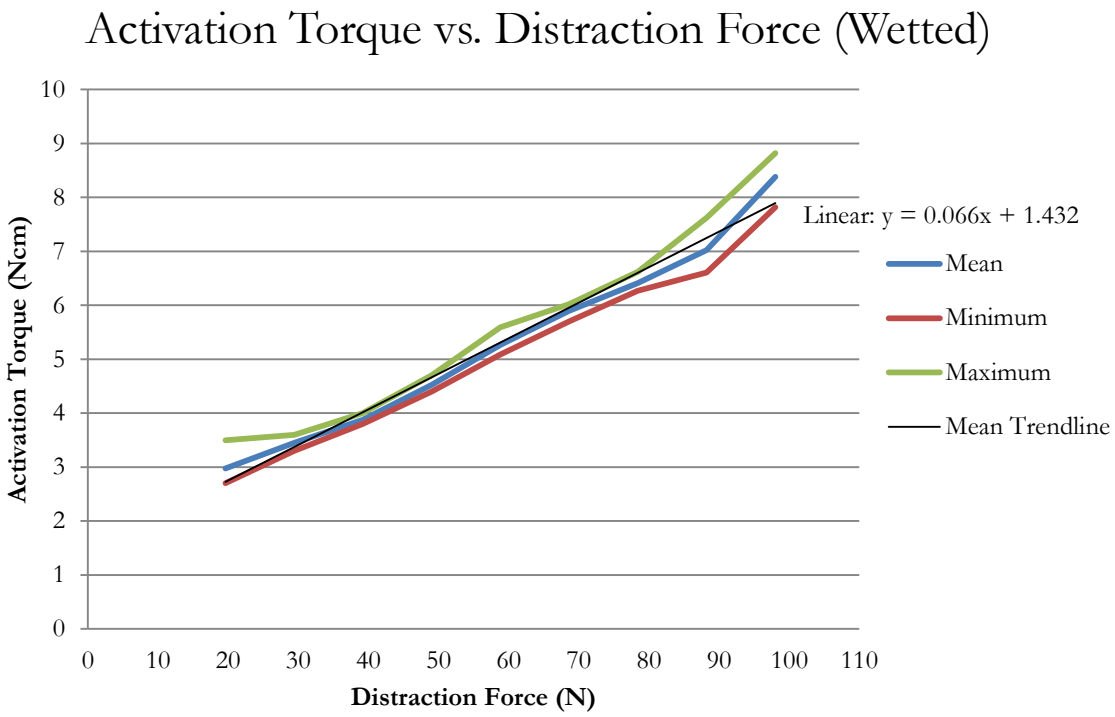

Figure 103: Activation Torque vs. Distraction Force, straight trajectory, wet.

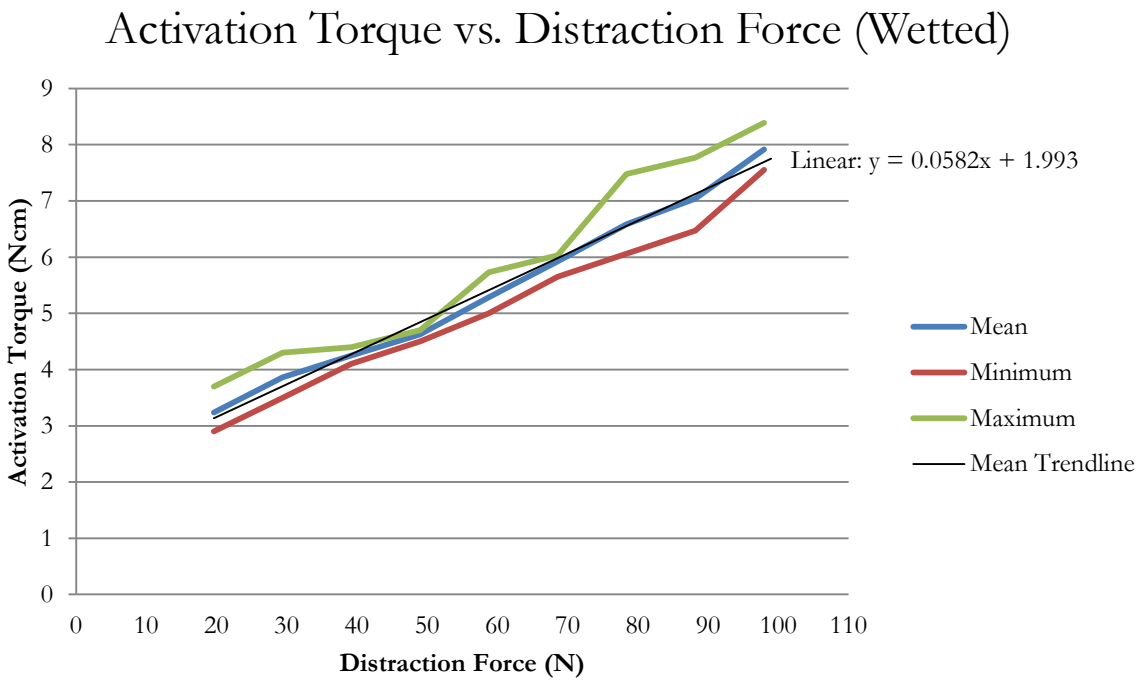

Figure 104: Activation Torque vs. Distraction Force, straight trajectory, wet.

Discussion:

The relationship between the distraction force and the required activation torque was expected to be a straight line, since the worm-rack mechanism introduces simple mechanical advantage and the effects of friction between the sliding surfaces are proportional to the distraction force. Thus, the relationship should be of the form y = mx, where y is the activation torque and x is the distraction force. Over the range tested, the relationship approximated a straight line, though a better approximation was achieved using an exponential function.

In the case of the non-lubricated test, the linear trend-lines were had the formulae (y = 0.1888x - 1.449) and (y = 0.1802x - 0.692). The similar x-coefficients suggest a consistent response of the device to loading. However, as is visible on the charts above, the exponential trend-lines were more accurate, suggesting a more complex relationship.

The data between the two non-lubricated tests were consistent, suggesting repeatable behaviour. Furthermore, over the range of interest, the straight line approximation is accurate and consistent between the two data sets. It is thus reasonable to assume that a reliable correlation can be found between the activation torque and axial load.

In the case of the lubricated test, the relationship was directly proportional, but does not pass through the origin, suggesting that the device has inherent resistance to activation that is not dependent on the presence of an applied load. The straight line approximations to the lubricated data sets were (y = 0.066x + 1.432) and (y = 0.058x + 1.993). Again, similar x-coefficients were observed.

The device was tested over the range 0-100 N, which spans the expected range of loads found in the literature. The device performed predictably and consistently, requiring a maximum activation torque of less than 20 Ncm in the non-lubricated case and less than 10 Ncm is the lubricated case. The operating environment of the device involves lubrication with saliva and protein-containing bodily fluids. Thus, the lubricated data set is taken as the design case. Since the worm has a torque-carrying capacity of at least 35 Ncm before plastic deformation and the maximum activation torque for the lubricated case is 10 Ncm, the mechanism provides a safety factor of at least 3.

Conclusions:

The device performed satisfactorily, generating the maximum expected distraction force with an activation torque of less than 20 Ncm, thereby satisfying the requirements of the PRS. The mechanism provides a safety factor of 3 against breakage of the worm screw; the weakest element.

Graphs were generated that relate the activation torque to the distraction load. A consistent correlation was found between applied distraction load and required activation torque for the non-lubricated and lubricated control conditions.

It is found that, using this correlation, a study of the in vivo distraction force can be carried out by measuring, in vivo, the torque required to activate the device and consulting the graphical data for the corresponding distraction force.

Lubrication of the mechanism causes a significant decrease in the torque required for activation, reducing the required activation torque to less than half for a given load.

G. 2. TEST: CURVILINEAR DISTRACTION SIMULATION UNDER LOAD AND CORRELATION OF ACTIVATION TORQUE WITH DISTRACTION FORCE.

Aims: To evaluate the performance of the device under a range of distraction loads up 100 N on a curved trajectory rail.

Test specimen: *V3* distractor with trajectory rail curved with a radius of 25mm over 100°.

Apparatus:

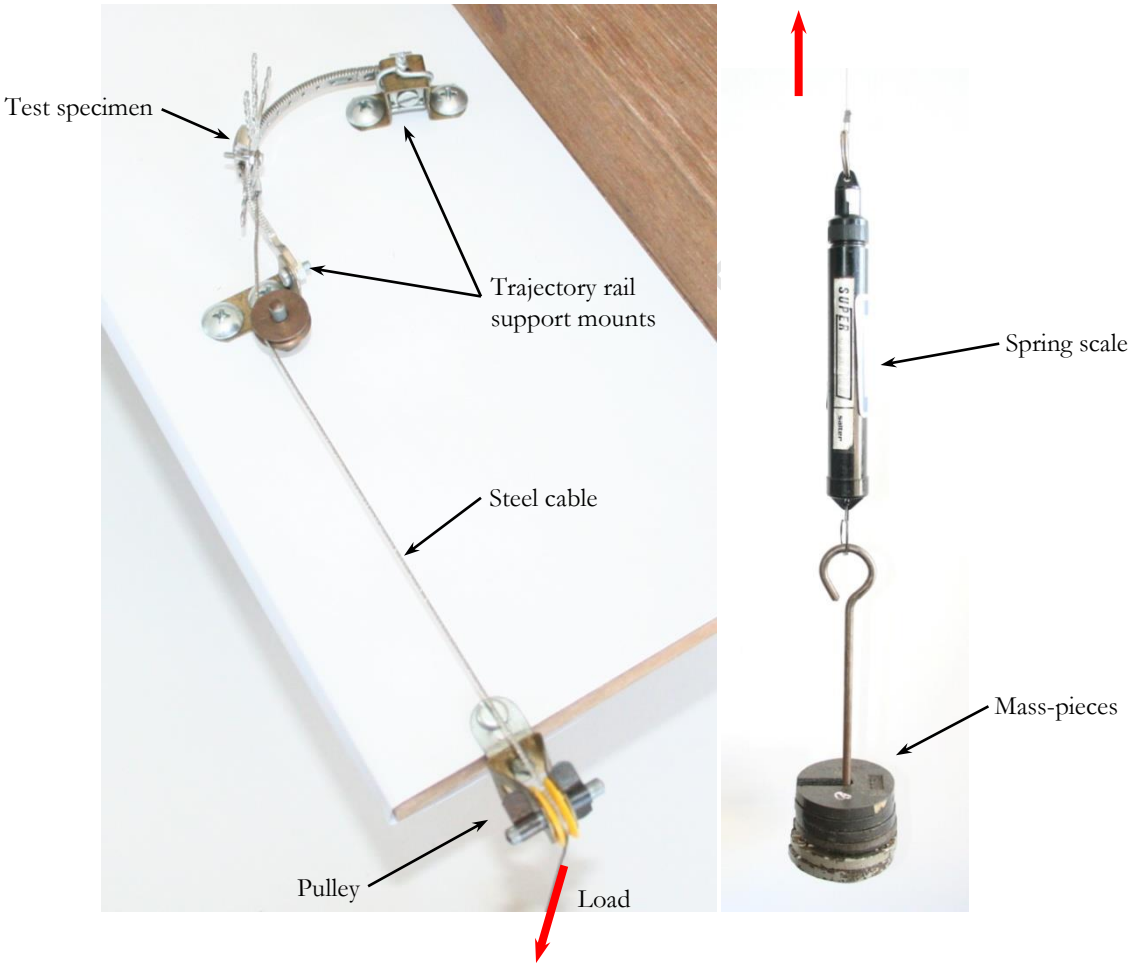

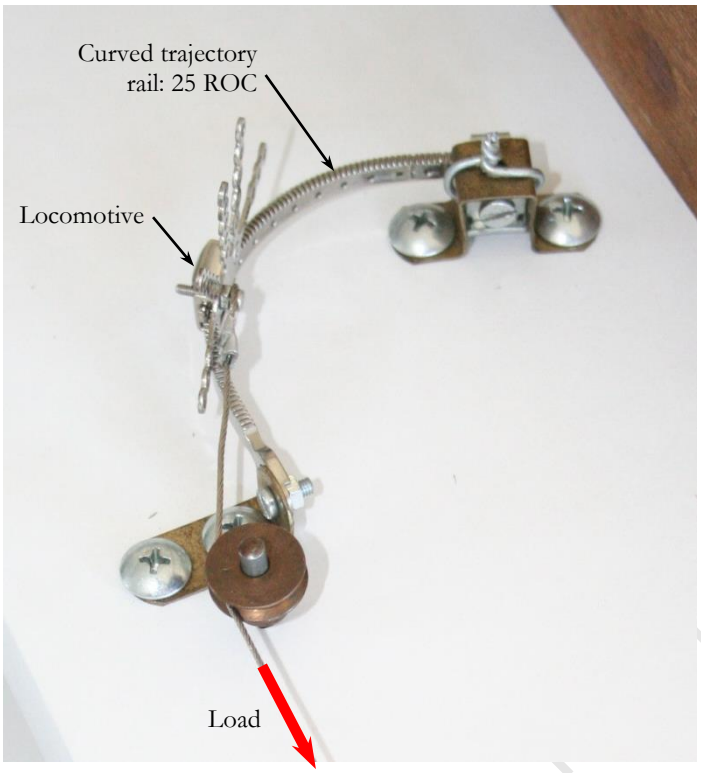

- Base - 16mm MDF board
- 1.5mm steel cable
- 200 N x 2 N spring scale, k_{spring}= 250kg/m
- Distraction driver adapter: ¼" Square (male) to 1.75mm square (female)
- BMS MS050S electronic torque driver:
  - Torque range: 5-50 Ncm range
  - Resolution: 0.01 Ncm
  - Accuracy: +-0.25%
- Detergent solution

Method:

A test rig was constructed on the MDF board that allowed the curved rail to be secured at both ends in the horizontal plane. A 1.5mm steel cable was connected to the locomotive at a distance of 4mm from the peaks of the rack teeth. This was then passed over a pulley, where it was connected to mass-pieces via the spring-scale. It was desired that the resisting force vector act approximately tangential to the rail. To this end, pins in the base provided a series of guides for the cable. As the locomotive progressed the cable was passed over the appropriate pin to approximate the tangent to the curve at that point.

The device was cleaned with a toothbrush in warm, detergent solution to ensure that it was free of any debris or oily residue.

The device was subjected to loads from 0-100 N in increments of 10 N. For each load, the traction mechanism was lubricated with a solution of detergent in water, applied to the worm-rack engagement using a syringe. The worm was activated 40 times in increments of a quarter turn, equating to 10 full rotations of the worm. The peak torque for each quarter turn was recorded using the PEAK function of the torque screwdriver, and tabulated in Microsoft Excel. The locomotive was then returned to its starting point by reversing the worm by 10 full rotations.

The process was carried out on two distinct portions of the curved rail.

Using Excel, the average, maximum and minimum reading was found for set of four readings. These were then plotted against the corresponding distraction force and a linear trend-line was added that was not forced through the origin.

Results:

The device exhibited a relationship between activation torque and distraction load that was exponential. Trend-lines fitted to the curves had the equations ($y = 1.818e^{0.0201x}$) and ($y = 1.927e^{0.0191x}$). The similar coefficients suggest consistent behaviour of the device under different loading conditions, despite the curvilinear trajectory and the fact that the test was repeated over two distinct portions of the rail.

The test results showed an increasing range of activation torque readings for an increasing distraction load, especially visible in the graphs below. The maximum activation torque readings for the 100 N load were 15.4 Ncm and 16.2 Ncm for the data sets. And the minimum readings were 9.4 Ncm and

8.8 Ncm. On average, for a given distraction load, the difference between the minimum and maximum torque readings was approximately 40% of the mean activation torque.

Conclusions:

The device requires a maximum torque of less than 20 Ncm, satisfying the requirements of the Product Requirement Specification. The data recorded was found to be consistent between two test cases, and thus the graphical data above may be used for in vivo correlation of activation torque with distraction load.

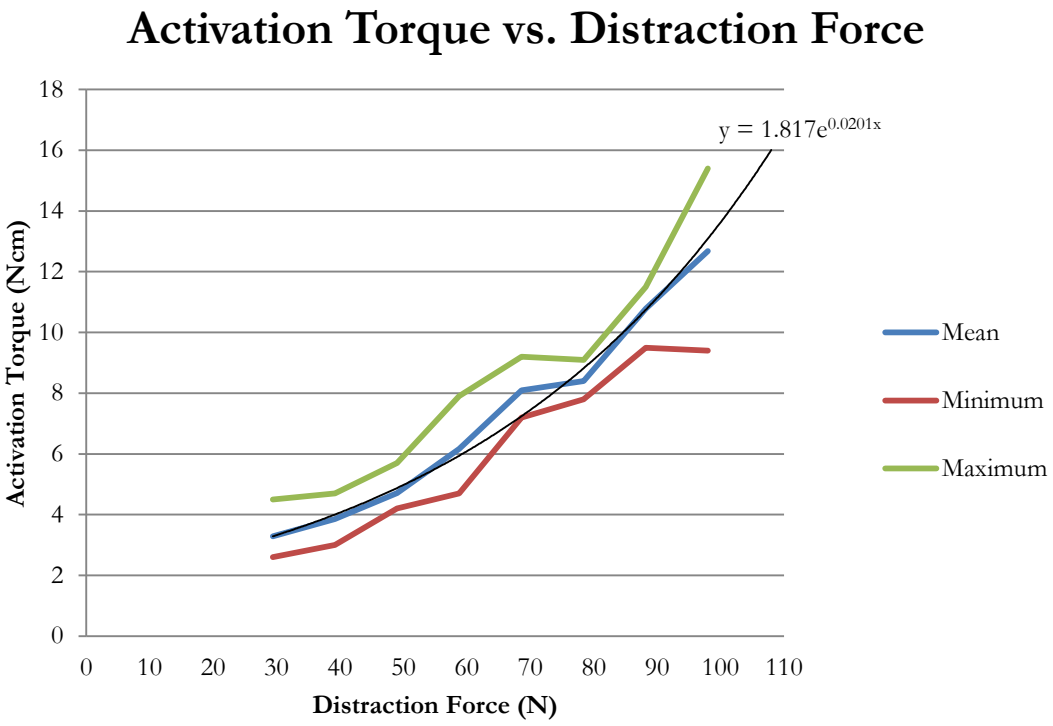

Figure 105: Activation torque vs. distraction force on a curvilinear trajectory, 4mm offset load.

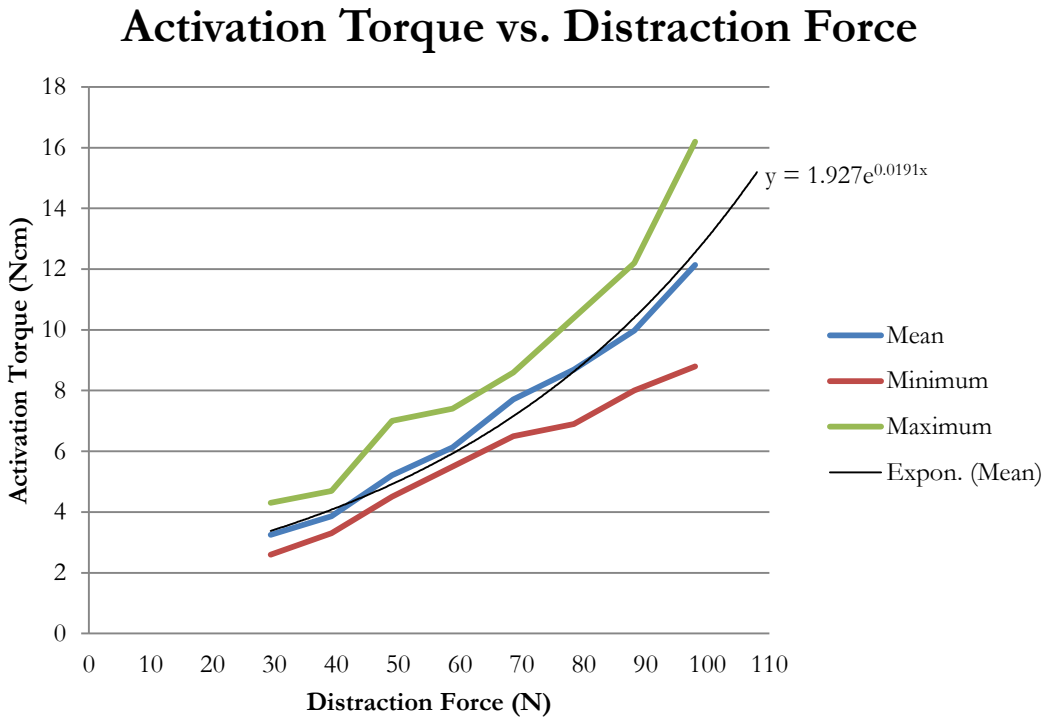

Figure 106: Activation torque vs. distraction force on a curvilinear trajectory, 4mm offset load.

APPENDIX H: DISCUSSION OF DESIGN DECISIONS

H. 1. CONFLUENCE BRACKET DESIGN CONSIDERATIONS

The major considerations for design of the confluence bracket were:

1. Limited Access
2. Constrained approach angles (i.e. directional access with screwdriver etc.)
3. The use of loose (non-captive) components must be avoided.
4. Difficulty aligning multiple plates simultaneously at confluence.
5. Minimised size is a critical criterion.
6. Confluence bracket cannot obscure more than 10mm of the trajectory rail.

The following points were suggested to address the above:

- If the confluence bracket requires alignment of holes, the bracket should provide a protrusion onto which the respective buttress plates may be fitted individually. This mitigates the need to align multiple holes simultaneously.
- The bracket should be captive on at least one of the buttress plates before installation.
- Any small components should be held captive on a larger component.
- A clamp rather than and nut-bolt arrangement is recommended as it achieves clamping without alignment of holes.

A discussion of the two most promising solution concepts follows.

H. 1. 1. SIMPLE WIRED CONFLUENCE CONCEPT

In the first clinical case the confluence joint made use of titanium wire that was tightened by twisting. It was noted that this solution can be easily adapted to a variety cases. By threading the wire through each plate separately and then tightening it was not necessary to align multiple holes simultaneously as would be required by a rigid bolt-nut arrangement.

Advantages of wired confluence:

- Small size
- Can be adapted to any geometry
- Trajectory rail is hardly obscured
- Involves no threaded fasteners, which require good access
- Low-cost

Disadvantages:

- Due to lack of rigidity, working with wire can be frustrating for the surgeon.
- In VT case wire was clamped by twisting ends until desired tension was achieved. This method was deemed crude by the surgeon.

If a wire device can be streamlined for the surgeon, then this offers an ideal solution.

H. 1. 2. CONFLUENCE GROMMET CONCEPT

To this end, a grommet-type component was conceptualised (see Figure 107). Protrusions at opposite ends of the grommet fit snugly into both the Ø1.2mm holes of the trajectory rail and the Ø2.5mm holes of the buttress plates. The grommet is sandwiched between the rail and the buttress plates and the entire stack is clamped together with a single loop of titanium wire. To avoid the hassle of manipulating the small grommet in the confines of the mouth, the grommet was designed to clip into the hole of the palatal plate before installation, where it is held captive for the remainder of the operation. Once both buttress plates have been installed, the zygomatic plate can be attached, producing a captive assembly of the two buttress plates, ready and available for attachment to the trajectory rail. Once the rail is in place, the confluence is quickly and easily connected by inserting the small pin-like protrusion into the appropriate Ø1.1mm hole in the trajectory rail. These holes are spaced 5mm apart, which provides a choice of where to connect the confluence, which can be adjusted repeatedly to ascertain the ideal confluence position. Once the geometry of the assembly has been finalised the plates, grommet and rail are secured together with a single loop of 0.6mm annealed titanium wire.

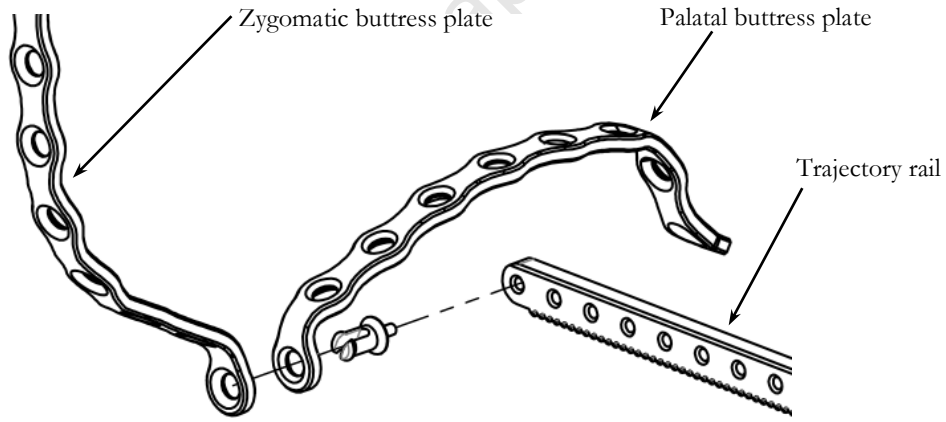

Figure 107: Exploded view of confluence assembly, illustrating the arrangement of the zygomatic and palatal buttress plates, and the trajectory rail.

This solution offers the surgeon maximum versatility and on-the-fly modifiability of the confluence that is completely secure and repeatable. Furthermore, since the buttress plates can be assembled separately to the rail and prior to making the osteotomy, the time taken to assemble the confluence is minimised, as well as the associated frustration of the surgeon. The confluence is easily dismantled by simply cutting the wire and separating the plates and rail.

The surgeon felt that because of its small size, the grommet confluence would be impractical, preferring the simple wired confluence. As such the grommet component was not manufactured and

thus has not been evaluated for its effectiveness in practice. It should be viewed as a recommendation for further enhancement, should the wired confluence prove unsatisfactory.

H. 2. JUSTIFICATION FOR THE BASE PLATE

A major concern with the first two in-vivo trials was the fact that the maxillary bone anchorage was disturbed repeatedly due to the insertion and removal of anchorage screws when attaching/removing the trajectory rail. This repeated attachment/removal was necessary for:

1. Shaping of the trajectory rail to match the desired facial geometry
2. Shaping of the cradle plate, attached to the trajectory rail
3. Removal of the rail to allow for the transport disc osteotomy to be performed.

A solution was thus required which allows the trajectory rail to be repeatedly removed and attached without disturbing the maxillary anchorage screws.

The chosen solution concept was a maxillary base-bracket which allows repeated attachment of the rail through a clamp mechanism. This feature further improved functionality by permitting versatile placement of the trajectory rail, irrespective of dental root position, as the clamp mechanism allows adjustment of the attachment angle and possibly protrusion.

1. Permits removal of the rail the before performing the osteotomy, without disturbing the anterior maxillary bone anchorage.
2. Simplifies the removal and re-attachment of the trajectory rail when performing the osteotomy or making any adjustments to the device.

H. 3. LOCOMOTIVE DETACHABILITY

The current protocol for installation of the device, prepared in collaboration with the medical and engineering experts[27], is as follows:

1. **Finalise shaping of trajectory rail, confluence plates and mesh cradle**
2. **Install base plate and trajectory rail**
3. **Prepare and install buttress plates**
4. **Load locomotive (if not already loaded)**
5. **Remove locomotive to make final adjustments to transport disc cradle**
6. **Reinstall device and confirm all geometry**
7. **Remove trajectory rail and perform osteotomy**
8. **Reattach trajectory rail**
9. **Position locomotive and affix bone transport disc**
10. **Secure the confluence of the trajectory rail and buttress plates**
11. **Activate device to ensure that distraction effect is visible**
12. **Reverse distraction to compress fracture**

In the initial surgery it is essential that the surgeon finalises the geometry of the rail and bone transport cradle and that the surgeon has sufficient access for producing the transport disc osteotomy. It must thus be possible to repeatedly install and remove the bone transport cradle and the trajectory rail. This led to the concept of a clip-on interface that allows the locomotive to be separated from the trajectory rail in situ. Such an interface offers the following advantages:

1. Supports repeated attachment/detachment of the locomotive from the trajectory rail in situ, allowing the surgeon to easily adjust the geometry of the cradle outside the mouth, while leaving the trajectory rail in place.
2. If the locomotive is damaged for any reason, it can be easily replaced.
3. Multi-stage distraction: If a second stage of distraction is required, a second locomotive could be attached to the trajectory rail in situ. Multi-stage distraction is discussed in section 9.4.

The disadvantage of the clip-on feature is the complexity added to the locomotive, the increased size of the locomotive to accommodate the clip-on features and the risks associated with the added complexity. When considering the benefits of the locomotive detachability concept it was found that the base clamp feature already provided much of the desired functionality, i.e. detachability of the

[27] Dr Rushdi Hendricks (B.Ch.D, M.Ch.D) and Dr George Vicatos (Pr.Eng., Ph.D.)

trajectory rail. Therefore, it was decided that the few benefits of the locomotive detachability concepts did not justify the associated complexity and the risk of compromising reliability.

However, clinical observations demonstrated that more versatile detachability is required. It may be a useful compromise to enable the transport disc cradle plate to be separated from the locomotive in situ. The cradle plate could thus be quickly and repeatedly installed and removed, allowing careful and accurate shaping of the transport disc cradle. This is discussed in the Recommendations, (section 9.3).

APPENDIX I: TORQUE DRIVER CALIBRATION CERTIFICATE

BMS PADDY

Kalibrier - Zertifikat
Certificate of Calibration
Certificat d'etalonnage

DIN50049 2.3 ___
DIN50049 3.1B ___

Modell Model Modelo	MS050S	Serien-Nr. Serial No. Numero de Serie	201433	Kalibrierdatum Date of Calibration Date d'etalonnage	28/08/2012	Prufer Inspector Inspecteur	A.Wiewiorski

Höchstwert
Maximum Capacity
Capacite Maximale: 50

Einheit
Units
Mesure: cNm

Eingestelltes Drehmoment Set Torque Appareil Dynamometric	Grenzwerte Limits Limites unterer lower inferieures	 oberer upper superieures	Abgelesene Werte Actual readings Valeur reelle Rechts-Anzug Clockwise Attacher à droite	 Links-Anzug Counter-clockwise Attacher à gauche
10	9.90	10.10	10.08	9.92
30	29.70	30.30	30.25	29.85
50	49.50	50.50	49.60	49.95

Die aufgefuhrten Grenzwerte und das verwendete Prufgerat fur die Kalibrierung entsprechen den Anforderungen:
The Limits shown and the test equipment for this calibration comply with the requirements of:
Les limites mentionnees et le material experimental utilise pour cet etalonnage sont conformes aux exgences de la norme:

ISO 6789.2003
EN ISO 6789 / 2003

Die Abweichung des eingesetzten Prufgerates liegt bei:
The uncertainty of measurement of the test equipment used is
L'ecart de mesure du materiel experimental est: ***+/- 0.25%***

Internationale Ruckfuhrbarkeit durch Kalibrierlabros gemaß DIN/ISO 9000.
International traceability through calibration laboratories acc. to ISO 9000.
Reperes internationaux etablis par les laboratoires d'etalonnage selon la norme ISO 9000.

Modell des Prufgergerates Tester Model Modelo experimental	MD MeBzelle MD Transducer Re decteur MD	Anpasser/Ausgeber Amplifier/Display Amplificateur/Affichage
Fabrikat Manufacturer Fabricant	NORBAR	NORBAR
Typ Type Type	50024ETS	40320
Seriennummer Serial Number Numero de serie	43675	42169
Kalibrierschein Nr. Calibration Cert. No. Certificat d'etalonnage No.	141192	UKAS 0256 -141187

APPENDIX J: ETHICAL APPROVAL CERTIFICATES

UNIVERSITY OF CAPE TOWN

Faculty of Health Sciences
Faculty of Health Sciences Research Ethics Committee
Room E52-24 Groote Schuur Hospital Old Main Building
Observatory 7925
Telephone [021] 406 6338 • **Facsimile** [021] 406 6411
e-mail: sumayah.ariefdien@uct.ac.za

28 May 2012

HREC REF: 147/2012

Dr R Hendricks
Department of Plastics & Reconstructive Surgery
J-Floor
OMB

Dear Dr Hendricks

PROJECT TITLE: EVALUATION OF THE CLINICAL OUTCOME OF CURVILINEAR TRANSPORT DISTRACTION OSTEOGENESIS AND REVASCULARISED FIBULA FREE FLAPS IN THE RECONSTRUCTION OF LARGE POST-MAXILLECTOMY DEFECTS.

Thank you for addressing the issues raised by the committee.

It is a pleasure to inform you that the Ethics Committee has **formally approved** the above mentioned study.

Approval is granted for one year till the 15 June 2013.

Please submit a progress form, using the standardised Annual Report Form (FHS016), if the study continues beyond the approval period. Please submit a Standard Closure form (FHS010)if the study is completed within the approval period.
(Forms can be found on our website:www.health.uct.ac.za/research/humanethics/forms)

Please note that the ongoing ethical conduct of the study remains the responsibility of the principal investigator.

Please quote the REC. REF in all your correspondence.

Yours sincerely

PROFESSOR M BLOCKMAN
CHAIRPERSON, HSF HUMAN ETHICS

Federal Wide Assurance Number: FWA00001637.

sAriefdien

EBE Faculty: Assessment ofEthics in Research Projects (Rev2)

Any person planning to undertake research in the Faculty of Engineering and the Built Environment at the University of Cape Town is required to completethis formbefore collecting or analysing data.When completed it should be submitted to the supervisor (where applicable) and from there to the Head of Department. If any of the questions below have been answered YES, and the applicant is NOT a fourth year student, the Head should forward this form for approval by the Faculty EIR committee: submit toMs Zulpha Geyer (Zulpha.Geyer@uct.ac.za; ChemEngBuilding, Ph021 650 4791).
NB: A copy of this signed form must be included with the thesis/dissertation/report when it is submitted for examination

This form must only be completed once the most recent revision EBE EiR Handbook has been read.

Name of Principal Researcher/Student: James Boonzaier Department: Mech. Eng.

Preferred email address of the applicant: jbee87@gmail.com

If a Student: Degree: MSc Supervisor: Dr George Vicatos

If a Research Contract indicate source of funding/sponsorship:

Research Project Title: Reconstruction of Cranial Maxillofacial Anatomy by Transport Distraction Osteogenesis.

Overview of ethics issues in your research project:

Question 1: Is there a possibility that your research could cause harm to a third party (i.e. a person not involved in your project)?	YES	NO x
Question 2: Is your research making use of human subjects as sources of data? If your answeris YES, please complete Addendum 2.	YES	NO x
Question 3: Does your research involve the participation of or provision of services to communities? If your answeris YES, please complete Addendum 3.	YES	NO x
Question 4: If your research is sponsored, is there any potential for conflicts of interest? If your answeris YES, please complete Addendum 4.	YES	NO x

If you have answered YES to any of the above questions, please append a copy of your research proposal, as well as any interview schedules or questionnaires (Addendum 1) andplease complete further addenda as appropriate. Ensure that you refer to the EiR Handbook to assist you in completing the documentation requirements for this form.

I hereby undertake to carry out my research in such a way that

there is no apparent legal objection to the nature or the method of research; and
the research will not compromise staff or students or the other responsibilities of the University;
the stated objective will be achieved, and the findings will have a high degree of validity;
limitations and alternative interpretations will be considered;
the findings could be subject to peer review and publicly available; and
I will comply with the conventions of copyright and avoid any practice that would constitute plagiarism.

Signed by:

	Full name and signature	Date
Principal Researcher/Student: James Boonzaier	James Angus Boonzaier	22-01-2012
This application is approved by:		
Supervisor(if applicable):		
HOD (or delegated nominee): *Final authority for all assessments with NO to all questions and for all undergraduate research.*		
Chair : Faculty EIR Committee For applicants other than undergraduate students who have answered YES to any of the above questions.		